Hypolimnetic Oxygenation Mitigates the Effects of Nutrient Loading on Water Quality in a Eutrophic Reservoir

Alexandra Beth Gerling

Thesis submitted to the faculty of the Virginia Polytechnic Institute and State University in partial fulfillment of the requirements for the degree of

Master of Science
In
Biological Sciences

Cayelan C. Carey, Chair
John C. Little
John E. Barrett

29 July 2015
Blacksburg, Virginia

Keywords: hypoxia, oxygenation, internal loading, external loading, water quality

Hypolimnetic Oxygenation Mitigates the Effects of Nutrient Loading on Water Quality in a Eutrophic Reservoir

Alexandra Beth Gerling

Abstract

Climate change is predicted to have many diverse effects on freshwater lakes and reservoirs by increasing both hypolimnetic hypoxia and runoff, which will increase nutrient concentrations and degrade water quality. Hypoxic conditions can trigger the release of metals and nutrients from the sediments, i.e., internal loading, while storms can increase external nutrient loading to a waterbody. One potential solution for combating hypoxia is to use side stream supersaturation (SSS), a novel form of hypolimnetic oxygenation. First, in Chapter 1, I tested the efficacy of SSS operation to improve water quality in Falling Creek Reservoir (FCR), a shallow, eutrophic, drinking water reservoir. I found that SSS operation successfully increased hypolimnetic oxygen concentrations in FCR and suppressed internal loading of iron, manganese, and phosphorus. In Chapter 2, I manipulated inflow volumes to FCR and used SSS as a tool to alter hypolimnetic oxygen conditions in whole-ecosystem manipulations of internal and external nutrient loading. I observed that internal nitrogen and phosphorus loading during hypoxic conditions largely controlled the hypolimnetic mass of nutrients in FCR, regardless of inflow volumes, presumably as a result of the accumulated nutrients in its sediment from historical agriculture. Additionally, FCR consistently functioned as net sink of N and P throughout almost all of the treatments and substantially reduced nutrient export to downstream ecosystems. In summary, my research demonstrates the sensitivity of reservoir water quality to global change.

Acknowledgements

I would like to express my deepest appreciation to my advisor, Dr. Cayelan Carey, for providing an incredible amount of support, guidance, and encouragement these past two years. I am grateful for her willingness to go above and beyond her role as my advisor. My research endeavors would not have been possible without her constant enthusiasm, patience, and understanding. I would also like to thank my committee member, Dr. John Little, for providing continual support and for sharing his unlimited knowledge and research expertise. Additional thanks goes to my committee member, Dr. Jeb Barrett, for providing valuable feedback and stimulating new ideas.

I sincerely thank the staff at the Western Virginia Water Authority for their substantial support and funding. In particular, I would like to thank Cheryl Brewer, Jamie Morris, Jeff Booth, Greg Belcher, Bob Benninger, Gary Robertson, and Rodney Witt. Their support both in the field and in the lab was invaluable.

In addition, I am very grateful for the enthusiastic support and assistance from the members of the Carey Lab, Reservoir Group, and Stream Team. Special thanks to Kevin Bierlein, Jon Doubek, Kate Hamre, Ryan McClure, and Zack Munger for their continual support and friendship. Thank you to Rick Browne, Chris Chen, Miranda Flood, Zach Gajewski, Mariah Haberman, Charlotte Harrell, Maddie Ryan, and Christina Urbanczyk for their assistance in the field and in the lab. My sincere appreciation goes to Bobbie Niederlehner, whom provided critical help and great company in the lab. To Paul Gantzer, thank you for sharing your time, energy, and expertise at Falling Creek.

Finally, this journey would not have been possible without the endless love, support, and encouragement I received these past two years from my parents, brothers, and great friends.

Table of Contents

List of Tables

List of Figures

Attribution

Several colleagues aided in the research and writing behind the two chapters presented as part of my thesis. Brief descriptions of their contributions are below.

Chapter 1: First Report of the Successful Operation of a Side Stream Supersaturation Hypolimnetic Oxygenation System in a Eutrophic, Shallow Reservoir

Richard G. Browne is a former graduate student in the Department of Civil and Environmental Engineering at Virginia Tech. He assisted with the field work, data collection, and data interpretation.

Dr. Paul A. Gantzer is an engineer at Gantzer Water Engineering, LLC. in Kirkland, Washington. He designed and installed the side stream supersaturation system in the reservoir.

Mark H. Mobley is an engineer at Mobley Engineering, Inc. in Norris, Tennessee. He designed and installed the side stream supersaturation system in the reservoir.

Dr. John C. Little is a professor in Department of Civil and Environmental Engineering at Virginia Tech. He contributed to designing the research, analyzing the data, and writing the paper.

Dr. Cayelan C. Carey is a professor in the Department of Biological Sciences at Virginia Tech. She helped design the research, analyze the data, and write the paper.

Chapter 2: Whole-Ecosystem Manipulations of Internal and External Loading Reveal the Sensitivity of a Century-Old Reservoir to Hypoxia

Zackary W. Munger is a graduate student in the Department of Geosciences at Virginia Tech. He assisted with field work and analyzing the data.

Jonathan P. Doubek is a graduate student in the Department of Biological Sciences at Virginia Tech. He assisted with field work at the reservoir.

Kathleen D. Hamre is a graduate student in the Department of Biological Sciences at Virginia Tech. She also assisted with field work at the reservoir.

Dr. Paul A. Gantzer is an engineer at Gantzer Water Engineering, LLC. in Kirkland, Washington. He designed and installed the side stream supersaturation system in the reservoir.

Dr. John C. Little is a professor in Department of Civil and Environmental Engineering at Virginia Tech. He helped design the research, analyze the data, and write the paper.

Dr. Cayelan C. Carey is a professor in the Department of Biological Sciences at Virginia Tech. She contributed to designing the research, analyzing the data, and writing the paper.

Introduction

Climate change is projected to have widespread impacts on freshwater lake and reservoir water quality and ecosystem functioning worldwide (Delpla et al. 2009, Jiménez Cisneros et al. 2014, Paerl and Huisman 2009, Smith and Schindler 2009, Williamson et al. 2009). For example, increasing air temperatures will warm surface waters in many waterbodies, resulting in stronger thermal stratification and decreased oxygen concentrations in the bottom waters (Sahoo and Schladow 2008, Sahoo et al. 2010, Tranvik et al. 2009, Williamson et al. 2009). Hypolimnetic hypoxia (defined as dissolved oxygen (DO) concentrations <2 mg/L in the bottom stratum of a waterbody; Wyman and Stevenson 1991) alters many biogeochemical processes in lakes and reservoirs and ultimately degrades water quality.

Hypoxic conditions in the hypolimnion stimulate the release of nutrients (specifically, nitrogen (N) and phosphorus (P)) and reduced metals (iron (Fe) and manganese (Mn)) from the sediments and leads to their accumulation in the hypolimnion (Matthews and Effler 2006a, McGinnis and Little 2002, Mortimer 1941). Maintaining an oxygenated environment is critical for controlling these nutrients and metals as excess N, P, Fe, and Mn in the water column can lead to undesirable outcomes for lake and reservoir managers. N and P can stimulate algal growth and exacerbate eutrophication (Schindler 1974, 1977, Schindler et al. 2008, Smith 1982), while Fe and Mn can cause taste, odor, and color problems for drinking water (AWWA 1987, Zaw and Chiswell 1999).

One solution to promoting oxic conditions in lakes and reservoirs is the use of hypolimnetic oxygenation (HOx) systems (Beutel and Horne 1999, Singleton and Little 2006). HOx systems operate by adding oxygen to bottom waters while preserving thermal stratification (Beutel and Horne 1999). HOx systems are commonly deployed and successful in deep (>10 m)

lakes and reservoirs (reviewed by Beutel and Horne 1999, Singleton and Little 2006). However, it is much more difficult to add oxygen to shallow (<10 m) waterbodies. Shallow lakes and reservoirs lack sufficient depth to ensure that the injected oxygen bubbles dissolve in the hypolimnion and that thermal stratification is not disrupted by HOx operation (Beutel 2006, Cooke et al. 2005). Thus, a novel technique known as side stream supersaturation (SSS) is a potential solution to oxygenation in shallow waterbodies (Beutel and Horne 1999).

Freshwater reservoirs are especially important to study because of their ubiquity and the critical role they play in biogeochemical processes. Artificial waterbodies cover more than 0.25 million km^2 of earth's surface (Downing et al. 2006a) and are increasingly being constructed for water supply, hydropower, irrigation, and recreation (Downing et al. 2006a, Rosenberg et al. 2000, Smith et al. 2002). Since the 1950s, over 10,000 km^3 of water have been impounded into reservoirs globally (Chao 1995, Rosenberg et al. 2000) and over 2 million small, artificial waterbodies exist across the United States alone (Smith et al. 2002). Reservoirs play a critical role in the landscape because they generally function as nutrient sinks and reduce nutrient export to downstream ecosystems (Nowlin et al. 2005, Powers et al. 2015, Teodoru and Wehrli 2005).

In Chapter 1 of this thesis, I tested the efficacy of SSS operation to improve water quality in a shallow, eutrophic, drinking water reservoir. First, I evaluated if SSS operation could successfully increase hypolimnetic oxygen concentrations without destratifying the water column or warming of the sediments. Second, I assessed how well SSS operation prevented the release of Fe, Mn, and P from the reservoir sediments.

In Chapter 2 of this thesis, I used SSS as a tool for whole-ecosystem manipulations to simulate the effects of different potential climate scenarios and measure their effects on reservoir N and P budgets. In this whole-ecosystem experiment, I controlled hypolimnetic oxygen

conditions as well as the volume of inflow water to the reservoir from an upstream tributary. My overarching goal was to determine the relative importance of internal versus external nutrient loads for the reservoir's N and P budgets and to determine if the reservoir was a net nutrient sink or source of N and P to downstream ecosystems.

Chapter 1: First Report of the Successful Operation of a Side Stream Supersaturation Hypolimnetic Oxygenation System in a Eutrophic, Shallow Reservoir

Alexandra B. Gerling, Richard G. Browne, Paul A. Gantzer, Mark H. Mobley, John C. Little, Cayelan C. Carey

Gerling, A.B., Browne, R.G., Gantzer, P.A., Mobley, M.H., Little, J.C., Carey, C.C., 2014. First report of the successful operation of a side stream supersaturation hypolimnetic oxygenation system in a eutrophic, shallow reservoir. *Water Research* 67, 129-143. doi:10.1016/j.watres.2014.09.002. Used with permission of RightsLink, 2015.

Abstract

Controlling hypolimnetic hypoxia is a key goal of water quality management. Hypoxic conditions can trigger the release of reduced metals and nutrients from lake sediments, resulting in taste and odor problems as well as nuisance algal blooms. In deep lakes and reservoirs, hypolimnetic oxygenation has emerged as a viable solution for combating hypoxia. In shallow lakes, however, it is difficult to add oxygen into the hypolimnion efficiently, and a poorly designed hypolimnetic oxygenation system could potentially result in higher turbidity, weakened thermal stratification, and warming of the sediments. As a result, little is known about the viability of hypolimnetic oxygenation in shallow bodies of water. Here, we present the results from recent successful tests of side stream supersaturation (SSS), a type of hypolimnetic oxygenation system, in a shallow reservoir and compare it to previous side stream deployments. We investigated the sensitivity of Falling Creek Reservoir, a shallow (Z_{max} = 9.3 m) drinking

water reservoir located in Vinton, Virginia, USA, to SSS operation. We found that the SSS system increased hypolimnetic dissolved oxygen concentrations at a rate of ~1 mg/L/week without weakening stratification or warming the sediments. Moreover, the SSS system suppressed the release of reduced iron and manganese, and likely phosphorus, from the sediments. In summary, SSS systems hold great promise for controlling hypolimnetic oxygen conditions in shallow lakes and reservoirs.

Introduction

Hypolimnetic hypoxia (defined as dissolved oxygen concentrations < 2 mg/L; Wyman and Stevenson 1991) in lakes and reservoirs degrades water quality and can prevent recovery from eutrophication (Cooke and Kennedy 2001, Cooke et al. 2005, Smith 2003, Wetzel 2001). Maintaining an oxygenated environment in the bottom waters prevents the release of nutrients and reduced metals – namely, phosphorus (P), iron (Fe), manganese (Mn) – and their accumulation in the hypolimnion (Matthews and Effler 2006a, McGinnis and Little 2002, Mortimer 1941). Controlling these nutrients and metals is essential for improving water quality. Phosphorus can stimulate algal growth and exacerbate eutrophication (Schindler 1974, 1977, Schindler et al. 2008, Smith 1982), while Fe and Mn in the hypolimnion can cause taste, odor, and color problems for drinking water suppliers (AWWA 1987, Zaw and Chiswell 1999). Ultimately, maintaining an oxygenated hypolimnion is paramount for controlling these nutrients and metals and simplifying the water treatment process.

Hypolimnetic oxygenation systems are commonly used to increase dissolved oxygen (DO) concentrations in the hypolimnia of lakes and reservoirs (Beutel and Horne 1999, Singleton and Little 2006). Hypolimnetic oxygenation systems aim to maintain thermal stratification while

adding oxygen to bottom waters (Beutel and Horne 1999). Two primary advantages of hypolimnetic oxygenation systems are higher oxygen solubility in comparison to hypolimnetic aeration systems, and higher oxygen transfer efficiencies (percent uptake of delivered oxygen; Beutel and Horne 1999). As a result, >30 hypolimnetic oxygenation systems have been deployed in lakes and reservoirs around the world, as documented in the literature (Liboriussen et al. 2009, Noll 2011, Singleton and Little 2006, Søndergaard et al. 2007, Yajima et al. 2009, Zaccara et al. 2007).

Despite its promise, the process of hypolimnetic oxygenation has three major potential drawbacks - destratification, hypolimnetic warming, and induced sediment oxygen demand - that must be taken into account when designing a system. First, hypolimnetic oxygenation aims to raise the oxygen content of the hypolimnion without destratifying the overlying water column (Ashley 1985). Such mixing could result in the entrainment of nutrients that were once isolated in the hypolimnion to the epilimnion, resulting in elevated nutrient concentrations in the photic zone and increased nutrient availability. Furthermore, partial destratification increases the hypolimnetic volume over which oxygen must be delivered to maintain desired DO concentrations, leading to inefficiency and added costs. Second, hypolimnetic oxygenation aims to avoid warming of the hypolimnion, which could lead to premature overturn, and poses a potential problem for benthic, cold-water organisms (Beutel and Horne 1999, Wu et al. 2003). Third, hypolimnetic oxygenation may also stimulate increases in sediment and water column oxygen uptake, thereby accelerating hypolimnetic oxygen depletion and diminishing overall performance of the system (Bryant et al. 2011, Gantzer et al. 2009b). Although somewhat counter-intuitive, hypolimnetic oxygenation systems can increase oxygen demand by stimulating

aerobic decomposition and chemical demand (Ashley 1981, Gantzer et al. 2009b, Lorenzen and Fast 1977, Moore et al. 1996, Soltero et al. 1994).

There are several different types of oxygenation systems that are commonly deployed in deep (>10 m) lakes and reservoirs. These primarily include bubble-plume diffusers (linear and circular) and submerged down-flow bubble contact chambers such as the Speece Cone (reviewed by Beutel and Horne 1999, Singleton and Little 2006). However, these types of systems are generally only deployed in deep lakes and reservoirs because shallow (<10 m) water bodies lack sufficient depth to ensure that bubbles of injected oxygen dissolve in the hypolimnion or that thermal stratification is not disrupted by system operation (Beutel 2006, Cooke et al. 2005). Thus, for implementing hypolimnetic oxygenation in shallow lakes and reservoirs, a technique known as side stream supersaturation (SSS) represents a potential alternative (Beutel and Horne 1999).

SSS may hold great promise for successful hypolimnetic oxygenation of shallow ecosystems. This technique involves withdrawing hypolimnetic water from the lake, injecting concentrated oxygen gas at high pressure, and returning the oxygenated water to the hypolimnion (Singleton and Little 2006). Due to the small hypolimnetic volume in shallow water bodies, SSS systems may be more effective than other systems in increasing hypolimnetic DO concentrations because they can add more oxygen with low water flow rate, thereby causing less mixing and maintaining thermal structure.

In a comprehensive review of published studies and other reports, we found that side stream systems have been deployed thus far in at least five lakes or reservoirs and three river or tidal ecosystems worldwide (Table 1). We note the difference in our review between side stream systems that inject oxygen into the hypolimnion of water bodies at saturated concentrations

(hereafter, side stream hypolimnetic oxygenation) and SSS systems, which inject oxygen at supersaturated concentrations.

The outcome of the previous side stream and SSS deployments has been mixed. While the earliest known deployment in Ottoville Quarry in 1973 (Z_{max} = 18 m) demonstrated that a side stream system could successfully increase hypolimnetic DO concentrations without destratification of the water column (Fast et al. 1975, 1977), later deployments of side stream systems, one an SSS, in Attica Reservoir (Fast and Lorenzen 1976, Lorenzen and Fast 1977), Lake Serraia (Toffolon et al. 2013), and Lake Thunderbird (OWRB 2012, 2013), all exhibited premature destratification (Table 1). Consequently, there has been no successful deployment of a side stream or SSS system in a shallow (<10 m) lake or reservoir to date.

Given that most lakes and reservoirs worldwide are small and shallow (Downing et al. 2006b, Scheffer 2004), and that improving water quality is a major goal worldwide (MEA 2005), we investigated the utility of SSS application in a shallow drinking water reservoir. We had two primary objectives. First, we assessed if the SSS system could successfully overcome induced sediment oxygen demand to increase hypolimnetic DO concentrations without triggering destratification or sediment warming. Second, we evaluated how well the system prevented the release of Fe, Mn, and P from the reservoir sediments.

Materials and Methods

Study site

Falling Creek Reservoir (FCR) is a small, eutrophic drinking water reservoir near Vinton in Bedford County, southwestern Virginia, USA (37° 18' 12" N, 79° 50' 14" W). FCR is operated and maintained by the Western Virginia Water Authority (WVWA) and provides drinking water

for residents of Roanoke, VA. FCR is located in an undisturbed, forested watershed and receives water primarily from one inflowing stream. The reservoir has a surface area of 1.19×10^{-1} km^2, maximum depth of 9.3 m, mean depth of 4 m, and a volume of 3.1×10^5 m^3, making it substantially smaller and shallower than other lakes and reservoirs in which hypolimnetic oxygenation has been previously studied. Despite the reservoir's small size, FCR does exhibit stable thermal stratification, typically from May to early October, producing a well-defined and discrete hypolimnion suitable for oxygenation. Mean residence time in the reservoir is 200 to 300 days. During its recent monitoring history, FCR has exhibited summer cyanobacterial blooms associated with taste and odor problems and long periods of hypolimnetic anoxia linked to internal nutrient loading of Fe, Mn, and P.

Data collection and nutrient analysis

We monitored FCR twice a week during the experimental period from April to September 2013. Water column depth profiles of temperature, DO, conductivity, and turbidity were measured at seven sites on a transect from the reservoir dam to its upstream tributary (Figure 1.1) using a SBE 19plus (Seabird Electronics, Bellevue, WA) high-resolution (4 Hz sampling rate) Conductivity, Temperature, and Depth (CTD) profiler. The response time of the DO probe on the CTD was 1.4 s at 20°C, allowing data to be collected at ~0.1 m increments from the water's surface to just above the sediments. A YSI (YSI Inc., Yellow Springs, OH) ProODO meter was substituted for the CTD's dissolved oxygen (DO) profile measurements from 3 July to 15 August and measured DO profiles at the seven sites on 0.5 m increments. Comparison of CTD and YSI profiles on the same sampling days yielded nearly identical measurements of DO (within 0.1 mg/L).

We collected water samples to measure total and soluble Fe, Mn, and P concentrations along a depth profile (at the eight discharge depths of the reservoir: 0.1, 0.8, 1.6, 2.8, 3.8, 5.0, 6.2, and 8.0 m) using a 1.2 L Kemmerer bottle (Wildlife Supply Company, Yulee, FL) at the deep hole as well as in the upstream tributary before it entered the reservoir. Samples for total and soluble analyses at each depth were poured directly from the Kemmerer bottle into plastic bottles that had been acid-washed with 1.2 N hydrochloric acid. Soluble samples were filtered through 0.7 μm Whatman GF/F filters, and total and soluble samples were preserved with 15.9 N nitric acid until analysis. We analyzed the samples for total and soluble Fe and Mn following the EPA Method 200.8, Rev. 5.4 (1994) using an Agilent 7700x ICP-MS (Agilent Technologies, Santa Clara, CA). We analyzed the samples for total phosphorus (TP) following the EPA Method 365.3 (1978) and soluble reactive phosphate (SRP) on a spectrophotometer following the QuikChem Method 10-115-10-1-B.

Finally, we measured the flow rate into the reservoir from the upstream tributary using a rectangular weir with a notch width of 1.10 m. An INW Aquistar PT2X pressure sensor (INW, Kirkland, WA) recorded the water level above the weir every 15 minutes, which we used to calculate the flow rate of the stream into the reservoir using (Chow 1959, Grant 1991):

$$q = K \times (L - 0.2 \times H) \times H^{1.5} \quad \text{(eqn. 1)}$$

where q is flow rate (m^3/min), K is 110.29, a unit conversion constant, L is the crest length of the weir (m), and H is the head on the weir (m). The residence time of FCR was calculated at 15 minute increments using the flow rate of the upstream tributary and assuming the reservoir volume was at full pond, 3.1×10^5 m^3.

Data Analysis

We examined how SSS operation affected hypolimnetic oxygen demand (HOD) and estimated the corresponding induced oxygen demand (IOD) caused by SSS operation. HOD is the rate of change of total oxygen content in the hypolimnion over time, which is measured on both (1) a mass basis (HOD_{mass}) yielding a rate in kg/day, and (2) a concentration basis (HOD_{conc}) yielding a rate in mg/L/day. HOD encompasses all oxygen-consuming processes in the hypolimnion, including oxygen demand from sediment, the water column, and any redox reactions.

We determined HOD and IOD by performing a regression analysis on the volume-weighted oxygen content in the hypolimnion (following the methods of Gantzer et al. 2009b), and then compared HOD and IOD during multiple periods of SSS activation and deactivation. During periods without SSS operation, the rate of change of hypolimnetic oxygen content (HOD_{mass} and HOD_{conc}) was observed to decrease linearly. During SSS operation, the rate of oxygen addition from SSS operation was subtracted from the observed hypolimnetic oxygen accumulation rate, yielding HOD. IOD represents the increased demand above background HOD (calculated only when the SSS was off), which is used to validate the factor of safety employed during system design.

Schmidt stability, an index of the strength of thermal stratification (Idso 1973), was calculated from the temperature profiles using Lake Analyzer (Read et al. 2011) in Matlab statistical software (version R2013a 8.1.0.604; Mathworks, Natick, MA). Schmidt stability (in J/m^2) indicates the resistance to mechanical mixing due to the potential energy inherent in the stratification of the water column, and was our primary metric for assessing the effect of SSS operation on thermal stratification.

Determining thermocline depth and hypolimnetic oxygen content

We calculated the hypolimnetic volume of the reservoir using the discrete depth temperature data on each sampling day. The thermocline depth was identified by analyzing temperature profiles and identifying the depth that exhibited the maximum rate of change in temperature for each day, following Wetzel (1975). The region of the reservoir below the thermocline depth was identified as the hypolimnion.

We determined hypolimnetic oxygen mass following Gantzer et al. (2009b). As described above, dissolved oxygen profiles were collected at seven sites along the length of the reservoir with a CTD profiler (Figure 1.1). We first partitioned the surface area and corresponding volume of the reservoir into seven sections centered around each sampling site. Second, we used the CTD profiles from each sampling site to create a dataset of the DO concentration in 0.1 m thick layers in each reservoir section on every sampling day. Third, we multiplied the oxygen concentration in each 0.1 m layer by the respective volume for that layer to calculate the hypolimnetic oxygen mass. Summing the hypolimnetic layers for each section yielded the total hypolimnetic oxygen mass for that section, and summing all the hypolimnetic sections yielded the oxygen mass for the total hypolimnion. Finally, the summed total hypolimnion oxygen mass was divided by the total hypolimnetic volume to calculate the volume-weighted hypolimnetic oxygen concentration for the reservoir on each sampling day.

We calculated hypolimnetic oxygen addition and depletion rates using the regression protocol of Lorenzen and Fast (1977), following the methods outlined by Gantzer et al. (2009b). Because hypolimnetic volume was observed to fluctuate between sampling days due to thermocline movement, HOD was calculated both on a mass basis (HOD_{mass}) corrected for volume fluctuations and on a concentration basis (HOD_{conc}) using the volume-weighted

hypolimnetic oxygen concentration multiplied by the mean volume for the sampling time period. Both methods yielded similar estimates, within 1%, and thus we report the average of the two calculated HOD estimates here.

Hypolimnetic oxygen system description and operation

The SSS system was designed and deployed in FCR in September 2012 under the direction of Gantzer Water Resources Engineering, LLC. (Kirkland, WA) and Mobley Engineering, Inc. (Norris, TN).

SSS system components

SSS overview: The SSS system installed at FCR consisted of six main components: a submersible pump, inlet piping, oxygen source, oxygen contact chamber, outlet piping, and distribution header (Figure 1.2). SSS operation can be summarized as follows. First, hypolimnetic water from a depth of 8.5 meters was drawn by a submersible pump into the inlet piping, which transported the water into the oxygen contact chamber. In the oxygen contact chamber, oxygen gas from the oxygen source was injected into the water, resulting in oxygenated water that was super-saturated relative to the oxygen concentrations in the hypolimnion. The oxygenated water exited the oxygen contact chamber through the outlet piping to the distribution header, which was positioned at the same depth as the submersible piping (8.5 m). The distribution header was where the oxygenated water was injected back into the hypolimnion and was located at the end of the outlet piping. Details for each of the six components are given below.

Submersible pump: Water was withdrawn from the hypolimnion into the inlet piping at a depth of 8.5 m by a Franklin Electric FPS 4400 (10.2 cm) high-capacity submersible pump (Franklin Electric, Fort Wayne, IN) with a corrosion-resistant motor and a delivery capacity of up to 227 liters per minute (LPM). We chose to use a submersible pump for the SSS because a submersible pump, unlike a conventional surface pump, would not lose suction capacity if the reservoir volume was drawn down during drought conditions. A Varispeed P7 pump controller (Yaskawa America, Inc., Waukegan, IL) was used to control and program pump operation. An INW 98i pressure transducer was installed at the highest point of the inlet piping and connected to the pump controller to enable the pump to be pressure-controlled.

Inlet and outlet piping: The inlet and outlet piping systems were each composed of anchoring attached to a three-pipe configuration of a separate supply pipe (inlet or outlet), a ballast pipe, and a buoyancy pipe connected together. The anchoring system consisted of concrete weights connected to the three-pipe configuration with stainless steel cables, and enabled the pipes to be suspended at a fixed depth in the water column (8.5 m depth, or 0.8 m above the reservoir sediments). Of the three pipes in the three-pipe configuration, only the supply pipe was connected into and out of the oxygen contact chamber for the inlet and outlet piping systems, respectively. The supply and ballast pipes were constructed of two 5.1 cm standard-dimension ratio (SDR)-11 high-density polyethylene (HDPE) pipes, and the buoyancy pipe was constructed from 7.6 cm SDR-21 HDPE pipe.

Traditionally, these piping systems are used for distributing air or oxygen gas to the water column through the supply pipe, and thus the presence of a gas in the supply pipe doubles as ballast. For this system, however, since the mode of oxygen addition was via oxygenated water, an additional pipe filled with gas was needed for ballast. The ballast pipe ensured sufficient

flotation to suspend the three-pipe configuration above the reservoir sediments. The larger buoyancy pipe was designed to be able to bring the entire system to the surface, anchors included, for maintenance and was controlled by the volume of water in the pipe. When the water in the buoyancy pipe was ejected, the piping system would rise to the reservoir's surface; it would then be filled with water to sink the system back to the 8.5 m depth in the hypolimnion.

Oxygen source: The oxygen source for the SSS system was a Centrox (AirSep, Buffalo, NY) pressure swing adsorption (PSA) unit. The PSA was capable of delivering enriched oxygen gas (93% nominal purity) up to 15 LPM. The Centrox unit was microprocessor controlled and fed a 227 L volume receiving tank, which was connected to the oxygen contact chamber through a MCP-100SLPM-D-I-485 mass controller (Alicat Scientific, Tucson, AZ).

Oxygen contact chamber: The oxygen contact chamber was constructed from HDPE piping increasing in diameter from 5.1 cm at the top to 30.5 cm at the bottom, with an overall length of 2.7 m.

Distribution header: The distribution header was located at the end of the outlet piping and used evenly-spaced 4:1 eductor nozzles (BEX Inc., Ann Arbor, MI) to eject the oxygenated water into the hypolimnion while promoting uniform oxygen distribution. Eductor nozzles were chosen for this application for two reasons: 1) to provide a near-instant dilution of the oxygenated water, which was super-saturated relative to *in situ* conditions, into the hypolimnion; and 2) to promote mixing throughout the hypolimnion via induced flow. For every one liter of pressurized oxygenated water pumped through an eductor nozzle, four liters of non-oxygenated water from the hypolimnion were suctioned into the nozzle, resulting in five liters of volume ejected from the nozzle into the reservoir. Thus, for example, if the pressurized flow from the

submersible pump was 10 LPM, the eductor portion of the nozzle suctioned 40 LPM of water from the hypolimnion into the nozzle, and the flow exiting the nozzle was 50 LPM.

We designed the distribution header to cover the length of the deepest region of the reservoir (see Figure 1.1) and positioned it to promote uniform mixing throughout the hypolimnion. The distribution header was 76.2 m long with 15 evenly-spaced eductor nozzles installed at 4.5 m intervals on alternate sides of the pipe at 8.5 m depth. The nozzles were oriented at a 10 degree angle above horizontal to minimize re-suspension of sediment. The eductor nozzles were sized to maintain adequate back pressure for optimal oxygen transfer in the contact chamber, while at the same time reducing the exit velocity to avoid sediment re-suspension and thermocline mixing in the hypolimnion.

Ideally, it would be useful to compare the system design and components used in this FCR SSS system with the other side stream systems deployed previously (Table 1). However, we found from our literature review that the engineering designs of those systems were not published or publically available, or they were lacking sufficient detail to conduct a full comparison.

SSS operational design

The SSS design was based on historical oxygen demand, determined from regression analysis of the volume-weighted HOD during 2008, using the same methods that were applied in 2013 and described above. During the 2008 sampling campaign, we collected DO profiles bi-weekly at the reservoir's deepest site in June and July and observed that the hypolimnion became anoxic on 28 July. We applied a safety factor of five to the background HOD to account for induced demand from SSS operation (Gantzer et al. 2009b) and make-up capacity. Make-up

capacity provides an oxygenation system with the ability to recover DO content following an unexpected period of shut down. From the 2008 sampling, we determined that the resulting required oxygen input capacity for summer conditions in FCR was 25 kg/d.

Following the oxygen input requirement determination, we calculated the pumping capacity, minimum velocities for dispersed bubble flow, and system operating pressures needed for successful oxygen transfer into the side stream water flow. We modeled the oxygen contact chamber and corresponding distribution piping with CSFSIM (Compressible Steady Flow SIMulation). CSFSIM modeling was used to determine the duration of time water spent in the distribution pipe, head losses, water velocities, and contact time in the oxygen contact chamber. Henry's law was used to determine the theoretical oxygen concentration for different water flow rates, pressures, and maximum summer temperatures, which follows similar estimates by Ashley (1985) and Ashley et al. (1987).

SSS system startup and testing

During SSS system testing, the oxygen concentration leaving the distribution header was predicted using observed water and applied gas flow rates, and compared to saturation conditions using Henry's law and pressure and temperature values measured with the pressure transducer installed in the inlet piping. Hamilton Oxyferm FDA ARC (Hamilton Company, Reno, NV) oxygen sensors were positioned on the effluent of the oxygen contact chamber and just prior to the first nozzle to validate oxygen transfer capacity and identify system operational limitations. Differences measured between the two readings provided operational guidelines and indicated the overall oxygen transfer efficiency in the oxygen contact chamber.

We activated the SSS system on 14 May 2013 and operated it continuously for five weeks. The system was deactivated on 20 June 2013 and remained off until it was reactivated on 1 August 2013. After the system was reactivated a second time, it remained on for the duration of the experimental monitoring period.

During both activation periods, the SSS was operated to add oxygen to the hypolimnion at 25 kg/d with a pump flow rate set at 227 LPM. At this pump flow rate, the mean hypolimnetic volume during both activation periods (43.5 ML) was actively circulated through the SSS system every 133 days. However, the active circulation induced in the hypolimnion from pump discharge through the eductor nozzles was estimated to be 1,135 LPM, thus mixing the mean hypolimnetic volume every 26 days.

Results

Dissolved oxygen and thermal structure

At the beginning of our sampling period in early April 2013, DO was uniformly distributed throughout an isothermal water column (Figure 1.3). As thermal stratification intensified in April and early May, volume-weighted hypolimnetic DO concentrations steadily declined at a mean rate of 0.13 mg/L/d (Figure 1.4; we excluded the first three sampling days from this calculation because thermal stratification did not fully develop until 25 April). Prior to SSS activation on 14 May, DO concentrations in the hypolimnion decreased to 5.2 mg/L just above the reservoir sediments.

We observed that SSS activation successfully increased hypolimnetic DO concentrations up to 600 m from the SSS system (Figure 1.5) without warming the bottom waters or destratifying the water column (Figure 1.6). SSS activation on 14 May resulted in a steady

increase in volume-weighted hypolimnetic DO, which linearly increased throughout the operational phase at a mean rate of 0.18 mg/L/d (Figure 1.4). Due to the 4:1 eductor nozzles on the distribution header, SSS operation resulted in a well-mixed hypolimnion, with uniform DO concentrations between the thermocline and the sediments. Oxygen concentrations increased both above and below the distribution header at 8.5 m depth.

Importantly, SSS activation did not decrease thermal stability. On the contrary, Schmidt stability increased throughout the operational phase to its seasonal maximum (48.34 J/m^2) in early July (Figure 1.6). The thermocline was located at a mean depth of 4.7 m throughout this first operational phase and ranged from 4.4 to 5.0 m. A defined metalimnetic oxygen minimum between ~3 and 4 m depth developed and persisted throughout this operational phase, indicating minimal to no mixing between the hypolimnion and epilimnion.

SSS deactivation on 20 June led to an immediate decrease in DO concentrations (Figure 1.3), with the greatest DO depletion occurring near the sediments. During this phase, volume-weighted hypolimnetic DO linearly decreased at a mean rate of 0.18 mg/L/d (Figure 1.4), resulting in hypoxic conditions throughout the hypolimnion by 35 days after SSS deactivation. However, DO concentrations at the sediments decreased much more rapidly than in the bulk hypolimnion. Within two weeks after SSS deactivation, the DO concentration had decreased from 11.7 to 3.9 mg/L just above the reservoir sediments, at a rate of 0.57 mg/L/day. Similarly, hypoxia in the metalimnetic region intensified during this period, from 8.8 to 1.4 mg/L. Immediately prior to SSS re-activation on 1 August, DO concentrations were <0.5 mg/L at the sediments. This period also coincided with 7 large (>1 cm/day) rain events, temporarily causing small fluctuations in Schmidt stability (Figure 1.6).

We re-activated the SSS system on 1 August, which again triggered an immediate increase in DO and restoration of well-mixed conditions in the hypolimnion (Figure 1.3). During the second activation phase, volume-weighted hypolimnetic DO linearly increased at the mean rate of 0.09 mg/L/d (Figure 1.4). The sediment-water interface exhibited a rapid increase in DO from 0.42 to 4.67 mg/L in the 4 days after activation. Similar to the first operational phase, the thermocline was located at a mean depth of 4.9 m (ranging from 4.6 to 5.6 m) during the second operational phase, with no major visible effects of the SSS on Schmidt stability until thermal stratification naturally weakened in mid-September.

Hypolimnetic oxygen demand

We observed an increase in hypolimnetic oxygen demand (HOD) during both SSS operational phases compared to the deactivation phases. The HOD in May prior to system activation was 6.5 kg/d, whereas HOD in the first activation phase was 18.6 kg/d, representing an increase of 186%. Similarly, HOD was 6.9 kg/d and 20.7 kg/d during the second deactivation and activation phases, respectively, representing an increase in HOD of 200% when the SSS was activated. During the first operational phase, the induced oxygen demand (IOD), which represents the relative increase in oxygen consumption due to SSS system operation, was estimated to be 2.86, while the IOD in the second operational phase was 3.01.

Iron, manganese, and phosphorus

Throughout the sampling period, we observed that total and soluble fractions of both Fe and Mn exhibited similar patterns of nutrient release from the sediments (Figure 1.7A-D). Figure 1.7 displays concentrations of nutrients and metals during the sampling period. The data are

interpolated between sampling days, which are denoted by inverted black triangles, and between sampling depths. The observed hypolimnetic Fe and Mn concentrations throughout the sampling period are displayed in Figure 1.8 (A-D) without interpolation.

From the beginning of May until the end of July, the concentrations of both fractions of Fe and Mn were below 1 mg/L. On 1 August, after 7 days of hypoxia at the sediment-water interface during SSS deactivation, we observed a large increase in Fe and Mn at the two deeper sampling depths. At 8 m depth, total and soluble Fe concentrations reached maxima of 11.6 mg/L and 2.2 mg/L, respectively, while total and soluble Mn concentrations reached maxima of 4.7 mg/L and 4.7 mg/L, respectively. As shown in Figure 1.8, when the SSS was activated on 1 August, Fe and Mn decreased rapidly, and the concentrations of Fe and Mn at the three hypolimnetic sampling depths tended to converge within 1 week after reactivation, indicating mixing of the hypolimnion. During the remainder of the sampling period, total Fe concentrations in the hypolimnion remained between 1.5 and 2 mg/L, while total Mn concentrations remained near 1 mg/L in the hypolimnion. Likewise, soluble Fe and Mn concentrations remained lower than 1 mg/L after 1 August.

In contrast to Fe and Mn, we observed more variable patterns in TP and SRP during the sampling period (Figure 1.7E-F). Release of P from the sediments, as indicated by an increase in P concentrations at the bottom of the hypolimnion, was greater overall during SSS deactivation phases than activation phases with peak TP and SRP concentrations of 98.0 μg/L and 9.8 μg/L, respectively, at 8 m depth on 25 July (Figure 1.8E-F). We also observed elevated P concentrations in the epilimnion during the second SSS deactivation phase that coincided with the large rain events (Appendix A). TP in the surface waters reached a maximum of 118.8 μg/L and SRP of 22.2 μg/L at 0.8 m on 11 July, a day after the upstream tributary exhibited the

maximum flow rate observed during the entire sampling period (21.4 m^3/min) due to a large rain storm (10 cm over the preceding 24 hours). Despite this variability in the epilimnion, the total loads of P in the hypolimnion decreased by 50% within 1 week after SSS reactivation, representing a decrease in 1.14 kg of P from the hypolimnion. No increases in any of the measured elements – Fe, Mn, or P – were observed in the hypolimnion during the second oxygenation period.

Discussion

SSS successfully oxygenated the hypolimnion of FCR

Our results indicate that SSS operation was successful in increasing hypolimnetic DO concentrations in FCR, a eutrophic, shallow reservoir. The two major issues that plagued previous side stream deployments – namely, warming of the hypolimnion and altered thermal stratification (Table 1.1) – were not observed during the sampling period. Schmidt stability throughout the activation and deactivation phases reflected a pattern typical of seasonal variability, rather than a response to SSS operation. We observed that stratification continued to strengthen during the first SSS operational period, demonstrating that the SSS system was able to successfully oxygenate the hypolimnion uniformly from the sediments to the thermocline without causing the entire water column to mix. The thermal structure was slightly disturbed in July; however, this disturbance coincided with several large rain events and was likely not related to SSS operation.

Furthermore, the consistent strength of the thermocline was likely why a metalimnetic oxygen minimum developed throughout the summer months in FCR. Beginning in July, algae from the epilimnion began to accumulate in the thermocline and decompose, as evident from the

DO data (Figure 1.3). This detrital buildup resulted in a disproportionate oxygen demand at this depth, resulting in a metalimnetic oxygen minimum and further demonstrating the strength of the thermocline.

As shown in Table 1, three out of the four previously installed side stream systems resulted in premature destratification. In the three systems that failed, the mixing energy introduced into the hypolimnion was presumably too high, resulting in substantial erosion of the thermocline, warming of the hypolimnion, and subsequent mixing of the destabilized water column. In contrast, the SSS system in FCR added the required amount of oxygen in a relatively low volume of water. One of the advantages of SSS over other hypolimnetic oxygenation systems is that the DO can be raised to higher levels by increasing the pressure in the oxygen contact chamber; i.e., a large amount of oxygen can be added in a small amount of water. Although the DO in the water being delivered to the hypolimnion may be supersaturated at its discharge depth, the discharge jets rapidly dilute the DO, preventing the formation of gas bubbles that are large enough to escape from the hypolimnion. At the same time, energy is needed to spread the oxygenated water throughout the hypolimnion, raising DO to the required concentration. Thus, successful design requires a balance between providing sufficient energy to spread the oxygen, but not so much that thermal stratification in the reservoir is destabilized. As noted above, it would be useful to compare the system design and components used in our SSS system with the other side stream systems deployed previously (Table 1.1). However, we found from our literature review that the engineering designs of those systems were not published or publically available, or they were lacking sufficient detail to conduct a full comparison.

Prior to the activation of the SSS in FCR, the side stream system deployed in Ottoville Quarry was the only known system that had successfully increased hypolimnetic DO

concentrations while preserving thermal stratification. Ottoville Quarry's maximum depth (18 m) was twice as deep as FCR, thus possessing a larger hypolimnetic volume for oxygenation. Unfortunately, Fe, Mn, and P concentrations were not reported for Ottoville Quarry, so it is unknown if that SSS system was able to suppress internal loading. In addition, little information is available on its SSS engineering design or operation. However, it was reported that the oxygen depletion averaged 1.0 mg/L/week and oxygen addition averaged 0.9 mg/L/week in Ottoville Quarry (Fast et al. 1975), which were coincidentally the same depletion and addition rates observed in FCR. While the system deployed in Ottoville Quarry was based on side stream pumping, not SSS, it provides an important early example of the great potential of side stream hypolimnetic oxygenation in lakes and reservoirs.

Higher induced oxygen demand during oxygenation

Hypolimnetic oxygen demand encompasses all oxygen-consuming processes in the hypolimnion. In FCR, HOD is likely driven primarily by organic matter decomposition (Davis et al. 1987, Gantzer et al. 2009b). During SSS operation, we observed increased HOD, likely due to higher rates of organic matter decomposition at the sediments (biological demand) and increased chemical demand from nutrient and metal release. Higher oxygen demand during oxygenation has been observed in several other water bodies, including Carvins Cove Reservoir and Spring Hollow Reservoir (Gantzer et al. 2009b) and Newman Lake (Moore et al. 1996), and is thought to be able to exceed an induced oxygen demand, or IOD, of 6 (Gantzer et al. 2009b). The increase in IOD of ~3 that we observed in FCR is within the range of previously observed IODs, also referred to as the induced HOD factor, reported from other oxygenation systems in the literature (1.5 to 4.0; Beutel 2003, Gantzer et al. 2009b, Moore et al. 1996, Prepas et al. 1997,

Soltero et al. 1994). Shallow reservoirs such as FCR are expected to experience induced HOD factors at the high end of this range due to the larger fraction of oxygen demand exerted at the sediments compared to the overlying shallow water column (Beutel 2003).

Between the two operational periods, we observed a very small increase in the IOD from 2.86 to 3.01, most likely due to the greater biological and chemical oxygen demand in the hypolimnion during the second operational phase compared to the first operational phase. In the second operational phase, the water column was much warmer, thereby accelerating respiration and decomposition processes, and there was much higher chemical demand: reduced Fe, Mn, and P concentrations were much higher in the hypolimnion than in the first operational phase. Despite the increase in HOD due to SSS operation, the observed ability of the SSS system to linearly raise DO concentrations during both operational phases indicates that the SSS system design appears to be adequate in its capacity to overcome the corresponding increases in oxygen demand in FCR, regardless of the starting hypolimnetic oxygen concentrations.

Although SSS operation increased HOD in this short term experiment, it has been hypothesized that HOD will decrease after several years of oxygenation (Gantzer et al. 2009b). Long-term (several year) monitoring programs should be implemented to determine the behavior of HOD after continuous SSS operation.

SSS suppressed the internal loading of reduced elements

Our data indicate that SSS operation was able to suppress Fe and Mn release from the sediments. After seven days of hypoxia at the sediment-water interface, soluble Fe and Mn release coincided with maximum oxygen depletion prior to SSS reactivation. Upon the re-

activation of the SSS on 1 August, the release of Fe and Mn, and potentially P, decreased from the sediments, indicating that the SSS was able to suppress additional internal loading.

During the entire sampling period, almost all of the total Mn in the hypolimnion was in the soluble form, while most of the total Fe was in the particulate form because Fe oxidizes much more rapidly than Mn (Davison 1993, Balzer 1982, Bryant et al. 2011). Evidence of the different kinetic rates is shown in Figure 1.8 following reactivation of the SSS on 1 August. First, the extreme vertical gradients in the concentrations of both soluble and particulate metals were essentially eliminated before the next sampling event on 7 August, indicating that the hypolimnion was close to completely mixed due to SSS operation. As shown in Figure 1.3, the mixing from the SSS also eliminated the oxygen concentration gradient in the hypolimnion, exposing the soluble Fe and Mn initially present in the anoxic bottom of the hypolimnion to higher oxygen concentrations. Simultaneously, oxygen introduced by the SSS raised the mean oxygen concentration in the hypolimnion. As a result, the soluble Fe concentrations decreased slowly, presumably forming particulate Fe. Indeed, total Fe continued to increase at 8 m depth until 21 August, suggesting an initial accumulation of suspended particulate Fe forming as a result of rapid oxidation in the bottom of the reservoir. After 28 August, total Fe began to decrease in the hypolimnion, suggesting that particulate Fe was removed from the hypolimnion via settling onto the reservoir sediments.

The different behavior of the total and soluble Mn concentrations in the hypolimnion is quite noticeable in Figure 1.8. Although the vast majority of the measured Mn was in the soluble form throughout the entire monitoring period, the vertical hypolimnetic gradient in Mn was again eliminated by the initial mixing following SSS reactivation on 1 August. In contrast to Fe,

however, the soluble Mn concentration remained relatively constant for the remainder of the sampling period.

Adding oxygen to the hypolimnion of a lake or reservoir does not stop the reduction of Fe and Mn. What it does do, when effectively applied, is to push the oxic-anoxic boundary out of the water column and into the sediments (Gantzer et al. 2009a, Bryant et al. 2011). This means that the oxidation process due to oxygenation can begin within the sediments, effectively reducing the accumulation of soluble Fe and Mn in the water column. The fact that Fe oxidizes much more rapidly than Mn (Davison 1993, Balzer 1982, Bryant et al. 2011) means that it is easier to control the accumulation of soluble Fe in the hypolimnion than it is to control the accumulation of soluble Mn. Beginning oxygenation early in the summer prior to the onset of thermal stratification may be an effective strategy to prevent the accumulation of soluble metals in the hypolimnion.

The suppression of Fe and Mn internal loading and accumulation in the water column by hypolimnetic oxygenation was also reported in Carvins Cove Reservoir, a reservoir with a linear bubble-plume diffuser system (Bryant et al. 2011, Gantzer et al. 2009a). However, to the best of our knowledge, there have been no reports of the successful control of Fe and Mn - or P - due to SSS or side stream operation.

It is not clear why there was a 6-week delay in Fe and Mn internal loading during the deactivation period in July, despite prolonged hypoxia at the sediment-water interface. One explanation may be that our deepest nutrient and metal samples were collected 1.3 m above the reservoir sediments, and therefore there was likely nutrient and metal release that we were unable to capture. Another plausible explanation is that there may have been a shift in the sediment microbial community as a result of oxygenation, altering nutrient transformations and

sediment release. As observed in Carvins Cove Reservoir, the delayed response in nutrient release may be explained by microbes adapting to altered fluxes in oxygen concentrations (Bryant et al. 2012).

Our data suggest that SSS operation may have altered P release from FCR sediments, but the evidence was not as conclusive as it was for Fe and Mn. Throughout July, during the second deactivation phase, FCR received high external P loads due to large rain events, which potentially may have contributed P to the hypolimnion. However, the strong thermal structure throughout this period, as demonstrated by the metalimnetic oxygen minimum, likely prevented entrainment of P from epilimnion to hypolimnion: consequently, it is unlikely that these external nutrients entering FCR during the rain events reached the hypolimnion. Furthermore, the much shorter hydraulic residence time of the reservoir during the rain events in mid-July further supports our hypothesis that the external P loads did not contribute to the increased P observed in the hypolimnion. The residence time during these rain events decreased from a mean of 247 days to approximately 10 days, and in turn likely flushed the external loads of P out of the reservoir quickly. The increase in epilimnetic P due to the storm events occurred 14 days before the largest increase in P at the sediments (Figure 1.7E); therefore, with a residence time of 10 days and strong thermocline at that time, those epilimnetic and hypolimnetic P dynamics were likely not linked to one another.

Conclusion

Our data strongly suggest that SSS is a viable option for improving water quality in FCR, a shallow, eutrophic drinking water reservoir. However, longer-term studies are recommended to evaluate the efficacy of SSS operation. Specifically, multiple years of monitoring will be

required to determine if HOD decreases over time, as well as if long-term hypolimnetic oxygenation is able to suppress the internal loading of P. In summary, side stream supersaturation hypolimnetic oxygenation systems may be a favorable management strategy for shallow (<10 m) water bodies.

References

Ashley, K.I., 1985. Hypolimnetic aeration: practical design and application. Water Res. 19(6), 735-740.

Ashley, K.I., Hay, S., Scholten, G.H., 1987. Hypolimnetic aeration: field test of the empirical sizing method. Water Res. 21, 223-227.

AWWA, 1987. Research needs for the treatment of iron and manganese. American Water Works Assn. 79, 119-122.

Balzer, W., 1982. On the distribution of iron and manganese at the sediment/water interface: thermodynamic versus kinetic control. Geochim. Cosmo. Acre 46, 1153-1161.

Beutel, M.W., 2003. Hypolimnetic anoxia and sediment oxygen demand in California drinking water reservoirs. Lake Res. Mgmt. 19(3), 208-221.

Beutel, M.W., 2006. Inhibition of ammonia release from anoxic profundal sediments in lakes using hypolimnetic oxygenation. Ecol. Eng. 28(3), 271-279.

Beutel, M.W., Horne, A.J., 1999. A review of the effects of hypolimnetic oxygenation on lake and reservoir water quality. Lake Res. Mgmt. 15(4), 285-297.

Bryant, L.D., Hsu-Kim, H., Gantzer, P.A., Little, J.C., 2011. Solving the problem at the source: Controlling Mn release at the sediment-water interface via hypolimnetic oxygenation. Water Res. 45(19), 6381-6392.

Bryant, L.D., Little, J.C., Burgmann, H., 2012. Response of sediment microbial community structure in a freshwater reservoir to manipulations in oxygen availability. FEMS Microbiol. Ecol. 80(1), 248-263.

Chow, V.T., 1959. Open-Channel Hydraulics, McGraw-Hill Book Company, New York, New York.

CH2M HILL, 2013. Assessment of Technologies for Dissolved Oxygen Improvement in J.C. Boyle Reservoir, CH2M HILL, Portland, Oregon.

Cooke, G.D., Kennedy, R.H., 2001. Managing drinking water supplies. Lake Res. Mgmt. 17(3), 157-174.

Cooke, G.D., Welch, E.B., Peterson, S., Nichols, S.A., 2005. Restoration and Management of Lakes and Reservoirs, 3rd ed., CRC Press, Boca Raton, Florida.

Davis, W.S., Fay, L.A., Herdendorf, C.E., 1987. Overview of USEPA/ Clear Lake Erie sediment oxygen demand investigations during 1979. J. Great Lakes Res. 13(4), 731-737.

Davison, W., 1993. Iron and manganese in lakes. Earth-Sci. Rev. 34, 119-163.

Downing, J.A., Prairie, Y.T., Cole, J.J., et al., 2006. The global abundance and size distribution of lakes, ponds, and impoundments. Limnol. Oceanogr. 51(5), 2388–2397.

Fast, A.W., Lorenzen, M.W., 1976. Synoptic survey of hypolimnetic aeration. J. Env. Eng. Div. 102, 1161-1173.

Fast, A.W., Overholtz, W.J., Tubb, R.A., 1975. Hypolimnetic oxygenation using liquid oxygen. Water Resources Res. 11(2), 294-299.

Fast, A.W., Overholtz, W.J., Tubb, R.A., 1977. Hyperoxygen concentrations in the hypolimnion produced by injection of liquid oxygen. Water Resources Res. 13(2), 474-476.

Gantzer, P.A., 2011. Grand Bay, MS SDOX Oxygen Injection Monitoring, Gantzer Water Resources Engineering, LLC, Kirkland, Washington.

Gantzer, P.A., Bryant, L.D., Little, J.C., 2009a. Controlling soluble iron and manganese in a water-supply reservoir using hypolimnetic oxygenation. Water Res. 43(5), 1285-1294.

Gantzer, P.A., Bryant, L.D., Little, J.C., 2009b. Effect of hypolimnetic oxygenation on oxygen depletion rates in two water-supply reservoirs. Water Res. 43(6), 1700-1710.

Grant, M.G., 1991. Isco Open Channel Flow Measurement Handbook, 3rd ed., Isco, Inc., Lincoln, Nebraska.

Idso, S.B., 1973. On the concept of lake stability. Limnol. Oceanogr. 18(4), 681-683.

Liboriussen, L., Søndergaard, M., Jeppesen, E., et al., 2009. Effects of hypolimnetic oxygenation on water quality: results from five Danish lakes. Hydrobiologia 625(1), 157-172.

Lorenzen, M.W., Fast, A.W., 1977. A Guide to Aeration/ Circulation Techniques For Lake Management, Report EPA-600/3-77-004, U.S. EPA, Corvallis, Oregon.

Matthews, D.A., Effler, S.W., 2006. Assessment of long-term trends in the oxygen resources of a recovering urban lake, Onondaga Lake, New York. Lake Res. Mgmt. 22(1), 19-32.

McGinnis, D.F., Little, J.C., 2002. Predicting diffused-bubble oxygen transfer rate using the discrete-bubble model. Water Res. 36, 4627-4635.

MEA, 2005. Ecosystems and Human Well-Being: Synthesis, Island Press, Washington, D.C.

Moore, B.C., Chen, P.H., Funk, W.H., Yonge, D., 1996. A model for predicting lake sediment oxygen demand following hypolimnetic aeration. Water Resources Bull. 32, 723-731.

Mortimer, C.H., 1941. The exchange of dissolved substances between mud and water in lakes. J. Ecol. 29, 280-329.

Noll, M.R., 2011. Phosphorus cycling in a managed lake ecosystem: Seasonal and longer-term trends. Appl. Geochem. 26, S234-S237.

OWRB, 2012. Lake Thunderbird Water Quality 2011, Oklahoma Water Resources Board, Oklahoma City, Oklahoma.

OWRB, 2013. Lake Thunderbird Water Quality 2012, Oklahoma Water Resources Board, Oklahoma City, Oklahoma.

Read, J.S., Hamilton, D.P., Jones, I.D., Muraoka, K., et al., 2011. Derivation of lake mixing and stratification indices from high-resolution lake buoy data. Env. Model. Software 26(11), 1325-1336.

Scheffer, M., 2004. Ecology of shallow lakes, Kluwer Academic Publishers, Dordrecht, Netherlands.

Schindler, D.W., 1977. Evolution of phosphorus limitation in lakes. Science 195(4275), 260-262.

Schindler, D.W., Hecky, R.E., Findlay, D.L., et al., 2008. Eutrophication of lakes cannot be controlled by reducing nitrogen input: results of a 37-year whole-ecosystem experiment. Proc. Natl. Acad. Sci. USA 105(32), 11254-11258.

Sherman, B., Bryant, L.D., Mobley, M.H., Ford, P., McGinnis, D.F., Singleton, V.L., Schafran, G., Little, J.C., 2012. Review of oxygenation technologies with special reference to application in the Canning River, CSIRO. Report to W. Australia Dept. of Water.

Singleton, V.L., Little, J.C., 2006. Designing hypolimnetic aeration and oxygenation systems - A Review. Env. Sci. Technol. 40(24), 7512-7520.

Smith, V.H., 1982. The nitrogen and phosphorous dependence of algal biomass in lakes - and empirical and theoretical analysis. Limnol. Oceanogr. 27(6), 1101-1112.

Toffolon, M., Ragazzi, M., Righetti, M., Teodoru, C.R., et al., 2013. Effects of artificial hypolimnetic oxygenation in a shallow lake. Part 1: phenomenological description and management. J. Env. Mgmt. 114, 520-529.

Wetzel, R.G., 2001. Limnology: Lake and River Ecosystems, 3rd ed., Academic Press, San Diego, California.

Wu, R.S.S., Zhou, B.S., Randall, D.J., Woo, N.Y.S., Lam, P.K.S., 2003. Aquatic hypoxia is an endocrine disruptor and impairs fish reproduction. Env. Sci. Technol. 37(6), 1137-1141.

Wyman, B., Stevenson, L.H., 1991. Dictionary of Environmental Science, Facts On File, Inc., New York, New York.

Yajima, H., Imberger, J., Dallimore, C., 2009. Evaluation of the intrusion generated by a submerged contact chamber of hypolimnetic oxygenator in a reservoir. Intl. J. River Basin Mgmt. 7(4), 415-422.

Zaccara, S., Canziani, A., Roella, V., Crosa, G., 2007. A northern Italian shallow lake as a case study for eutrophication control. Limnology 8(2), 155-160.

Zaw, M., Chiswell, B., 1999. Iron and manganese dynamics in lake water. Water Res. 33(8), 1900-1910.

Tables

Table 1.1. Overview of known side stream oxygenation systems, listed chronologically by deployment. The dotted line separates systems deployed in lakes and reservoirs (listed first) from river and tidal ecosystems.

Lake Name	Location	Z_{max} (m)	Type of System	Year Deployed	Outcome	Reference
Ottoville Quarry	Ottoville, Ohio, USA	18	Side Stream Pumping	1973	Increased DO and maintained thermal stratification	1,2
Attica Reservoir	Attica, New York, USA	9.4	Side Stream Pumping	1973	Increased DO; premature destratification due to increased turbulence	3,4
Lake Serraia	Trentino, Italy	18	Side Stream Pumping	2006	Increased DO; water column heating and premature destratification	5
Lake Thunderbird	Norman, Oklahoma, USA	17.7	Supersaturated Dissolved Oxygen (SDOX) System	2011	Increased DO; sediment heating, water column mixing, premature destratification, oxic water did not penetrate the entire hypolimnion	6,7
Falling Creek Reservoir	Vinton, Virginia, USA	9.3	Side Stream Supersaturation	2013	Increased DO and maintained thermal stratification	This study
Canning-Swan River	Western Australia, Australia	Typically <1.5, 3-6 m depressions	Side Stream Supersaturation	1997	Increased DO and reduced internal nutrient loading	8
Grand Bay (estuarine reach of Mississippi Tidal River)	Mississippi, USA	6	Portable Side Stream Supersaturation	2011 (4 day test period)	Difficulty maintaining elevated DO due to diel tidal fluctuations	9
J.C. Boyle Reservoir (riverine portion)	Klamath County, Oregon, USA	12.8	Portable Supersaturated Dissolved Oxygen (SDOX) System	2011 (5 day test period)	Increased DO; no other parameters are reported	10

[1]Fast et al. (1975); [2]Fast et al. (1977); [3]Lorenzen and Fast (1977); [4]Fast and Lorenzen (1976); [5]Toffolon et al. (2013); [6]OWRB (2012); [7]OWRB (2013); [8]Sherman et al. (2012); [9]Gantzer (2011); [10]CH2M HILL (HILL (2013).

Figures

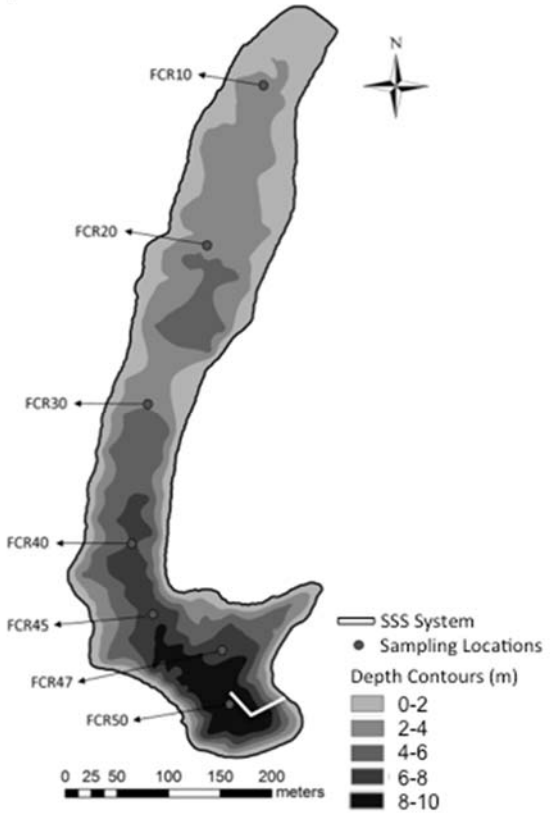

Figure 1.1. Falling Creek Reservoir bathymetry and sample sites, located in Vinton, Virginia, USA. The dots represent sampling locations on a transect from the SSS system to its upstream tributary. The sample locations were labeled based on increasing depths; FCR10 is the shallowest sample location and FCR50 the deepest sample location.

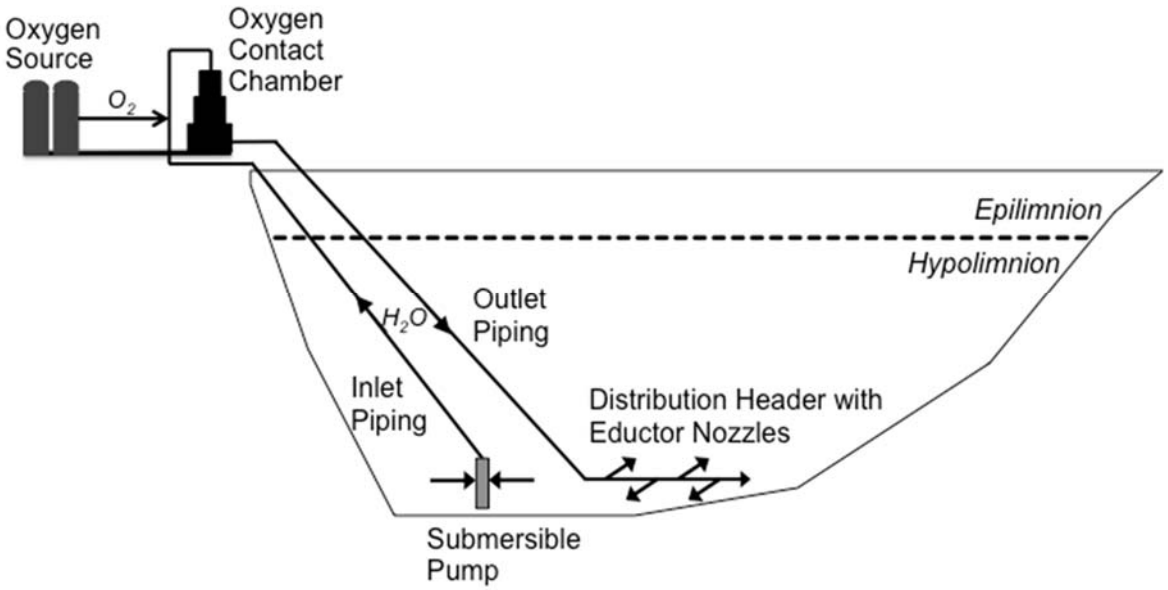

Figure 1.2. A cross-sectional schematic of the SSS system in Falling Creek Reservoir (FCR). The SSS system installed at FCR consisted of six main components: a submersible pump, inlet piping, oxygen source, oxygen contact chamber, outlet piping, and distribution header. As noted in the text, hypolimnetic water from a depth of 8.5 meters was drawn by a submersible pump into the inlet piping, which transported the water into the oxygen contact chamber. In the oxygen contact chamber, oxygen gas from the oxygen source was injected into the water, resulting in oxygenated water that was super-saturated relative to the oxygen concentrations in the hypolimnion. The oxygenated water exited the oxygen contact chamber through the outlet piping to the distribution header, which was positioned at the same depth of the submersible piping (8.5 m). The distribution header was located at the end of the outlet piping and was where the oxygenated water was injected back into the hypolimnion.

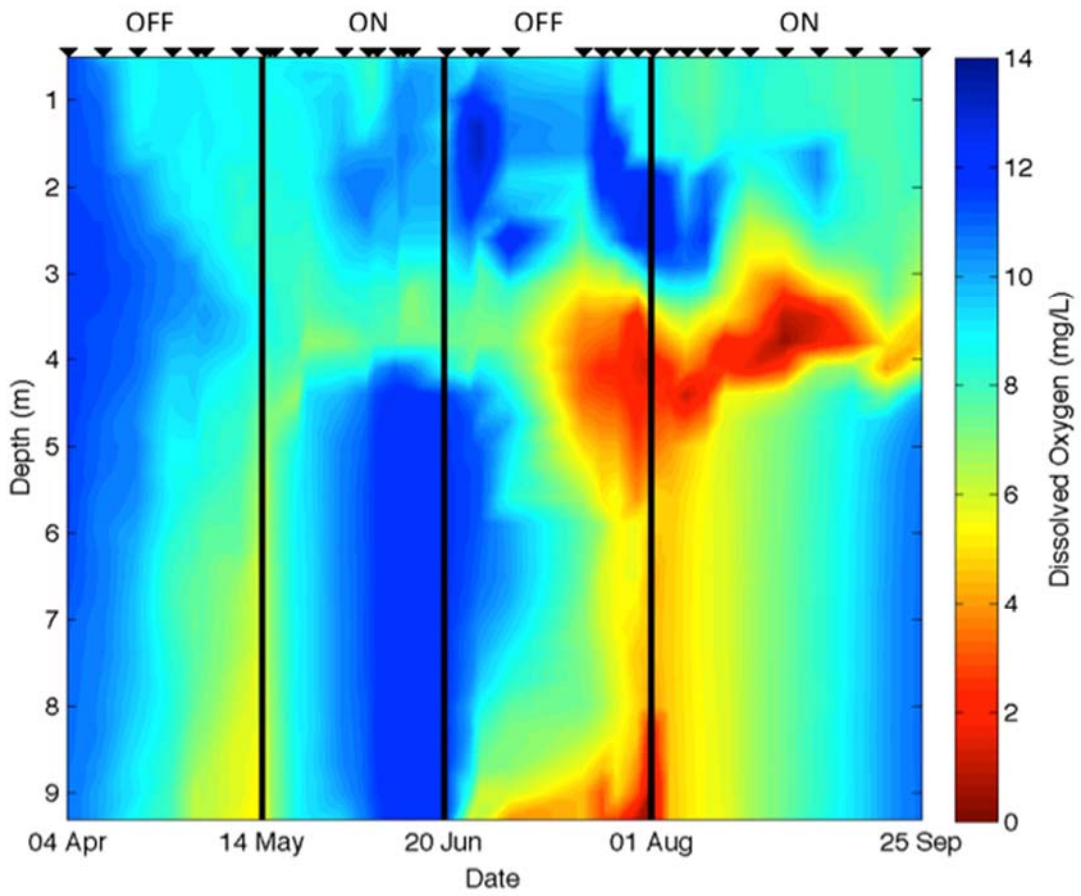

Figure 1.3. Dissolved oxygen concentrations from the deep hole of the reservoir from 4 April to 25 September 2013. The system was deactivated until 15 May (denoted by the "OFF"), activated until 20 June (denoted by the "ON"), deactivated again until 1 August (denoted by the "OFF"), and finally reactivated for the remainder of the sampling period (denoted by the "ON"). All sample days are denoted by inverted black triangles; data were interpolated between sample days for the figure. The distribution header was located at 8.5 m depth.

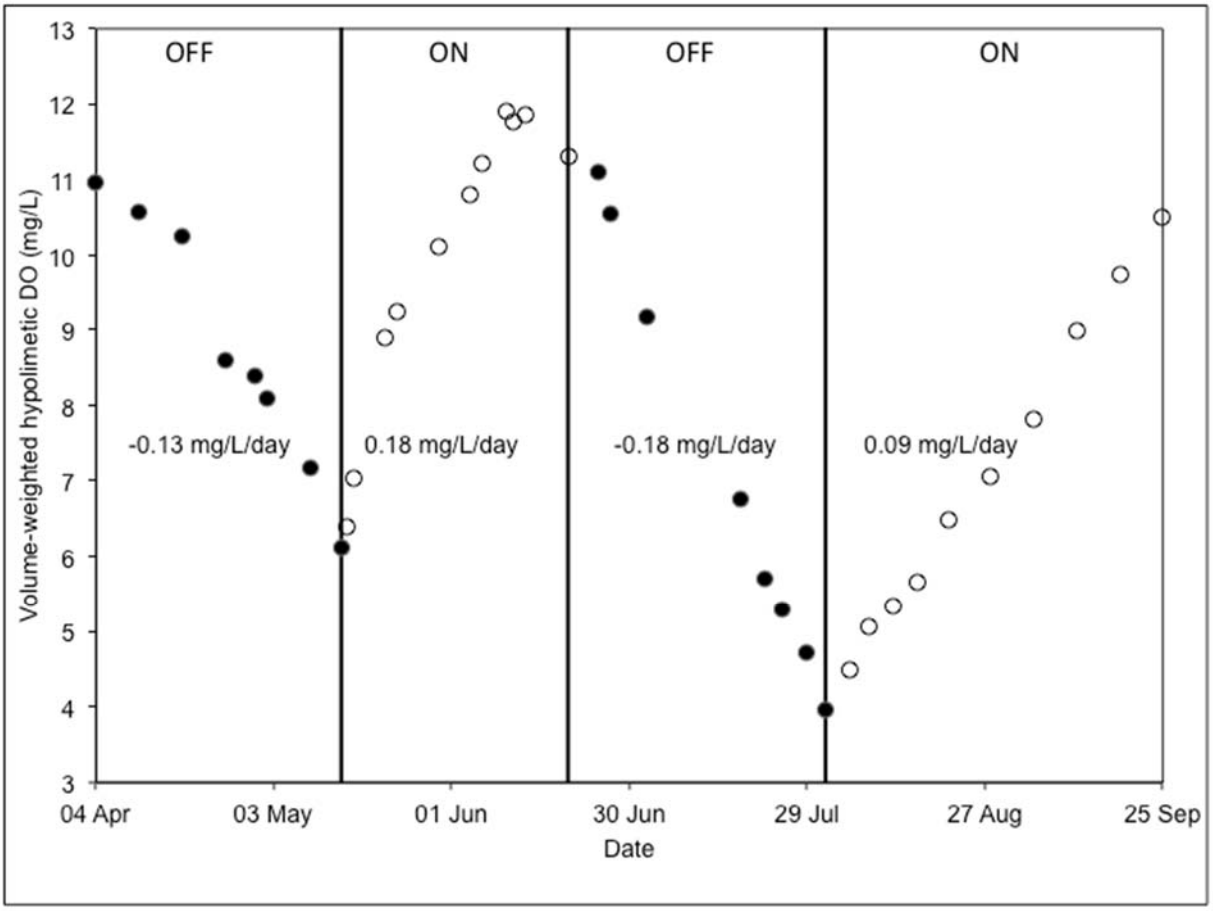

Figure 1.4. Volume-weighted hypolimnetic dissolved oxygen addition and depletion rates in mg/L/day from 4 April to 25 September 2013. The black dots represent when the SSS was deactivated (denoted by the "OFF"), and the white dots represent when the SSS was activated (denoted by the "ON"). The mean depletion and addition rate for each period are embedded in the figure; the first three sampling days were excluded from the first depletion rate calculation because thermal stratification did not fully develop until 25 April).

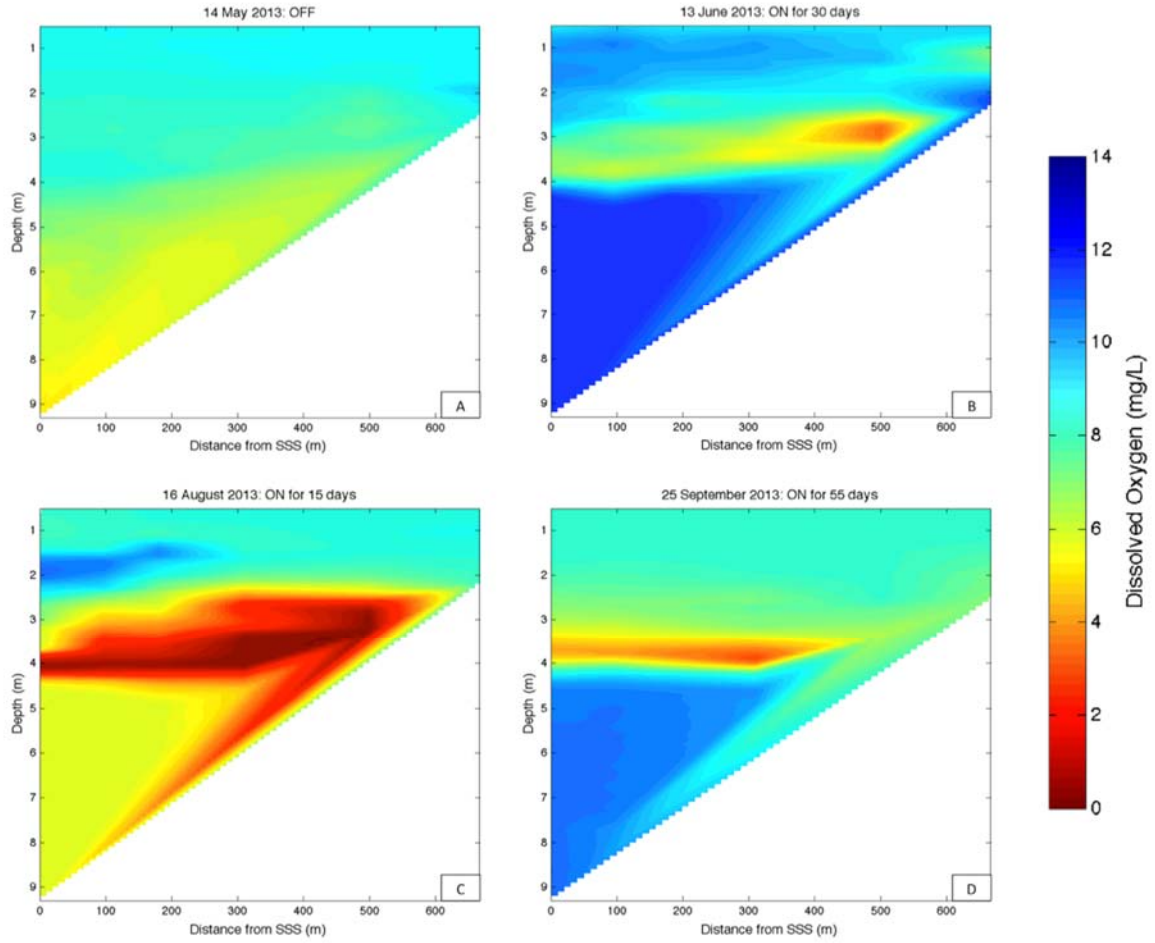

Figure 1.5. Dissolved oxygen concentrations on a transect up the reservoir from the side stream supersaturation (SSS) system to the upstream tributary on four select dates: (A) 14 May 2013, immediately before the SSS was activated for the first time; (B) 13 June, after the SSS was continuously activated for 30 days; (C) 16 August, after the SSS had been deactivated for 42 days and subsequently reactivated for 15 days; and (D) 25 September, after the SSS had been reactivated for 55 days.

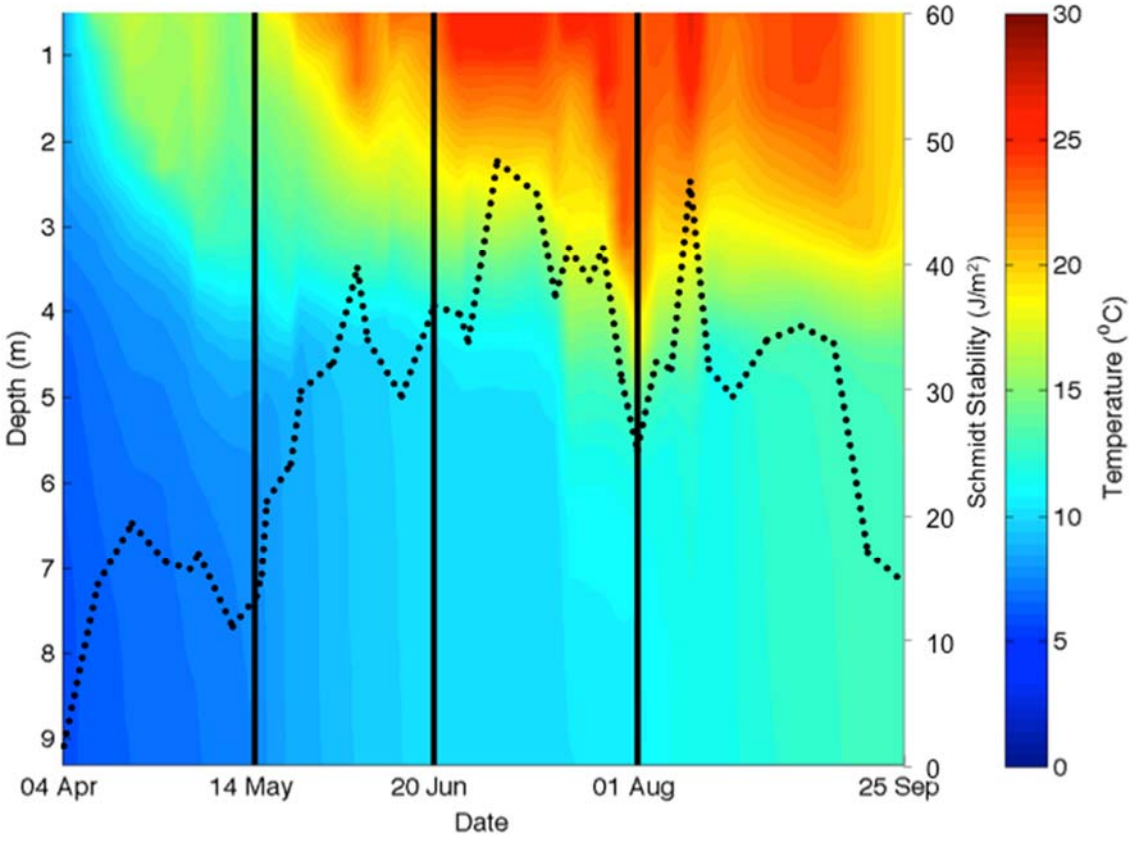

Figure 1.6. Temperature (°C, colored heat map) and Schmidt stability values (J/m^2, dotted line) measured at the deep hole of the reservoir from 4 April to 25 September 2013. The system was deactivated until 15 May (denoted by the "OFF"), activated until 20 June (denoted by the "ON"), deactivated again until 1 August (denoted by the "OFF"), and finally reactivated for the remainder of the sampling period (denoted by the "ON"). The sampling days used to generate the figure were the same as used in Figure 1.1.

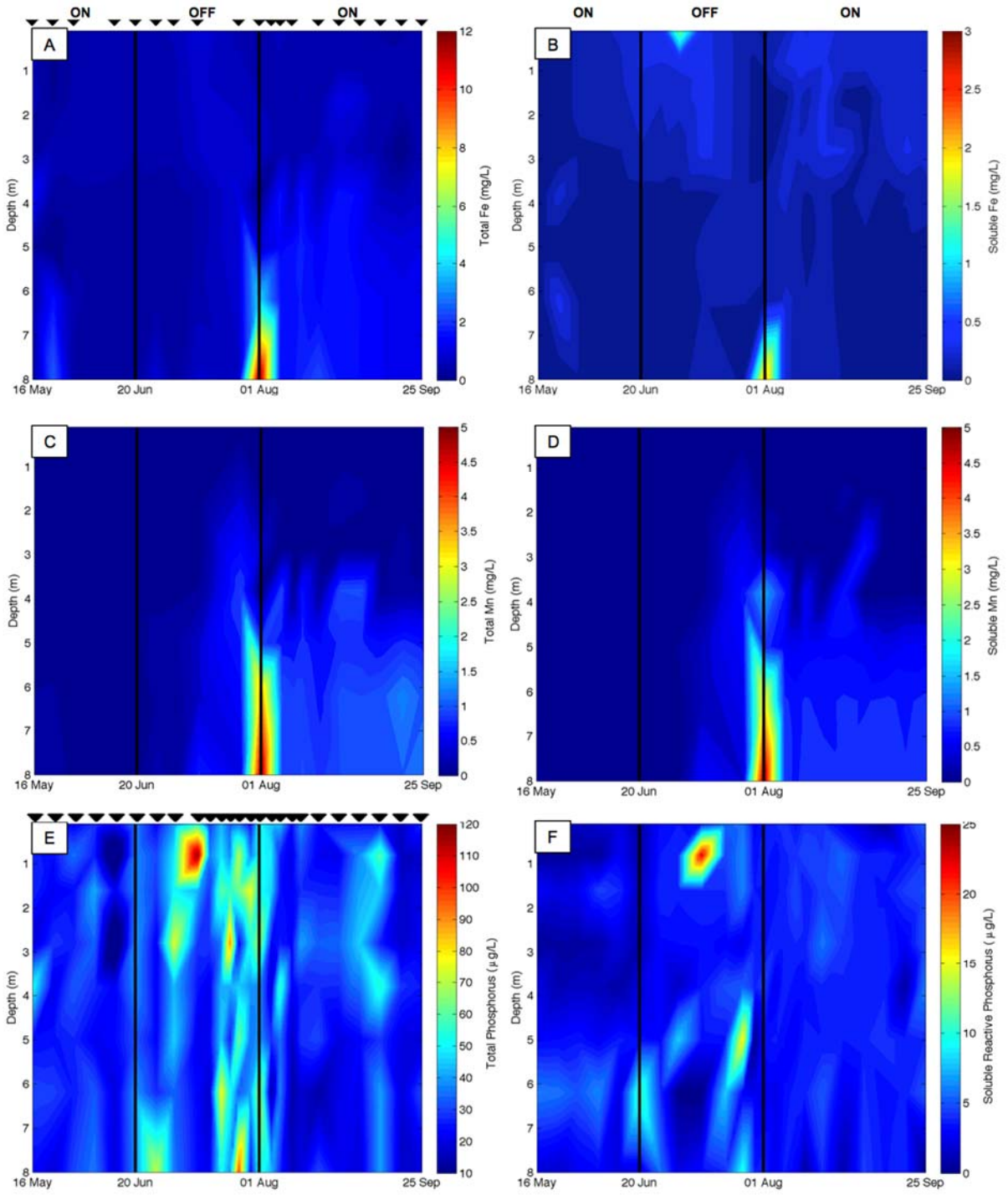

Figure 1.7. The total and soluble fractions of iron (A, B), manganese (C, D), and phosphorus (E, F), respectively. Iron and manganese concentrations are given in mg/L, phosphorus concentrations are given in µg/L. All measurements were sampled at the deepest site of the reservoir from 16 May to 25 September 2013. All sample days are denoted by inverted black

triangles; data were interpolated between sample days for the figures. The total and soluble fractions of iron and manganese (panels A-D) had the same sample days, while the total and soluble reactive phosphorus had the same sample days (panels E,F). The system was activated until 20 June (denoted by the "ON"), deactivated again until 1 August (denoted by the "OFF"), and finally reactivated for the remainder of the sampling period (denoted by the "ON").

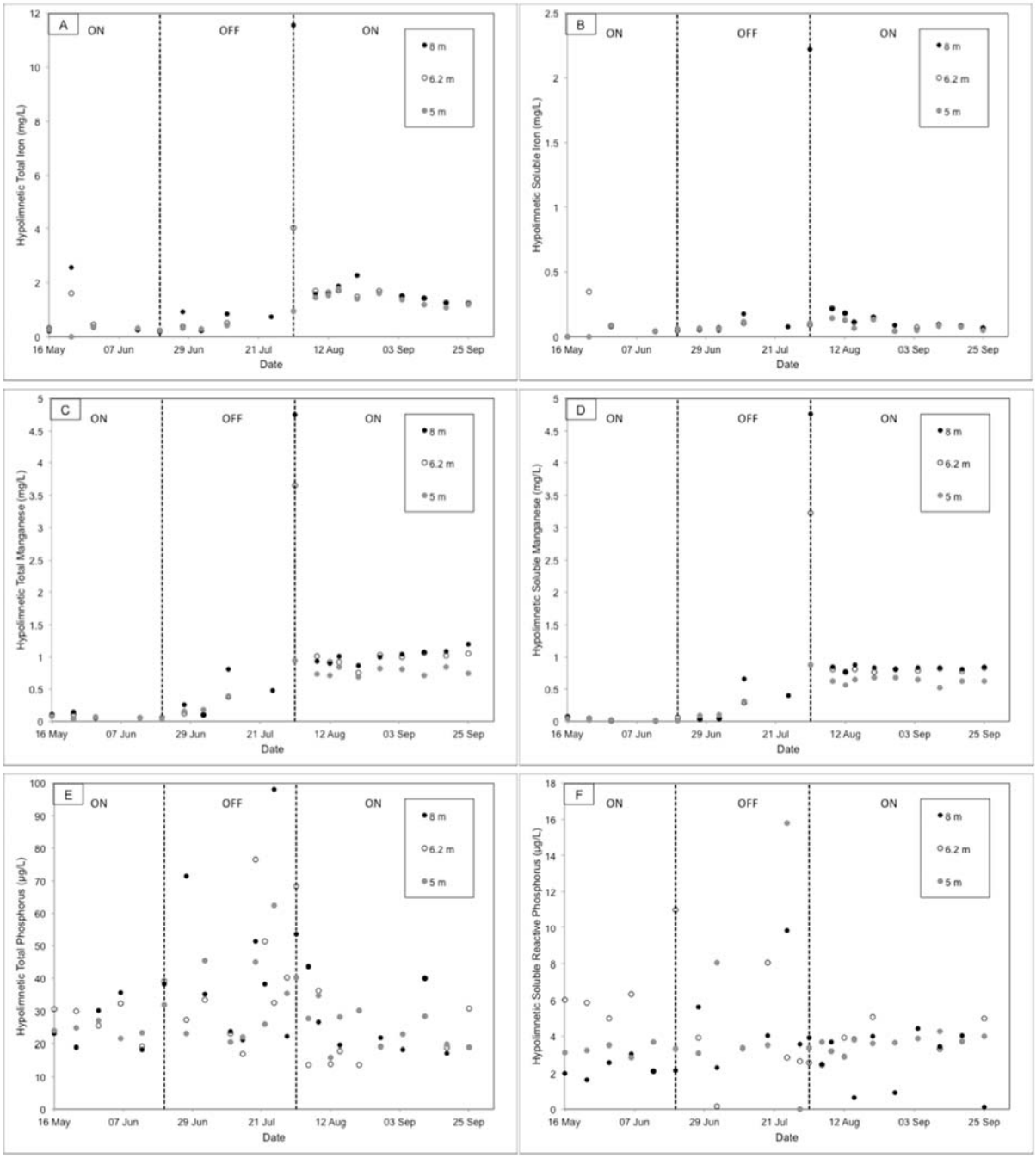

Figure 1.8. The total and soluble fractions of hypolimnetic iron (A, B), manganese (C, D), and phosphorus (E, F), respectively, measured at 5 m, 6.2 m, and 8 m depths in the hypolimnion. Iron and manganese concentrations are given in mg/L, phosphorus concentrations are given in µg/L. All measurements were collected at the deepest site of the reservoir from 16 May to 25 September 2013. The system was activated until 20 June (denoted by the "ON"), deactivated

again until 1 August (denoted by the “OFF”), and finally reactivated for the remainder of the sampling period (denoted by the “ON”).

Chapter 2: Whole-Ecosystem Manipulations of Internal and External Loading Reveal the Sensitivity of a Century-Old Reservoir to Hypoxia

Alexandra B. Gerling, Zackary W. Munger, Jonathan, P. Doubek, Kathleen D. Hamre, Paul A. Gantzer, John C. Little, Cayelan C. Carey

Abstract

Climate change is predicted to have widespread impacts on freshwater lake and reservoir nutrient budgets by altering both hypolimnetic hypoxia and runoff, which will in turn alter the magnitude of internal and external nutrient loads. To examine the effects of these potential climate scenarios on nitrogen (N) and phosphorus (P) budgets, we manipulated hypolimnetic hypoxia and external loads to Falling Creek Reservoir (FCR), an old, eutrophic reservoir in a reforested catchment with a legacy of historical agricultural land use. We conducted a full factorial whole-ecosystem manipulation of hypolimnetic oxygen conditions and external nutrient loads to FCR to determine the relative importance of internal versus external loads for the reservoir's nutrient budget and if the reservoir was a net nutrient sink or source of N and P to downstream. In addition, we conducted sediment core incubations in the laboratory that provided estimates of the potential release rates of N and P from the reservoir's sediments. Our field observations and sediment core incubations demonstrated that the internal N and P loads during hypoxic conditions largely controlled the hypolimnetic mass of nutrients in FCR, regardless of changes in external loads, presumably as a result of the accumulated nutrients in its sediment from historical agriculture practices. Our study is notable in the length of time (>80 years since catchment reforestation) that a reservoir with a short residence time (<1 year) is still exhibiting

high internal loading rates during hypoxia. During our two-year monitoring period, FCR commonly functioned as net sink of N and P (especially nitrate-nitrite (NO_3^- – NO_2^-) and soluble reactive P (SRP)) across the treatments, except during hypoxic conditions, when the reservoir was a net source of ammonium (NH_4^+) to downstream. Throughout the experiment, we observed extremely high NO_3^- – NO_2^- retention rates, indicating that the reservoir removed on average >70% of NO_3^- – NO_2^- inputs through denitrification. Our study highlights the importance of understanding how multiple aspects of global change, waterbody and catchment characteristics, and land use history will interact to alter nutrient budgets in the face of global change.

Introduction

Climate change is predicted to have many diverse effects on freshwater lake and reservoir water quality and ecosystem functioning worldwide (e.g., Adrian et al. 2009, Delpla et al. 2009, Paerl and Huisman 2009, Smith and Schindler 2009, Williamson et al. 2009). For example, in many regions, it is expected that warmer air temperatures will increase water temperatures, resulting in stronger thermal stratification and decreased hypolimnetic oxygen concentrations (Sahoo and Schladow 2008, Sahoo et al. 2010, Tranvik et al. 2009, Williamson et al. 2009). Hypolimnetic hypoxia (defined as dissolved oxygen (DO) concentrations <2 mg/L in the bottom stratum of a waterbody; Wyman and Stevenson 1991) alters many biological and chemical processes, including increased loading of nutrients from the sediments into the water column (i.e., internal loading; Boström et al. 1988a, Diaz 2001, Mortimer 1941, Søndergaard et al. 2003), and thus is of much interest to lake and reservoir managers.

In concert with predictions of increased thermal stratification and hypolimnetic hypoxia, many lakes and reservoirs are also predicted to experience increased storm frequency and

intensity (Bindoff et al. 2013, Easterling et al. 2000, Min et al. 2011, Westra et al. 2013). Storms mobilize nutrients and sediments from the catchment and result in increased nutrient runoff into water bodies (i.e., external loading; Beaulac and Reckhow 1982, Park et al. 2010). In comparison to the number of analyses conducted on warming water temperatures (e.g., Adrian et al. 2009, Schneider and Hook 2010, Williamson et al. 2009), there have been fewer published studies that have explored the impacts of increased storm frequency and intensity on nutrient loading to lakes and reservoirs. The studies that have investigated this aspect of climate change found that storms are able to substantially increase external loading of nitrogen (N) and phosphorus (P) to waterbodies (e.g., Jeppesen et al. 2009, Jeppesen et al. 2011). However, it is not clear if those ecosystems serve as nutrient sinks or sources of nutrients exported downstream.

Consequently, through increasing water temperatures and thermal stratification and increasing storm magnitude and frequency, climate change has the potential to initiate an increase in both internal and external nutrient loads, which may have cascading impacts on freshwater ecosystems. These two predicted stressors – increased hypolimnetic hypoxia and increased runoff – will have substantial effects on lake and reservoir nutrient dynamics, especially because waterbodies in many regions will experience both stressors simultaneously (Bindoff et al. 2013, Palmer et al. 2014, Sahoo et al. 2010, Whitehead et al. 2009). However, little is known about the interacting relationship of these two stressors and how they will influence lake and reservoir nutrient budgets.

Determining the relative importance of hypolimnetic hypoxia and increased runoff and how they will interact to alter nutrient budgets is critically important because they may have substantial implications for water quality and nutrient cycling in lakes and reservoirs. N and P are considered the two most important limiting nutrients for primary productivity (Conley et al.

2009, Schindler 1974, 1977, Schindler et al. 2008, Smith 2003) and increased internal and external loads of the two nutrients can promote the formation of phytoplankton blooms and potentially an increase in trophic state (Carpenter 2005, Nürnberg 1991). Here, we focus on the dissolved forms of both N and P (ammonium (NH_4^+), nitrate-nitrite ($NO_3^- - NO_2^-$), and soluble reactive phosphorus (SRP)), because the dissolved species of the two nutrients are most readily available for uptake by phytoplankton and microbes (Berman 1997, Boström et al. 1988b, Schindler 1977, Schindler et al. 2008). If the main stock of nutrients in the reservoir was contributed from internal sources, then the reservoir may function as a nutrient source to downstream during hypoxic conditions as a result of accumulating sediments and nutrients from external sources over time.

Examining these interactions in freshwater reservoirs is especially important because of the ubiquity of reservoirs and the critical role they play in nutrient cycles. Reservoirs are abundant worldwide and are continually being built for water supply, hydropower, irrigation, and recreation (Downing et al. 2006a, Rosenberg et al. 2000, Smith et al. 2002). Over 10,000 km^3 of water has been impounded into reservoirs since the 1950s globally (Chao 1995, Rosenberg et al. 2000), with >2 million small, artificial waterbodies currently present across the United States (Smith et al. 2002). Recent studies have indicated that reservoirs retain a substantial amount of N and P globally (Brown et al. 2011, Harrison et al. 2009, Wollheim et al. 2008) and consequently may have considerable impacts on biogeochemical cycles (Cole et al. 2007, David et al. 2006, Harrison et al. 2009, Knoll et al. 2014, Renwick et al. 2005). Reservoirs generally function as N and P sinks and reduce nutrient export to downstream ecosystems (Nowlin et al. 2005, Powers et al. 2015, Teodoru and Wehrli 2005); though, the efficiency of reservoir nutrient retention is

predicted to decrease as external nutrient loads increase (Kõiv et al. 2011, Powers et al. 2015, Shostell and Bukaveckas 2004).

The hypolimnetic oxygen concentration of a reservoir is a key determinant of its nutrient budget because of the different biogeochemical processes that alter dissolved N and P cycles under hypoxic versus oxic conditions at the sediments, where the biggest stock of N and P in a reservoir is located. For example, NH_4^+ accumulates in the sediment pore water from the decomposition of organic matter via the process of ammonification (Canfield et al. 2010, Mengis et al. 1997, Seitzinger 1988, Stumm and Morgan 1996). Under hypoxic conditions in the hypolimnion, this NH_4^+ is released from the sediments while NO_3^- and NO_2^- are denitrified to dinitrogen (N_2) (Canfield et al. 2010, Knowles 1982, Mengis et al. 1997, Painter 1970, Seitzinger 1988, Stumm and Morgan 1996). Similarly, decreased redox potential at the sediment – water interface during hypoxia promotes the reduction of Fe (III) to Fe (II) in the sediments, leading to the release of phosphate, commonly measured as SRP, into the water column (Boström et al. 1988a, Einsele 1936, Mortimer 1941). In oxic conditions, by comparison, NH_4^+ concentrations are generally low as a result of bacterial nitrification in which the oxidation of NH_4^+ to NO_2^- occurs, followed by the oxidation of NO_2^- to NO_3^- (Canfield et al. 2010, Seitzinger 1988, Stumm and Morgan 1996, Wetzel 2001). Similarly, if the water above the sediments is well-oxygenated, an oxidized microzone is formed at the sediment – water interface which effectively prevents the upward diffusion of phosphate into the water column (Boström et al. 1988a, Einsele 1936, Mortimer 1941).

Finally, the sensitivity of a reservoir to different scenarios of hypoxia and increased runoff may depend on land use in the catchment. While several studies have quantified nutrient budgets in reservoirs located in catchments dominated by current agricultural land use (Downing

et al. 2008, Downing et al. 2006a, Renwick et al. 2005, Smith et al. 2002), less is known about the effects of historical agriculture on N and P dynamics in reforested catchments. Because agriculture can substantially increase sediment and nutrient export from the landscape via runoff (Howarth et al. 1996, Powers et al. 2013, Turner and Rabalais 2003), and reservoirs are able to accumulate a considerable amount of sediments and nutrients over time, historical agriculture may influence the current sensitivity of reservoirs to hypoxia and runoff, even in completely reforested catchments. Dimictic, hypoxic reservoirs may be more vulnerable to the effects of historical agriculture land use as N and P are continually recycled into the hypolimnion every summer and consequently never completely buried in the sediments. Consequently, if the reservoir outflows do not remove water from the hypolimnion, the effects of high external nutrient loading may continue to affect hypolimnetic nutrient budgets for some time into the future.

Here, we conducted whole-ecosystem manipulations of an old, eutrophic reservoir in a reforested catchment to simulate the effects of potential climate scenarios and measure their effects on reservoir N and P budgets. We investigated the relative importance of internal versus external nutrient loads for the reservoir's dissolved N and P budgets using an innovative 2 x 2 experimental design. In this full factorial experiment, we manipulated hypolimnetic oxygen conditions and external nutrient loads by operating a hypolimnetic oxygenation system and controlling the volume of inflow water to the reservoir from an upstream tributary (Figure 2.1). Throughout the four treatments, we calculated if the reservoir was a net nutrient sink or source of nutrients to downstream during our two-year monitoring period. To complement the whole-ecosystem nutrient budgets, we conducted laboratory hypolimnetic sediment core incubations to

measure nutrient release rates. These incubations provided estimates of the potential release rates of dissolved N and P from the reservoir's sediments.

Through our experimental design, we were able to examine the effects of the potential climate change scenarios of increased hypoxia and increased runoff in isolation as well as in concert. We identified the four whole-ecosystem treatments with letters, as shown in Figure 2.1. Treatment A was the reference treatment, with oxic hypolimnetic conditions and low inflow volumes (low internal and low external loads). Treatment B had hypoxic hypolimnetic conditions and low inflow volumes (high internal and low external loads) and Treatment C was its converse, with oxic hypolimnetic conditions and high inflow volumes (low internal and high external loads). Finally, Treatment D had a hypoxic hypolimnion and high inflow volumes (high internal and high external loads). We hypothesized that hypoxic conditions would promote increased internal loading relative to oxic conditions, and that high inflow volumes to the reservoir would result in higher external loads relative to low inflow volumes, with Treatment D having the highest hypolimnetic mass of N and P of any of the treatments (Figure 2.1). In the absence of specific reservoir and catchment characteristics (e.g., catchment land use, size, and trophic state), we would expect relatively similar hypolimnetic masses between the treatments with hypoxic conditions and low external loads (Treatment B; Figure 2.1) and oxic conditions and high external loads (Treatment C; Figure 2.1). However, for a reservoir with historical agricultural land use in the catchment, we expect that the internal loads under hypoxic conditions would provide a more substantial contribution to the hypolimnetic mass than external loads due to the legacy of accumulated nutrients in the reservoir sediments.

Materials and Methods

Study site

We conducted the whole-ecosystem manipulations in Falling Creek Reservoir (FCR), which is located in Vinton, VA, USA (37° 18’ 12’’ N, 79° 50’ 14’’ W) and is managed by the Western Virginia Water Authority (WVWA) to provide drinking water for the residents of Roanoke, VA. This region is predicted to experience rising air and water temperatures, resulting in stronger thermal stratification and decreased hypolimnetic oxygen concentrations as well as increased storm frequency and intensity over the next few decades (Bindoff et al. 2013, Easterling et al. 2000, Min et al. 2011, Palmer et al. 2014, Westra et al. 2013). FCR is eutrophic (median total P concentrations > 20 $\mu g\ L^{-1}$), has a maximum depth of 9.3 m, and has a volume of $3.1 \times 10^5\ m^3$ (Gerling et al. 2014). The reservoir receives water primarily from one upstream tributary that flows from Beaverdam Reservoir (Figure 2.2). FCR was constructed in 1898, when the reservoir’s catchment was dominated by agricultural land use (WVWA, unpublished data). By the end of the 1930s, all of the farmland in FCR’s catchment was abandoned and reforested, resulting in a predominantly forested catchment today (Figure 2.2; WVWA, unpublished data).

To increase oxygen concentrations in FCR’s hypolimnion, the WVWA installed a hypolimnetic oxygenation (HOx) system in 2012 (see Gerling et al. 2014 for further details on the engineering of the HOx system). In brief, the side stream supersaturation HOx system installed at FCR consisted of six main components: a submersible pump, inlet piping, oxygen source, oxygen contact chamber, outlet piping, and distribution header. The HOx system withdrew hypolimnetic water from a depth of 8.5 m by a submersible pump into the inlet piping, which transported the water into the oxygen contact chamber on shore. In the oxygen contact chamber, oxygen gas from the oxygen source was injected into the water, resulting in

oxygenated water that was supersaturated relative to the oxygen concentrations in the hypolimnion. The oxygenated water exited the oxygen contact chamber through the outlet piping to the distribution header, which was also positioned at 8.5 m. The distribution header was located at the end of the outlet piping and was where the oxygenated water was injected back into the hypolimnion at the same depth and temperature through eductor nozzles. Although the distribution header is located at the deepest site of the reservoir near the dam, the HOx system is able to successfully increase the oxygen concentrations in the majority of the hypolimnion, extending 600 m up the reservoir (Gerling et al. 2014).

Whole-ecosystem manipulations of hypolimnetic oxygen and inflow volumes

We manipulated the hypolimnetic oxygen concentrations in the reservoir during our treatments by turning the HOx system sequentially on and off for periods of ~5-6 weeks in 2013 and ~4-5 weeks in 2014. We activated the HOx system in 2013 from 14 May to 20 June and 1 August to 25 September. In 2014, the HOx system was activated for 3 periods, from 6 May to 3 June, 29 June to 22 July, and 18 August to 29 September. During the two activation periods in 2013 and the last activation period in 2014, the HOx system was operated to add oxygen to the hypolimnion at rate of 25 kg d^{-1}; in the first two activation periods in 2014, it was operated to add oxygen at rate of 20 kg d^{-1}. At both oxygen addition rates, the mean hypolimnetic volume (4.4×10^7 L) was circulated through the HOx system every 133 days. However, the active circulation induced in the hypolimnion by HOx operation and release of the oxygenated water through the eductor nozzles circulated the mean hypolimnetic volume every 26 days. Because of this induced HOx mixing in the hypolimnion, our treatments were determined based on HOx

activation (Treatments A and C) or deactivation (Treatments B and D) rather than observed hypolimnetic conditions for consistency across treatments and years.

We manipulated external loading to FCR by controlling the amount of water released from Beaverdam Reservoir into FCR (hereafter, inflow volume; Figure 2.2). In 2013, for Treatments A and B, the inflow pipe from Beaverdam Reservoir into the FCR tributary was closed, so the only water entering FCR through the tributary was runoff from the catchment. On 28 April 2014, we manipulated the volume of water entering FCR by opening the inflow pipe at the upper Beaverdam Reservoir (Figure 2.2). We used the peak amount of inflow that occurred during extremely large precipitation events in July 2013 as the basis for the level of the 2014 inflow volume. The inflow pipe originates in the epilimnion of Beaverdam Reservoir and is underground for ~750 m until it reaches an open stream that flows ~950 m before entering FCR. Opening the inflow pipe resulted in increased volume at a gauged weir on the open stream ~150 m above the FCR within 24 hours. All inflow volumes for this experiment were recorded at the weir. The inflow pipe remained continuously open for the remainder of our monitoring period in 2014 as part of Treatments C and D. Throughout weekly or biweekly sampling in the summer of 2014, we observed that the median ± 1 S.D. epilimnetic NH_4^+, SRP, and nitrate + nitrite (hereafter, $NO_3^- - NO_2^-$) concentrations were 6.4 ± 10 μg L^{-1}, 4.1 ± 24 μg L^{-1}, and 2.8 ± 1.8 μg L^{-1}, respectively; in 2013, Beaverdam Reservoir was not monitored. Both reservoirs have similar geology and water chemistry (Gerling et al. 2014; WVWA, unpublished data).

As a result of the hypolimnetic oxygenation, inflow volume manipulations, and water chemistry analyses across the two years, Treatments A and B were composed of only one period in 2013 while Treatment C had three periods and Treatment D consisted of two periods in 2014.

Field data collection and nutrient analysis

We monitored the physics and chemistry of FCR following the protocols described in Gerling et al. (2014) a minimum of once to three times per week from June to September 2013 and May to September 2014, when the reservoir was completely thermally stratified. We used an SBE 19plus (Seabird Electronics, Bellevue, WA) high-resolution (4 Hz sampling rate) Conductivity, Temperature, and Depth (CTD) profiler to collect water column profiles of temperature and DO at five sites stretching from the reservoir dam to the upstream tributary. The CTD collected measurements at ~0.1 m increments from the water's surface to just above the sediments. From 3 July to 15 August 2013, an YSI (YSI Inc., Yellow Springs, OH) ProODO meter was substituted for the CTD's DO profile measurements. The YSI DO profiles were measured on 0.5 m increments at the same reservoir sites. The CTD and YSI measurements were compared on the same sampling days and produced nearly identical measurements of DO (within 0.1 mg L^{-1}).

We collected water samples to measure dissolved N and P concentrations in the upstream tributary from Beaverdam Reservoir ~150 m before it entered FCR at the gauged weir and throughout the water column at the deepest site of FCR (Figure 2.2). The samples were collected on a depth profile of the eight discharge depths of the reservoir: 0.1, 0.8, 1.6, 2.8, 3.8, 5.0, 6.2, and 8.0 m; 9.0 m was added in 2014. In 2013, the depth profile samples were collected with a 1.2 L Kemmerer bottle (Wildlife Supply Company, Yulee, FL); in 2014, the samples were collected using a 4 L Van Dorn bottle (Wildlife Supply Company). In both years, water samples from each depth were filtered through 0.7 μm Whatman GF/F filters in the field and were poured directly from the Van Dorn bottle into acid-washed (with 1.2 N hydrochloric acid) plastic bottles. We analyzed the samples for NH_4^+, SRP, and $NO_3^- - NO_2^-$ on a Lachat (Lachat Instruments,

Loveland, CO) following the Quik-Chem Method 10-115-10-1-B. During the two years of monitoring, the mean (± 1 S.D.) method detection limits were 3.3 ± 2.2 μg L^{-1}, 2.0 ± 0.8 μg L^{-1}, and 0.9 ± 0.6 μg L^{-1} for NH_4^+, SRP, and $NO_3^- - NO_2^-$, respectively.

We measured the flow from the tributary into FCR through a rectangular weir with a notch width of 1.10 m. Installed in the weir was an INW Aquistar PT2X pressure sensor (INW, Kirkland, WA), which recorded the temperature and water level above the notch every 15 min. We used the water level data to calculate the mean daily flow rate of the stream into the reservoir following Chow (1959) and Grant (1991), as described by Gerling et al. (2014). We calculated the hydraulic residence time of the reservoir using the flow rate of the upstream tributary and assuming the reservoir volume was at full pond, which corresponded well to water level observations during our monitoring periods.

Data analysis

We used the nutrient concentrations measured in the reservoir's deepest site and at the weir to calculate the internal and external contributions of the masses of NH_4^+, SRP, and $NO_3^- - NO_2^-$ in the hypolimnion during our four treatments. We focused on the hypolimnion and not the entire water column because the reservoir was thermally stratified throughout the entirety of our monitoring period and diffusion of NH_4^+, SRP, and $NO_3^- - NO_2^-$ across the thermocline boundary was minimal. During stratified conditions, the volume of water in a hypolimnion is largely isolated and therefore redox reactions and elemental budgets can readily be measured (Matthews et al. 2008, Mattson and Likens 1993). First, by analyzing the CTD temperature profiles, we identified the thermocline depth as the depth that exhibited the maximum rate of change in temperature for each day, following Wetzel (2001). We designated the volume of

water above the thermocline depth as the epilimnion and below the thermocline depth as the hypolimnion. Regardless of the inflow rate, the inflow water from Beaverdam Reservoir was consistently colder than the FCR water, resulting in underflow during both years. Thus, we were able to assume that all inflow water entering FCR went into the bottom of the hypolimnion. In addition, water was only extracted for drinking water from the surface of the reservoir during both years, and thus we assumed that the hypolimnion did not have any other outflows except for entrainment into the epilimnion.

In both years, the thermocline depth during the stratified summer period (June-September in 2013, May-September in 2014) was consistently observed between 3.8 m and 5.0 m. Because our sampling depth profile was determined by the reservoir discharge depths, which did not include any coverage between 3.8 and 5.0 m at the thermocline boundary, we designated depth samples collected at 0.1, 0.8, 1.6, 2.8, and 3.8 m as part of the epilimnion and 5.0, 6.2, and 8.0 m as part of the hypolimnion throughout our monitoring periods. We excluded the 2014 water samples collected from 9.0 m depth in this analysis for consistency between years.

To calculate the external loads from the inflow tributary, we first linearly interpolated the observed nutrient concentrations at the tributary weir between samplings to the daily scale. Next, we multiplied the observed mean flow rate on each day by the daily concentrations for NH_4^+, SRP, and $NO_3^- - NO_2^-$ to calculate the external load entering FCR in kg. We determined the hypolimnetic mass of NH_4^+, SRP, and $NO_3^- - NO_2^-$ by using our three sampling depths (5.0, 6.2, and 8.0 m) to partition the hypolimnetic volume of FCR into corresponding fixed layers encompassing each sampling depth. We linearly interpolated the observed hypolimnetic concentrations between sample days and then multiplied the NH_4^+, SRP, and $NO_3^- - NO_2^-$ concentrations observed at 5.0, 6.2, and 8.0 m by the respective water volume for each layer.

Because the hypolimnetic volume did not substantially change through the stratified period yet water was entering the bottom of the hypolimnion from the inflow tributary, we needed to account for water being transferred from the top of the hypolimnion to the epilimnion. To do this, we determined the proportion of entrainment from the hypolimnetic 5.0 m layer to the epilimnetic 3.8 m layer based on the inflow volume for every day, which entailed three steps. First, we divided the mean daily inflow volume by the 5.0 m layer volume and subtracted it from one to determine the proportion of the 5.0 m layer volume that was entrained into the epilimnion. This ranged during 2013 and 2014 from 0.02 to 0.37 during high inflow volume treatments, with a mean value of 0.18 ± 0.11. Second, we multiplied that proportion by the fixed 5.0 m layer volume for every day, resulting in a smaller 5.0 m layer volume, corrected for epilimnetic entrainment. Third, summing the nutrient masses of the three individual hypolimnetic layers (5.0 m corrected for epilimnetic entrainment, 6.2 m, and 8.0 m) yielded the total hypolimnetic mass for each nutrient. We assumed that groundwater sources of N and P were negligible.

We subtracted the observed external load from the hypolimnetic mass for each day during the monitoring periods and attributed the remainder of nutrient loading to internal sources. Internal loading rates were calculated by dividing the nutrient masses contributed by internal sources by the surface area of the hypolimnetic sediments and time in days.

To determine if FCR was a net nutrient sink or source of nutrients to downstream during each of the treatments, we calculated the net fluxes of NH_4^+, SRP, and $NO_3^- – NO_2^-$. The nutrient inputs to FCR were defined as the external loads, as described above. To determine the nutrient outputs, we assumed that the inflow volume was equivalent to the outflow volume downstream, which left FCR at 0.1 m depth. Similar to the external loads, we first linearly interpolated the observed nutrient concentrations at the surface (0.1 m depth) between samplings to the daily

scale. Next, we multiplied the observed mean inflow rate each day by the daily concentrations for NH_4^+, SRP, and $NO_3^- – NO_2^-$ to calculate the output of nutrients leaving FCR in kg. Finally, following Powers et al. (2015), we estimated the net reservoir fluxes of NH_4^+, SRP, and $NO_3^- – NO_2^-$ as a percentage of the inputs using the equation:

$$[F_{net} = 100 \times (Outputs - Inputs)/Inputs] \quad \text{(eqn. 1)}$$

where F_{net} is defined as the net flux of nutrients. Negative values indicated that the reservoir exhibited net nutrient retention as a nutrient sink, and positive values represented net nutrient export or a source to downstream.

Because we did not have a reference reservoir as part of our experimental design, the four treatments occurred sequentially, potentially confounding the comparison of nutrient budgets among treatments when the reservoir did not fully flush all water between treatment periods. Given this limitation, we standardized the hypolimnetic mass of each nutrient to compare the treatments by subtracting the last day of the previous treatment's observed hypolimnetic mass, weighted by the residence time of the reservoir, from every day of the subsequent treatment. Thus, we were able to account for any remaining nutrients in the hypolimnion that accumulated during the previous treatment, as those nutrients were flushed from the reservoir over time. This standardization allowed us to equally compare nutrient dynamics among the treatments over the two monitoring years.

Sediment Cores

Sediment cores were collected from FCR under hypoxic hypolimnetic conditions in 2014 to measure loading rates of dissolved N and P from the reservoir's sediments. Nine sediment cores were collected on 23 June 2014 (DO at the sediments at site of collection = 1.6 mg L^{-1})

using a K – B gravity sediment corer (Wildlife Supply Company). Each core had approximately 20 cm of sediment and 500 mL of overlaying water. We gently wrapped the tubes containing the sediment cores in aluminum foil to keep them dark after collection and immediately brought them back to the laboratory. Hypolimnetic reservoir water was used to replace any water lost in transportation (<50 mL).

Once in the laboratory, the sediment cores were incubated in parallel under oxic and hypoxic conditions. The cores were randomly assigned into treatments, resulting in five oxic cores and four hypoxic cores for the experiment. The cores were incubated in the dark at ambient room temperatures ranging from 20 – 24°C, with lids tightly sealing the top of the core tubes. Oxic conditions in the core water were maintained by bubbling with air at a rate of 19.3 standard cm^3 $minute^{-1}$. The bubbling occurred just above the sediment – water interface to prevent mixing of the sediments. In the non-aerated treatment, DO depletion occurred naturally over time in the water overlying the sediment cores and the cores achieved hypoxic conditions after one week. We monitored DO and temperature in the cores every three days after the incubation began by inserting an YSI ProODO dissolved oxygen probe as close to the sediment as possible without disturbing the sediment – water interface. After the probe was removed, we used tubing and a plastic syringe to withdraw 30 mL of water from as close to the sediments as possible to measure NH_4^+, SRP, and NO_3^- – NO_2^-. The water was passed through GF/F filters and analyzed on the Lachat as described above.

We used the nutrient measurements to calculate the internal loading rates from every sediment core. We determined the rates by multiplying the nutrient concentration measured in the overlying water by the volume of water in every core tube after each sample day and divided

by the number of days between sampling and the surface area of the core sediments (18 cm^2), to determine the release rates in the units of mg nutrient m^{-2} day^{-1}.

We used one-way repeated-measures analysis of variance (RM ANOVA) mixed models to determine if the oxygen treatments worked as planned and if there were significant main effects and interactions of our two factors (time and oxygen) on each nutrient. All statistical analyses were conducted in R v.3.1.1 (R CoreTeam 2014). For SRP and NO_3^- – NO_2^- loading rates, we used the lme4 and lmerTest R packages to estimate *p*-values using the Satterthwaite approximation (Chambers 1992, Wilkinson and Rogers 1973). We had to rescale the NH_4^+ loading rates and then we used the pbkrtest R package to estimate *p*-values using the Kenward-Roger approximation.

Results

We successfully manipulated both hypolimnetic oxygen conditions as well as inflow volumes to Falling Creek Reservoir through our series of four treatments (Figure 2.1). Below, we report the dissolved nitrogen and phosphorus budgets calculated for each of the four treatments.

Experimental manipulation of hypolimnetic oxygen concentrations and inflow volumes

In both 2013 and 2014, HOx activation successfully increased hypolimnetic DO concentrations throughout Treatments A and C (Figure 2.3). In both years, oxygenation continually produced a well-mixed hypolimnion, with uniform DO concentrations from the thermocline to the sediments. Regardless of oxygen addition rates, the HOx operation increased DO concentrations in the bulk hypolimnion by approximately 1 mg L^{-1} $week^{-1}$. HOx operation increased DO concentrations laterally in the hypolimnion up to 600 m from the oxygen diffuser

site, resulting in oxygenation of >90% of the total hypolimnetic volume of FCR (data not shown). A distinct metalimnetic oxygen minimum developed at ~3 to 4 m depth in 2013 and ~3 to 5 m depth in 2014, likely due to detritus accumulating as it settles more slowly into the cooler thermocline. This metalimnetic oxygen minimum persisted throughout all treatments, indicating that there was minimal mixing between the hypolimnion and epilimnion.

HOx deactivation to establish Treatments B and D in 2013 and 2014 resulted in an immediate decline in hypolimnetic DO concentrations, decreasing by 1 mg L^{-1} within six hours after oxygenation was terminated (Figure 2.3). During both years, DO concentrations at the sediments decreased much more rapidly than in the upper hypolimnetic water column during the deactivated periods. Excluding the first monitoring periods in spring 2013 and 2014 when thermal stratification was still developing, hypoxic conditions were consistently achieved at the sediments within approximately seven days of HOx deactivation across the years in Treatments B and D. For each of the two hypoxic treatments, the minimum DO concentrations observed in the hypolimnion just above the reservoir sediments were 0.42 mg L^{-1} (Treatment B; 1 August 2013), 0.22 mg L^{-1} (Treatment D; 29 June 2014), and 0.11 mg L^{-1} (Treatment D; 18 August 2014). Depending on the extent of hypoxia in the prior treatment, there were up to three days of hypoxic conditions in Treatments A and C after HOx activation until oxic conditions were achieved.

In 2013, the inflow pipe from Beaverdam Reservoir into the FCR tributary was closed during Treatments A and B, so the only water entering FCR through the tributary was runoff from the catchment. Overall, the mean flow through the weir remained low in 2013 (1.2 ± 0.9 m^3 min^{-1}; 1 S.D.), though there were intermittent high peaks during large storms (Figure 2.4). We observed more large precipitation events in 2013 compared to 2014; a maximum flow rate of

21.4 m^3 min^{-1} on 10 July 2013 was observed immediately after an extremely large precipitation event (10 cm in 24 hours).

As a result of opening the inflow pipe at Beaverdam Reservoir on 28 April 2014, base flow in summer 2014 was approximately four times higher than in 2013. The upstream tributary exhibited a mean flow rate of 4.9 ± 1.4 m^3 min^{-1} throughout the monitoring period of 2014 during Treatments C and D (Figure 2.4). As a result, the mean hydraulic residence time in the reservoir in 2013 during Treatments A and B was 247 ± 118 days and decreased to 67 ± 45 days in 2014 during Treatments C and D.

Treatment A: Oxic hypolimnion + low inflow volumes

Following our hypotheses (Figure 2.1), NH_4^+, SRP, and $NO_3^- - NO_2^-$ standardized hypolimnetic masses exhibited their lowest levels in the two-year monitoring period during Treatment A (Figure 2.5). Most notably, the hypolimnetic masses of NH_4^+ observed daily during Treatment A were considerably lower than observed in the other treatments (Figure 2.5i). During this treatment, NH_4^+, SRP, and $NO_3^- - NO_2^-$ concentrations were consistently low (mean SRP concentrations were <4 μg L^{-1}, mean $NO_3^- - NO_2^-$ concentrations were <8 μg L^{-1}, and mean NH_4^+ concentrations were <70 μg L^{-1}) throughout the water column (Figure 2.6i, iii, v; Figure 2.7i, iii, v).

During Treatment A, internal loading dominated the hypolimnetic masses of NH_4^+, SRP, and $NO_3^- - NO_2^-$ (Figure 2.8i, iii, v). On every day in Treatment A, external loads of NH_4^+ contributed less than 1% of the mass of NH_4^+ present in the hypolimnion; by difference, internal loads contributed >99% of the observed NH_4^+ mass. Similarly, internal sources contributed the majority (54% and 67%) of the hypolimnetic masses of SRP and $NO_3^- - NO_2^-$, respectively. On

all sampling days during Treatment A, the external loading rates were very low: less than 0.09 kg d^{-1} for NH_4^+, SRP, and $NO_3^- - NO_2^-$. FCR consistently functioned as a net nutrient sink during Treatment A, retaining 25% of NH_4^+ inputs, 76% of SRP inputs, and 90% of $NO_3^- - NO_2^-$ inputs (Table 2.1). Finally, the mean internal loading rates of NH_4^+, SRP, and $NO_3^- - NO_2^-$ standardized for the hypolimnetic sediment area were -290 ± 100 mg m^{-2} d^{-1}, 1.1 ± 0.8 mg m^{-2} d^{-1}, and -1.2 ± 8.1 mg m^{-2} d^{-1}, respectively, during Treatment A, indicating that the sediments were a sink of NH_4^+ and $NO_3^- - NO_2^-$.

Treatment B: Hypoxic hypolimnion + low inflow volumes

The hypolimnetic masses of NH_4^+, SRP, and $NO_3^- - NO_2^-$ were consistently larger during Treatment B compared to Treatment A for all three nutrients (Figure 2.5i-iii), following our hypotheses (Figure 2.1) (Figure 2.7i, iii, v). The highest NH_4^+ and SRP concentrations throughout Treatment B were observed just above the reservoir's sediments under hypoxic conditions (920 μg L^{-1} at 8 m on 1 August 2013 and 9.8 μg L^{-1} at 8 m on 25 July 2013, respectively), indicating that internal loading of NH_4^+ and SRP from the sediments occurred (Figure 2.6i, iii). In contrast to NH_4^+ and SRP, the maximum $NO_3^- - NO_2^-$ concentration during Treatment B, 77 μg L^{-1} at 8 m, was observed on 19 July 2013 in oxic conditions (DO at the sediments = 4.5 mg L^{-1}) (Figure 2.6v). The $NO_3^- - NO_2^-$ concentrations decreased as hypoxia intensified in Treatment B, reaching 11 μg L^{-1} on 1 August 2013, when DO at the sediments was 0.42 mg L^{-1} (Figure 2.6v). In comparison to the hypolimnion, the mean epilimnetic NH_4^+, SRP, and $NO_3^- - NO_2^-$ concentrations were all less than 10 μg L^{-1} during Treatment B, despite that SRP concentrations reached a maximum of 22 μg L^{-1} at 0.8 m depth during a storm event (Figures 2.4; 2.6i, iii, v).

Similar to Treatment A, the hypolimnetic masses of NH_4^+, SRP, and $NO_3^- - NO_2^-$ throughout Treatment B were also primarily driven by internal loading (Figure 2.8i, iii, v), though internal loading rates of NH_4^+ were on average 134% higher in Treatment B than A. On all days during Treatment B, external loading contributed 0-5% of the mass of NH_4^+ present in the hypolimnion; by difference, internal sources contributed 95-100% of the NH_4^+ mass. With such high internal loading rates, FCR was a net source for NH_4^+ downstream (exporting up to 300% of inputs, or three times the level of external loads) in this treatment (Table 2.1). SRP and $NO_3^- - NO_2^-$ were also dominated by internal sources, which contributed 70% and 65% of the mass of each nutrient in the hypolimnion, respectively. Unlike NH_4^+, however, FCR functioned as a net sink for $NO_3^- - NO_2^-$ and SRP, retaining ≥68% of both nutrients' external loads (Table 2.1), likely due to $NO_3^- - NO_2^-$ removal via denitrification during hypoxic conditions and because the mean internal loading rate of SRP was not substantially higher in hypoxic Treatment B relative to oxic Treatment A (0.018 ± 0.01 kg d^{-1} in Treatment A vs. 0.019 ± 0.01 kg d^{-1} in Treatment B). Throughout Treatment B, the mean internal loading rates of NH_4^+, SRP, and $NO_3^- - NO_2^-$ standardized for hypolimnetic sediment area were 100 ± 120 mg m^{-2} d^{-1}, 1.2 ± 5.9 mg m^{-2} d^{-1}, and 13 ± 19 mg m^{-2} d^{-1}, respectively, the highest internal loading rates for every nutrient observed across all treatments.

It is important to note that the external loads on some days were slightly larger during Treatment B compared to Treatment A due to a series of storms in July 2013 (Figure 2.4). On 4 July 2013, immediately after the largest storm, maximum external loading rates into FCR were 190%, 188%, and 64% higher for NH_4^+, SRP, and $NO_3^- - NO_2^-$, respectively, than mean base flow conditions during the rest of the treatment. However, the external loads on all other days throughout Treatment B were still much smaller than observed in Treatments C or D.

Treatment C: Oxic hypolimnion + high inflow volumes

Following our predictions for a reforested reservoir with a legacy of agricultural land use in the catchment, the hypolimnetic masses were consistently smaller for Treatment C compared to Treatment B for all three nutrients (Figure 2.5i-iii). Similar to Treatment A, the other treatment with oxic conditions, all three nutrient concentrations remained consistently low (all mean nutrient concentrations were <11 $\mu g\ L^{-1}$) throughout the water column (Figures 2.5ii, iv, vi; 6ii, iv, vi).

Despite much higher inflow volumes into FCR from the upper Beaverdam reservoir and largely oxic hypolimnetic conditions, internal sources still primarily dominated the nutrient budget of NH_4^+ in Treatment C, though the internal NH_4^+ loading rates were much lower than observed in Treatment B. During the three periods that composed Treatment C (7 May to 3 June 2014, 30 June to 22 July 2014, and 19 August to 29 September 2014), internal loading contributed 50%, 73%, and 87%, respectively, of the observed hypolimnetic NH_4^+ masses (Figure 2.8ii). The mean internal loading rates of NH_4^+ in the three Treatment C periods (-0.07 ± 0.06 kg d^{-1}, -0.3 ± 0.01 kg d^{-1}, and -0.5 ± 0.2 kg d^{-1}, respectively), however, were one to three orders of magnitude lower than in Treatment B (1.6 ± 2.0 kg d^{-1}; Figure 2.8: i, ii). For all three periods of Treatment C, FCR was consistently a sink of NH_4^+ and retained ≥58% of NH_4^+ inputs (Table 2.1; observed fluxes were -58 ± 27%, -70 ± 21%, -78 ± 9% for each period, respectively). The mean NH_4^+ internal loading rates for the three periods standardized for hypolimnetic sediment area were -4.5 ± 3.5 mg m^{-2} d^{-1}, -18.7 ± 6.63 mg m^{-2} d^{-1}, and -27.5 ± 13.3 mg m^{-2} d^{-1}, respectively.

In contrast to NH_4^+, the majority of the mass of SRP present in the hypolimnion was contributed by external loading during the three periods of Treatment C $^+$, as a result of increased

inflow volumes (Figure 2.8iv). During the three periods, external loading contributed 70%, 85%, and 52%, respectively, of the hypolimnetic SRP mass. Similar to NH_4^+, the mean internal SRP loads during the three periods of Treatment C (-0.01 ± 0.03 kg d^{-1}) were much smaller than the mean internal SRP loads in Treatment B (0.019 ± 0.01 kg d^{-1}; Figure 2.8iii, iv). FCR was also a sink for SRP during the three periods, retaining a mean of 39 ± 32%, 19 ± 20%, 47 ± 22% of SRP inputs, respectively (Table 2.1). The mean SRP internal loading rates standardized by sediment area varied across the three periods, with the last period indicating that the sediments served as a sink for SRP, at 0.7 ± 0.9 mg m^{-2} d^{-1}, 0.6 ± 0.4 mg m^{-2} d^{-1}, and -1.7 ± 1.8 mg m^{-2} d^{-1}, respectively.

Similar to SRP, external loads of NO_3^- – NO_2^- also dominated the hypolimnetic mass during all three periods of Treatment C, due to much higher inflow rates from Beaverdam Reservoir (Figure 2.8vi). Throughout the three periods of Treatment C, there was little variation in the internal and external loads. In each of the periods, external loading contributed 88%, 84%, and 72%, respectively, of the mass of NO_3^- – NO_2^- present in the hypolimnion. FCR was a substantial sink for NO_3^- – NO_2^- and consistently retained >90% of NO_3^- – NO_2^- inputs across the three treatment periods (Table 2.1; 91 ± 5%, 98 ± 0.4%, and 95 ± 6%, respectively). Finally, the mean internal loading rates standardized for hypolimnetic sediment area were -1.0 ± 0.4 mg m^{-2} d^{-1} from 7 May to 3 June 2014, -3.0 ± 1.1 mg m^{-2} d^{-1} from 30 June to 22 July 2014, and -5.6 ± 3.6 mg m^{-2} d^{-1} from19 August to 29 September 2014.

Treatment D: Hypoxic hypolimnion + high inflow volumes

Treatment D, which experienced both high internal and external nutrient loads, did not exhibit the largest hypolimnetic masses for every nutrient, contrary to our hypotheses (Figure

2.1): Treatment D's hypolimnetic nutrient masses were consistently at the level of, or slightly below, the masses observed in Treatment B (high internal and low external loads). Treatment D was composed of two periods, 4 June to 29 June 2014 and 23 July to 18 August 2014, with the two periods exhibiting very similar nutrient dynamics.

As also observed during the hypoxic conditions in Treatment B, internal NH_4^+ and SRP loads to the hypolimnion were consistently highest when dissolved oxygen concentrations were at their minimum at the sediments (Figure 2.6ii, iv, vi), indicating that the reservoir sediments were the source of internal loads. The highest concentrations of NH_4^+ (830 μg L^{-1}) and SRP (15 μg L^{-1}) in the hypolimnion were observed just above the sediments on the days with the lowest observed oxygen concentrations (0.11 mg L^{-1}) on 18 August 2014 (Figure 2.6ii, iv).

Throughout both periods of Treatment D, the epilimnetic nutrient concentrations remained low relative to the hypolimnion (Figure 2.7ii, iv, vi), with the exception of a peak of 45 μg L^{-1} of SRP at 0.8 m depth on 16 June 2014 (Figure 2.7iv). Similar to Treatment B, the maximum observed NO_3^- – NO_2^- concentration during Treatment D, 74 μg L^{-1} at 9 m, occurred on 9 June 2014 while the DO at the sediments was not yet hypoxic (2.2 mg L^{-1}; Figure 2.6vi). During maximum hypoxia in both Treatment D periods (when DO at the sediments was <0.3 mg L^{-1} on 29 June and 18 August 2014), the NO_3^- – NO_2^- concentrations at 9 m substantially decreased to 1.5 μg L^{-1} and 6.3 μg L^{-1}, respectively (Figure 2.6vi).

During hypoxic hypolimnetic conditions and high inflow volumes in Treatment D, we observed that internal sources largely dominated the nutrient budgets of NH_4^+. On every day in Treatment D, the majority of the NH_4^+ mass was from internal loading, as the external loads of NH_4^+ only contributed 13% and 28% of the mass of NH_4^+ present in the hypolimnion during the two Treatment D periods. The external contribution of SRP was slightly larger than NH_4^+

throughout the two periods of Treatment D, contributing 46% and 69%, respectively, of the mass of SRP present in the hypolimnion. FCR functioned as a nutrient sink during both periods of Treatment D for both NH_4^+ (retaining a mean of 1 ± 71% and 59 ± 40% of inputs, respectively) and SRP (retaining a mean of 54 ± 4% and 48 ± 37% of inputs, respectively). During both periods of Treatment D, the mean internal loading rates of NH_4^+ standardized for sediment area, 22.8 ± 12.9 mg m^{-2} d^{-1}, were considerably smaller than the mean internal loading rates of NH_4^+ in Treatment B, 100 ± 120 mg m^{-2} d^{-1}. However, the mean internal loading rates of SRP in Treatments B and D were very similar, 1.2 ± 5.9 mg m^{-2} d^{-1} and 1.2 ± 3.8 mg m^{-2} d^{-1}, respectively.

In comparison to NH_4^+ and SRP, external loading of NO_3^- – NO_2^- dominated the hypolimnetic mass of the nutrient during the two periods of Treatment D, due to much higher inflow volumes. External sources contributed over 80% of the mass of NO_3^- – NO_2^- present in the hypolimnion during both periods of Treatment D, peaking at 0.41 kg d^{-1} of NO_3^- – NO_2^- on 21 July 2014. The mean NO_3^- – NO_2^- external loads were very similar between the two periods within Treatment D, 0.29 ± 0.06 kg d^{-1} from 4 June to 29 June 2014 and 0.29 ± 0.04 kg d^{-1} from 23 July to 18 August 2014. In the hypoxic conditions of Treatment D, FCR was a major NO_3^- – NO_2^- sink during both periods of Treatment D, removing a mean of 95 ± 2% and 94 ± 1%, respectively, of NO_3^- – NO_2^- inputs (Table 2.1). The mean NO_3^- – NO_2^- internal loading rates standardized for sediment area were also larger during Treatment B compared to all of Treatment D (13.1 ± 19.1 mg m^{-2} d^{-1} and 1.2 ± 2.8 mg m^{-2} d^{-1}, respectively). The high NO_3^- – NO_2^- loading rates in Treatments B and D were largely driven by the oxic conditions at the beginning of the treatments prior to the onset of hypoxia. We did observe decreases in the NO_3^- – NO_2^- loading rates during hypoxic conditions in FCR.

Sediment Cores

The sediment cores were successfully incubated under oxic and hypoxic conditions in the laboratory to estimate potential nutrient loading rates from FCR. As a result of bubbling air in the water overlying the sediment cores in the oxic treatment, DO concentrations >8 mg L^{-1} were established within 24 hours and maintained for the duration of the experiment (Figure 2.9i). The water overlying the sediment cores in the hypoxic treatment exhibited DO concentrations <2 mg L^{-1} within four to seven days (Figure 2.9i), similar to the oxygen depletion rate observed within the hypolimnion of FCR. After the treatments were established, the cores exhibited relatively consistent DO concentrations (Figure 2.9i): the mean DO concentration in the oxic cores was 8.3 ± 0.3 mg L^{-1} (Days 1 – 21) and 1.8 ± 1.5 mg L^{-1} in the hypoxic cores (Days 4-21). DO concentrations in the cores exhibited significant effects of the time × treatment interaction, treatment, and time (RM ANOVA; all $p < 0.001$; see Table 2.2 for all statistical results). The time × treatment interaction in DO was largely driven by the extra days needed for hypoxic conditions to develop relative to the immediate oxic conditions in the oxic treatment.

The hypoxic sediment cores released a substantial mass of NH_4^+ while the oxic sediment cores absorbed NH_4^+ (Figure 2.9ii), as also observed in the hypolimnion of FCR (Figure 2.8i, ii). This effect varied over time, resulting in a significant interaction of time and treatment and significant main effects of treatment and time (all $p < 0.001$; Table 2.2) on NH_4^+ loading rates. After 18 days of incubation, the release of NH_4^+ in the hypoxic sediment cores decreased considerably. The mean NH_4^+ loading rates were an order of magnitude larger in the hypoxic sediment cores (7740 ± 10300 mg m^{-2} d^{-1}) than observed in FCR under hypoxic conditions (101 ± 125 mg m^{-2} d^{-1} in Treatment B and 22.8 ± 12.9 mg m^{-2} d^{-1} in Treatment D).

The peak internal loading of SRP from the hypoxic sediment cores was delayed until Day 18 of the incubation, and the SRP internal loading rates in the oxic sediment cores remained low throughout the entirety of the incubation (Figure 2.9iii). This delay in SRP loading in the hypoxic treatment resulted in a marginally significant interaction of time and treatment ($p = 0.06$), while the effects of time and treatment were not significant (both $p > 0.23$). The mean SRP loading rate observed in the hypoxic sediment cores (330 ± 650 mg m^{-2} d^{-1}) was approximately three orders of magnitude greater than the mean SRP loading rates observed in FCR during maximum hypoxic conditions (1.2 ± 5.9 mg m^{-2} d^{-1} in Treatment B and 1.2 ± 3.8 mg m^{-2} d^{-1} in Treatment D).

The $NO_3^- - NO_2^-$ loading rates observed in the sediment cores and in the hypolimnion of FCR were markedly different. There was an immediate release of $NO_3^- - NO_2^-$ from the sediments to the water column in the oxic cores, followed by absorption of $NO_3^- - NO_2^-$ in the sediments of both oxic and hypoxic cores after 3 days (Figure 2.9iv). The rapid decrease of $NO_3^- - NO_2^-$ coincided with a decrease in dissolved oxygen concentrations in the hypoxic treatment, resulting in a significant interaction of time and treatment ($p = 0.006$). We also observed a significant effect of time ($p < 0.001$) and treatment ($p = 0.003$) on $NO_3^- - NO_2^-$ loading rates. By comparison, under hypoxic treatments in FCR, the mean $NO_3^- - NO_2^-$ loading rates were larger (13.1 ± 19.1 mg m^{-2} d^{-1} in Treatment B and 1.2 ± 2.8 mg m^{-2} d^{-1} in Treatment D), due to the oxic conditions at the beginning of the treatments, than the mean $NO_3^- - NO_2^-$ loading rates in the hypoxic sediment cores (-300 ± 530 mg m^{-2} d^{-1}).

Discussion

We observed that the hypolimnetic nutrient dynamics in Falling Creek Reservoir were strongly affected by our manipulation of hypolimnetic oxygen conditions and inflow volumes to the reservoir. Below, we discuss the observed patterns of nutrient budgets in the reservoir, and the implications for reservoir biogeochemical cycles in the face of global change.

Internal loads dominated Falling Creek Reservoir's nutrient budgets

Our results provide substantial evidence that internal dissolved N and P loads greatly influence the hypolimnetic nutrient dynamics in FCR (Figure 2.8). Internal loads largely controlled the hypolimnetic masses of NH_4^+ and SRP, even when external volumes were experimentally increased by 400% from 2013 to 2014. Furthermore, the reservoir responded quite predictably to the multiple HOx activation and deactivation transitions across the two years: internal loads of NH_4^+ and SRP greatly increased during hypoxic conditions in the hypolimnion in both Treatments B and D. These increases in internal loading during hypoxia were likely due to the diffusion of NH_4^+ from the sediment pore water into the water column and redox-mediated SRP release from the sediments (Beutel 2006, Boström et al. 1988a, Mengis et al. 1997, Mortimer 1941, Painter 1970, Stumm and Morgan 1996).

We observed that Treatment B (hypoxic conditions and low inflow volumes) had the largest hypolimnetic masses for all three nutrients (Figure 2.5). Contrary to our hypotheses (Figure 2.1), the internal loads under hypoxic conditions in Treatment B were substantially larger than the internal loads in Treatment D, resulting in much higher nutrient concentrations in the reservoir during Treatment B than D, regardless of the period within the treatment. Because internal loading during hypoxia dominated FCR's nutrient budget, treatments with similar

hypolimnetic oxygen conditions (i.e., Treatments A and C with oxic hypolimnia versus Treatments B and D with hypoxic hypolimnia) exhibited similar trends of hypolimnetic masses (Figure 2.8).

The hypolimnetic masses of NH_4^+ and SRP were particularly sensitive to hypolimnetic oxygen conditions even during the treatments with higher external loads from Beaverdam Reservoir (Figure 2.8ii, iv). From 2013 to 2014, we calculated that the NH_4^+ and SRP external loading rates would have needed to additionally increase by ~1000% and ~350%, respectively, to have equaled the mass of nutrients contributed by internal loads in Treatment D. The largest release of NH_4^+ and SRP from the sediments occurred during the first period of Treatment D (Figure 2.6ii, iv), Figure 2.8ii, iv), which has also been observed in several other lakes that experience hypolimnetic hypoxia (e.g., Rydin 2000), largely because there are less nutrients remaining in the surface sediment that can be released as the season progresses. During the second Treatment D period of 22 July to 18 August 2014, the external contribution of the hypolimnetic mass of SRP was more prominent (Figure 2.8iv). During all periods of Treatments B and D, we observed more variability in the internal nutrient loads and hypolimnetic masses than in the periods of Treatments A and C (Figure 2.8). This variation may be an effect of the hypolimnetic DO concentrations decreasing throughout the treatments, resulting in more variability in the internal loading rates over time within the treatment periods.

In contrast to NH_4^+ and SRP, $NO_3^- - NO_2^-$ external loading was dominant in Treatments C and D. Consistently, the internal loads of $NO_3^- - NO_2^-$ were minimal throughout our monitoring period of 2014, suggesting accelerated rates of N removal, presumably denitrification, as a result of higher inflow volumes (Figure 2.8vi) (Koop-Jakobsen and Giblin 2010). Furthermore, in both years during maximum hypoxic conditions at the sediments, the

internal loading rates of NO_3^- – NO_2^- decreased considerably (Figure 2.8v,vi). As a result, the reservoir served as a large sink of NO_3^- – NO_2^-, as discussed below.

Our experimental design during the two-year monitoring period presented some limitations. For example, it was difficult to compare the strength of the hypolimnetic oxic and hypoxic conditions among all of the treatments and years. However, the comparison of oxic and hypoxic hypolimnetic conditions within the same year (i.e., Treatments A vs. B in 2013 and Treatments C vs. D in 2014) demonstrated that the hypolimnetic masses were strongly driven by internal loads under hypoxic conditions in the reservoir. Moreover, due to our experimental design, our treatments were autocorrelated and there were effects of interannual variability on the nutrient budgets. For example, there were several large storm events in 2013 compared to 2014, which varied the magnitude of the external loads within Treatment B. Although we did not have a reference system to analyze for comparison, standardization of the hypolimnetic masses allowed us to segregate the effects of nutrient dynamics between treatments. Even without standardization among the treatments, we found that internal loads still dominated the hypolimnetic masses of nutrients in the reservoir.

Falling Creek Reservoir as a net nutrient sink

Nutrient retention or removal in reservoirs are broadly affected by interacting internal and external dynamics, including residence time and loading from the catchment via runoff (Essington and Carpenter 2000, Kõiv et al. 2011, Powers et al. 2015, Seitzinger et al. 2002). During our two-year monitoring period, FCR commonly functioned as net nutrient sink, though there was variation in the magnitude of nutrient losses among treatments (Table 2.1). Nutrients were retained presumably by sedimentation, nutrient burial, and biological uptake, as well as N

removal via denitrification and other N removal processes (Burgin and Hamilton 2007, David et al. 2006, Essington and Carpenter 2000, Molot and Dillon 1993, Schindler et al. 1993, Vanni et al. 2011, Wodka and Effler 1985). The only time FCR served as a net nutrient source to downstream (i.e., positive net flux) was for NH_4^+ during Treatment B, due to very large internal NH_4^+ loads during hypoxic conditions.

The magnitude of net fluxes varied among the three nutrients (Table 2.1). Throughout all four treatments, FCR retained a mean of 38-76% of SRP inputs. SRP retention was lower in Treatments C and D than in A and B, presumably due to their higher external loads and shorter residence time (Table 2.1). By contrast, FCR was a sink for a remarkably large amount of NO_3^- – NO_2^- inputs (a mean of 70-95% across the four treatments), with the highest retention rates observed in Treatments C and D. After increasing the inflow volume from Beaverdam Reservoir in 2014, external NO_3^- – NO_2^- loads entering FCR increased by 240%. It is possible that these higher external loading rates may have accelerated the rate of denitrification in the reservoir during 2014, as also observed by Koop-Jakobsen and Giblin (2010), resulting in a much greater NO_3^- – NO_2^- sink that year. The site of the reservoir where the inflow enters FCR (Figure 2.2) is only ~3.5 m depth, yet still experiences thermal stratification and hypoxia (Gerling et al. 2014). These warm, shallow, littoral sediments with high organic material deposits near the inflow are likely a biogeochemical hotspot for N removal via denitrification (Bruesewitz et al. 2012), with much higher denitrification rates in years with increased loads of NO_3^- – NO_2^-.

In comparison to SRP and NO_3^- – NO_2^-, FCR served as both a sink and source of NH_4^+ downstream, which was largely controlled by the magnitude of internal loading rates. During Treatment B, which experienced the highest internal loads of NH_4^+ during the two-year monitoring period (up to 11 kg d^{-1}), the reservoir exported a mean of 0.05 ± 0.05 kg d^{-1} of NH_4^+

downstream. During all of the other treatments, the amount of dissolved N retention in FCR increased from low inflow volumes in 2013 (Treatments A and B) to high inflow volumes in 2014 (Treatments C and D) (Table 2.1). This again may suggest higher rates of sedimentation, nutrient burial, and biological uptake occurred in the reservoir in 2014 compared to 2013 (David et al. 2006, Koop-Jakobsen and Giblin 2010).

Previous studies (e.g., Harrison et al. 2009, Powers et al. 2015, Smith et al. 1997) have also reported net N and P retention in reservoirs. For example, Powers et al. (2015) found many reservoirs in currently agricultural catchments across the Midwestern U.S. retain >20% of N and P inputs. Additionally, reservoirs along large rivers across the United States retained 34% of P inputs while reservoir N retention represented 0-32% of inputs to 17 temperate reservoirs (Harrison et al. 2009). These reservoirs varied considerably in age, trophic status, size, catchment history, and magnitude of nutrient loads, but most were more eutrophic and much larger than FCR. FCR exhibited much higher nutrient retention rates than those measured in previous studies, likely due to its small size, shallow depth, and because it only had one outflow. The NH_4^+, SRP, and $NO_3^- - NO_2^-$ retention rates measured in this study for FCR are among the highest rates observed for a reservoir ecosystems (Harrison et al. 2009, Kelly 2001, Leavitt et al. 2006, Patoine et al. 2006, Salas and Martino 1991).

Aging reservoirs such as FCR play an important role in the landscape as sites for nutrient retention, thereby reducing the magnitude of nutrient export to downstream aquatic ecosystems. For the case of FCR, our results suggest that the reservoir has resilience to increased external nutrient loads expected with more frequent and powerful storm events. This observation is particularly relevant for $NO_3^- - NO_2^-$, which was demonstrated by the reservoir's increased retention rates in response to increased external loads in Treatments C and D. However,

hypolimnetic hypoxia may mediate the role of reservoirs as nutrient sinks or sources, as we observed for NH_4^+. Future increases in NH_4^+, SRP, and $NO_3^- - NO_2^-$ internal loading will undoubtedly modify nutrient delivery downstream and the ability of the reservoir to serve as a sink or source of N and P.

Sediment core incubations

Our results from the sediment core incubation emphasize that FCR has accumulated a substantial quantity of N and P in its sediments since its construction in 1898. In both the hypoxic sediment cores and hypoxic treatments (B and D) in the reservoir, we observed similar patterns of NH_4^+ and SRP release into the overlying water and absorption of $NO_3^- - NO_2^-$, though the NH_4^+ and SRP release rates were considerably larger (~100x) in the sediment cores than observed in FCR (Figure 2.8; Figure 2.9). Our observed field release rates correlated well with the range of reported release rates for other eutrophic lakes and reservoirs with hypoxic sediments (Auer et al. 1993, Graetz et al. 1973, Larsen et al. 1981, Mengis et al. 1997, Nürnberg 1984, Nürnberg 1988, Rysgaard et al. 1994, Shaw and Prepas 1990). In a survey of several eutrophic reservoirs on the west coast of the United States, reported sediment release rates were >15 mg $m^{-2}d^{-1}$ and 2-10 mg $m^{-2}d^{-1}$ for NH_4^+ and SRP, respectively, as well as very low, and sometimes negative, release rates of $NO_3^- - NO_2^-$, indicating denitrification (Beutel 2006, Beutel et al. 2008), similar to rates we observed in FCR.

The discrepancy in internal loading rates between the laboratory incubations and the field observations may be due to several reasons. The spatial heterogeneity of sediment characteristics varies within FCR from the site of the inflow to the dam, likely altering the sediment release rates substantially (Boström et al. 1988a, Holdren and Armstrong 1980, Søndergaard et al. 2003).

Spatial variation and composition may also be enhanced by hypolimnetic mixing at the sediment – water interface from HOx activation (Beutel 2003, Gantzer et al. 2009b, Matthews and Effler 2006b, Moore et al. 1996). Additionally, internal loading rates are dependent on the areal extent and duration of hypoxia (Nürnberg 1995, Nürnberg 2002). Finally, the water temperature at the sediments of FCR during Treatments B and D ranged from 9.9-11.3°C, whereas the sediment incubations occurred at ambient room temperature (20-24°C). These much warmer conditions likely enabled much higher microbial processing rates and nutrient release from the sediments (Boers et al. 1998, Jensen and Andersen 1992, Søndergaard et al. 2003, Søndergaard et al. 1999).

Long-term effects of Falling Creek Reservoir's agricultural legacy

As a result of its agricultural legacy, FCR has accumulated a substantial amount of nutrients in its sediments, despite little human activity in the catchment for the past ~80 years. Because the hypolimnion of FCR will become hypoxic during the summer stratified period in the absence of human intervention, it is likely that the nutrients that entered the reservoir prior to reforestation were continually recycled into the water column in the summer and then redeposited onto the sediments each year. Shallow reservoirs such as FCR exhibit high nutrient resuspension and recycling (Wetzel 2001). It is also possible that historical external nutrients may have accumulated in the hypolimnion of FCR since there is no substantial hypolimnetic outflow.

It is likely that the legacy of historical agricultural land use in the catchment still dominates the nutrient dynamics in the reservoir. Several studies have indicated that past land use activity, particularly agriculture, is responsible for long-term modifications to freshwater ecosystems due to the increased delivery of N and P and sediment, despite reforestation (Blann et

al. 2009, Carpenter et al. 1998, Foley et al. 2005, Foster et al. 2003, Harding et al. 1998, Surasinghe and Baldwin 2014). While previously high external loading is known to result in elevated internal loading rates over the long-term ("the ghost of loadings past"; Harding et al. 1998), our study is notable in the length of time (>80 years since catchment reforestation) that a reservoir with a relatively short residence time (<1 year) is still exhibiting high internal loading rates during hypoxia.

Our results suggest that it is critical to consider reservoir catchment history and waterbody characteristics when predicting the effects of hypolimnetic hypoxia and increased storms on reservoir nutrient budgets. Together, the small size of FCR (surface area of 1.19×10^{-1} km^2; maximum depth of 9.3 m) and FCR's legacy of >80 years of accumulated nutrients in the sediments likely contributed substantially to its high internal loads. Small reservoirs have been associated with long-term sediment storage (Powers et al. 2013, Renwick et al. 2005) partly due to higher nutrient settling velocities (Harrison et al. 2009). Furthermore, FCR's catchment is primarily forested and absent of current agriculture or anthropogenic sources, with only one contributing tributary (Figure 2.2).

It is possible that nutrient sources other than historical anthropogenic loading may have contributed to the high internal loads observed in FCR, such as weathering bedrock, but it is likely that FCR's agricultural legacy is the predominant factor driving current internal loading rates. Our findings emphasize that there are considerably more nutrients that have accumulated in the sediments than entering the reservoir through the inflow.

Looking ahead: the power of the whole-ecosystem experiment approach to studying the effects of future climate

The whole-ecosystem manipulations in FCR provided a rare opportunity to investigate the rates of nutrient transformations under different redox conditions. Microcosm experiments can be an effective research tool to study these nutrient transformations, though there are often difficulties scaling laboratory studies to the whole-ecosystem level, as observed in our sediment core incubations and field study. Reservoir processes are dynamic and complex, making it is critically important to understand their phenomena at multiple scales. Though not always feasible, whole-ecosystem experiments offer invaluable insight to biogeochemical processes that are crucial for understanding how to adaptively manage for future changes in ecosystems (Carpenter 1996, Carpenter 1999, Carpenter et al. 1995, Gardner et al. 2001), such as those expected with climate change.

Conclusion

As the construction of reservoirs increases globally (Chao 1995, Downing et al. 2006a, Rosenberg et al. 2000, Smith et al. 2002), reservoirs will increasingly play an increasingly important role in biogeochemical processes in the landscape over the long-term (decades to centuries). Consequently, the effects of climate change (i.e., increased water temperatures, intensified thermal stratification, and the subsequent hypoxic conditions in the hypolimnion) may amplify the magnitude of internal loads in the future (Sahoo and Schladow 2008, Sahoo et al. 2010, Whitehead et al. 2009), and some of these recycled nutrients may be exported downstream. In addition, external loads from storm events are predicted to vary in many regions globally, which can result in pulses of increased N and P entering into a waterbody. Our manipulations

demonstrated that the greatest climate change risk to FCR's water quality may be increased internal loads stimulated by hypoxic conditions in the hypolimnion, as expected under future scenarios of longer and more intense thermal stratification.

References

Adrian, R., C.M., O.R., Zagarese, H., Baines, S.B., Hessen, D.O., Keller, W., Livingstone, D.M., Sommaruga, R., Straile, D., Van Donk, E., Weyhenmeyer, G.A., Winder, M., 2009. Lakes as sentinels of climate change. Limnology and Oceanography 54, 2283–2297.

Auer, M.T., Johnson, N.A., Penn, M.R., Effler, S.W., 1993. Measurement and verification of rates of sediment phosphorus release for a hypereutrophic urban lake. Hydrobiologia 253, 301-309.

Beaulac, M.N., Reckhow, K.H., 1982. An examination of land use - nutrient export relationships. Water Resources Bulletin 18, 1013-1024.

Berman, T., 1997. Dissolved organic nitrogen utilization by an Aphanizomenon bloom in Lake Kinneret. Journal of Plankton Research 19(5), 577-586.

Beutel, M.W., 2003. Hypolimnetic anoxia and sediment oxygen demand in California drinking water reservoirs. Lake and Reservoir Management 19(3), 208-221.

Beutel, M.W., 2006. Inhibition of ammonia release from anoxic profundal sediments in lakes using hypolimnetic oxygenation. Ecological Engineering 28(3), 271-279.

Beutel, M.W., Leonard, T.M., Dent, S.R., Moore, B.C., 2008. Effects of aerobic and anaerobic conditions on P, N, Fe, Mn, and Hg accumulation in waters overlaying profundal sediments of an oligo-mesotrophic lake. Water Res 42(8-9), 1953-1962.

Bindoff, N.L., Stott, P.A., AchutaRao, K.M., Allen, M.R., Gillett, N., Gutzler, D., Hansingo, K., Hegerl, G., Hu, Y., Jain, S., Mokhov, I.I., Overland, J., Perlwitz, J., Sebbari, R., Zhang, X., 2013. Detection and Attribution of Climate Change: from Global to Regional. In: Climate Change 2013: The Physical Science Basis. Contribution of Working Group I to the Fifth Assessment Report of the Intergovernmental Panel on Climate Change. Stocker, T.F., Qin, D., Plattner, G.-K., Tignor, M., Allen, S.K., Boschung, J., Nauels, A., Xia, Y., Bex, V. and Midgley, P.M. (eds), Cambridge, United Kingdom and New York, NY, USA.

Blann, K.L., Anderson, J.L., Sands, G.R., Vondracek, B., 2009. Effects of Agricultural Drainage on Aquatic Ecosystems: A Review. Critical Reviews in Environmental Science and Technology 39(11), 909-1001.

Boers, P.C.M., Van Raaphorst, W., Van der Molen, D.T., 1998. Phosphorus retention in sediments. Water Science and Technology 37(3), 31-39.

Boström, B., Andersen, J.M., Fleischer, S., Jansson, M., 1988a. Exchange of phosphorus across the sediment-water interface. Hydrobiologia 170, 229-244.

Boström, B., Persson, G., Broberg, B., 1988b. Bioavailability of different phosphorus forms in freshwater systems. Hydrobiologia 170, 133-155.

Brown, J.B., Sprague, L.A., Dupree, J.A., 2011. Nutrient Sources and Transport in the Missouri River Basin, with Emphasis on the Effects of Irrigation and Reservoirs. J Am Water Resour Assoc 47(5), 1034-1060.

Bruesewitz, D.A., Tank, J.L., Hamilton, S.K., 2012. Incorporating spatial variation of nitrification and denitrification rates into whole-lake nitrogen dynamics. Journal of Geophysical Research 117.

Burgin, A.J., Hamilton, S.K., 2007. Have we overemphasized the role of denitrification in aquatic ecosystems? A review of nitrate removal pathways. Frontiers In Ecology And The Environment 5(2), 89-96.

Canfield, D.E., Glazer, A.N., Falkowski, P.G., 2010. The Evolution and Future of Earth's Nitrogen Cycle. Science 330, 192-196.

Carpenter, S.R., 1996. Microcosm experiments have limited relevance for community and ecosystem ecology. Ecology 77, 677-680.

Carpenter, S.R., 1999. Microcosm experiments have limited relevance for community and ecosystem ecology: Reply. Ecology 80, 1085-1088.

Carpenter, S.R., 2005. Eutrophication of aquatic ecosystems: bistability and soil phosphorus. Proc Natl Acad Sci U S A 102(29), 10002-10005.

Carpenter, S.R., Caraco, N.F., Correll, D.L., Howarth, R.W., Sharpley, A.N., Smith, V.H., 1998. Nonpoint pollution of surface waters with phosphorus and nitrogen. Ecological Applications 8(3), 559-568.

Carpenter, S.R., Chisholm, S.W., Krebs, C.J., Schindler, D.W., Wright, R.F., 1995. Ecosystem Experiments. Science 269, 324-327.

Chambers, J.M., 1992. Statistical Models in S. Chambers, J.M. and Hastie, T.J. (eds), Pacific Grove, California.

Chao, B.F., 1995. Anthropogenic impact on global geodynamics due to reservoir water impoundment. Geophysical Research Letters 22(24), 3529-3532.

Chow, V.T., 1959. Open-Channel Hydraulics, McGraw-Hill Book Company, New York, New York.

Cole, J.J., Prairie, Y.T., Caraco, N.F., McDowell, W.H., Tranvik, L.J., Striegl, R.G., Duarte, C.M., Kortelainen, P., Downing, J.A., Middelburg, J.J., Melack, J., 2007. Plumbing the Global Carbon Cycle: Integrating Inland Waters into the Terrestrial Carbon Budget. Ecosystems 10(1), 172-185.

Conley, D.J., Paerl, H.W., Howarth, R.W., Boesch, D.F., Seitzinger, S.P., Havens, K.E., Lancelot, C., Likens, G.E., 2009. Controlling Eutrophication: Nitrogen and Phosphorus. Science 323(1014-1015).

David, M.B., Wall, L.G., Royer, T.V., Tank, J.L., 2006. Denitrification and the nitrogen budget of a reservoir in an agriculture landscape. Ecological Applications 16, 2177-2190.

Delpla, I., Jung, A.V., Baures, E., Clement, M., Thomas, O., 2009. Impacts of climate change on surface water quality in relation to drinking water production. Environ Int 35(8), 1225-1233.

Diaz, R.J., 2001. Overview of hypoxia around the world. J Environ Qual 30, 275-281.

Downing, J.A., Cole, J.J., Middelburg, J.J., Striegl, R.G., Duarte, C.M., Kortelainen, P., Prairie, Y.T., Laube, K.A., 2008. Sediment organic carbon burial in agriculturally eutrophic impoundments over the last century. Global Biogeochemical Cycles 22(1), 1-10.

Downing, J.A., Prairie, Y.T., Cole, J.J., Duarte, C.M., Tranvik, L.J., Striegl, R.G., McDowell, R.W., Kortelainen, P., Caraco, N.F., Melack, J., Middelburg, J.J., 2006. The global abundance and size distribution of lakes, ponds, and impoundments. Limnology and Oceanography 51, 2388-2397.

Easterling, D.R., Meehl, G.A., Parmesan, C., Changnon, S.A., Karl, T.R., Mearns, L.O., 2000. Climate Extremes: Observations, Modeling, and Impacts. Science 289, 2068-2074.

Einsele, W., 1936. Über die Beziehung des Eisenkreislaufs zum Phosphorkreislauf im eutrophen. See. Arch. Hydrobiol. 29, 664–686.

Essington, T.E., Carpenter, S.R., 2000. Nutrient Cycling in Lakes and Streams: Insights from a Comparative Analysis. Ecosystems 3(2), 131-143.

Foley, J.A., DeFries, R., Asner, G.P., Barford, C., Bonan, G., Carpenter, S.R., Chapin, F.S., Coe, M.T., Daily, G.C., Gibbs, H.K., Helkowski, J.H., Holloway, T., Howard, E.A., Kucharik, C.J., Monfreda, C., Patz, J.A., Prentice, C., Ramankutty, N., Snyder, P.K., 2005. Global consequences of land use. Science 309(5734), 570-574.

Foster, D., Swanson, F., Aber, J., Burke, I., Brokaw, N., Tilman, D., A., K., 2003. The importance of land-use legacies to ecology and conservation. BioScience 53(1), 77-89.

Gantzer, P.A., Bryant, L.D., Little, J.C., 2009. Effect of hypolimnetic oxygenation on oxygen depletion rates in two water-supply reservoirs. Water Res 43(6), 1700-1710.

Gardner, R.H., Kemp, W.M., Kennedy, V.S., Peterson, J.E., 2001. Scaling Relations in Experimental Ecology, Columbia University Press, New York, NY.

Gerling, A.B., Browne, R.G., Gantzer, P.A., Mobley, M.H., Little, J.C., Carey, C.C., 2014. First report of the successful operation of a side stream supersaturation hypolimnetic oxygenation system in a eutrophic, shallow reservoir. Water Res 67, 129-143.

Graetz, D.A., Keeney, D.R., Aspiras, R.B., 1973. Status of lake sediment-water systems in relation to nitrogen transformations. Limnology and Oceanography 18(6), 908-917.

Grant, M.G., 1991. Isco Open Channel Flow Measurement Handbook, 3rd Edition, Isco, Inc., Lincoln, Nebraska.

Harding, J.S., Benfield, E.F., Bolstad, P.V., Helfman, G.S., Jones, E.B.D., 1998. Stream biodiversity: The ghost of land use past. Proc Natl Acad Sci U S A 95, 14843–14847.

Harrison, J.A., Maranger, R.J., Alexander, R.B., Giblin, A.E., Jacinthe, P.-A., Mayorga, E., Seitzinger, S.P., Sobota, D.J., Wollheim, W.M., 2009. The regional and global significance of nitrogen removal in lakes and reservoirs. Biogeochemistry 93(1-2), 143-157.

Holdren, G.C., Armstrong, D.E., 1980. Factors affecting phosphorus release from intact lake sediment cores. Environmental Science and Technology 14, 79-87.

Howarth, R.W., Billen, G., Swaney, D., Townsend, A.R., Jaworski, N.A., Lajitha, K., Downing, J.A., Elmgren, R., Caraco, N.F., Jordan, T., Berendse, F., Freney, J.R., Kudeyarov, V., Murdoch, P., Zhao-Liang, Z., 1996. Regional nitrogen budgets and riverine N and P fluxes for the drainages to the North Atlantic Ocean: Natural and human influeneces. Biogeochemistry 35, 75-139.

Jensen, H.S., Andersen, F.O., 1992. Importance of temperature, nitrate, and pH for phosphate releasefrom aerobic sediments of four shallow, eutrophic lakes. Limnology and Oceanography 37, 577-589.

Jeppesen, E., Kronvang, B., Meerhoff, M., Sondergaard, M., Hansen, K.M., Andersen, H.E., Lauridsen, T.L., Liboriussen, L., Beklioglu, M., Ozen, A., Olesen, J.E., 2009. Climate change effects on runoff, catchment phosphorus loading and lake ecological state, and potential adaptations. J Environ Qual 38(5), 1930-1941.

Jeppesen, E., Kronvang, B., Olesen, J.E., Audet, J., Sondergaard, M., Hoffmann, C.C., Andersen, H.E., Lauridsen, T.L., Liboriussen, L., Larsen, S.E., Beklioglu, M., Meerhoff, M., Ozen, A., Ozkan, K., 2011. Climate change effects on nitrogen loading from cultivated catchments in Europe: implications for nitrogen retention, ecological state of lakes and adaptation. Hydrobiologia 663, 1-21.

Jiménez Cisneros, B.E., Oki, T., Arnell, N.W., Benito, G., Cogley, J.G., Döll, P., Jiang, T., Mwakalila, S.S., 2014. Freshwater resources. In: Climate Change 2014: Impacts, Adaptation, and Vulnerability. Part A: Global and Sectoral Aspects. Contribution of

Working Group II to the Fifth Assessment Report of the Intergovernmental Panel on Climate Change. ield, C.B., Barros, V.R., Dokken, D.J., Mach, K.J., Mastrandrea, M.D., Bilir, T.E., Chatterjee, M., Ebi, K.L., Estrada, Y.O., Genova, R.C., Girma, B., Kissel, E.S., Levy, A.N., MacCracken, S., Mastrandrea, P.R. and White, L.L. (eds), pp. 229-269, Cambridge, United Kingdom and New York, NY, USA.

Kelly, V.J., 2001. Influence of reservoirs on solute transport: a regional-scale approach. Hydrological Processes 15(7), 1227-1249.

Knoll, L.B., Vanni, M.J., Renwick, W.H., Kollie, S., 2014. Burial rates and stoichiometry of sedimentary carbon, nitrogen and phosphorus in Midwestern US reservoirs. Freshwater Biology 59(11), 2342-2353.

Knowles, R., 1982. Denitrification. Microbiological Reviews 46(1), 43-70.

Kõiv, T., Nõges, T., Laas, A., 2011. Phosphorus retention as a function of external loading, hydraulic turnover time, area and relative depth in 54 lakes and reservoirs. Hydrobiologia 660(1), 105-115.

Koop-Jakobsen, K., Giblin, A.E., 2010. The effect of increased nitrate loading on nitrate reduction via denitrification and DNRA in salt marsh sediments. Limnology and Oceanography 55(2), 789–802.

Larsen, D.P., Schults, D.W., Malueg, K.W., 1981. Summer internal phosphorus supplies in Shagwa Lake, Minnesota. Limnology and Oceanography 26(4), 740-753.

Leavitt, P.R., Brock, C.S., Ebel, C., Patoine, A., 2006. Landscape-scale effects of urban nitrogen on a chain of freshwater lakes in central North America. Limnology and Oceanography 51, 2262–2277.

Matthews, D.A., Effler, S.W., 2006. Long-term changes in the areal hypolimnetic oxygen deficit (AHOD) of Onondaga Lake: Evidence of sediment feedback. Limnology and Oceanography 51(702-714).

Matthews, D.A., Effler, S.W., Driscoll, C.T., O'Donnell, S.M., Matthews, C.M., 2008. Electron budgets for the hypolimnion of a recovering urban lake, 1989–2004: Response to changes in organic carbon deposition and availability of electron acceptors. Limnology and Oceanography 53(2), 743-759.

Mattson, M.D., Likens, G.E., 1993. Redox reactions of organic matter decomposition in a soft water lake. Biogeochemistry 19, 149-172.

Mengis, M., Gächter, R., Wehrli, B., Bernasconi, S., 1997. Nitrogen elimination in two deep eutrophic lakes. Limnology and Oceanography 42(7), 1530-1543.

Min, S.K., Zhang, X., Zwiers, F.W., Hegerl, G.C., 2011. Human contribution to more-intense precipitation extremes. Nature 470(7334), 378-381.

Molot, L.A., Dillon, P.J., 1993. Nitrogen mass balances and denitrification rates in central Ontario Lakes. Biogeochemistry 20, 195-212.

Moore, B.C., Chen, P.H., Funk, W.H., Yonge, D., 1996. A model for predicting lake sediment oxygen demand following hypolimnetic aeration. Water Resources Bulletin 32, 723-731.

Mortimer, C.H., 1941. The exchange of dissolved substances between mud and water in lakes. Journal of Ecology 29, 280-329.

Nowlin, W.H., Evarts, J.L., Vanni, M.J., 2005. Release rates and potential fates of nitrogen and phosphorus from sediments in a eutrophic reservoir. Freshwater Biology 50(2), 301-322.

Nürnberg, G.K., 1984. The prediction of internal phosphorus load in lakes with anoxic hypolimnia. Limnology and Oceanography 29(1), 111-124.

Nürnberg, G.K., 1988. Prediction of phosphorus release rates from total and reductant- solube phosphorus in anoxic lake sediments. Can. J. Fish. Aquat. Sci. 45, 453-462.

Nürnberg, G.K., 1991. Phosphorus from internal sources in the Laurentian Great Lakes, and the concept of threshold external load. Journal of Great Lakes Research 17(1), 132-140.

Nürnberg, G.K., 1995. Quantifying anoxia in lakes. Limnology and Oceanography 40, 1100-1111.

Nürnberg, G.K., 2002. Quantification of Oxygen Depletion in Lakes and Reservoirs with the Hypoxic Factor. Lake and Reservoir Management 18(4), 299-306.

Paerl, H.W., Huisman, J., 2009. Climate change: a catalyst for global expansion of harmful cyanobacterial blooms. Environ Microbiol Rep 1(1), 27-37.

Painter, H.A., 1970. A review of literature on inorganic nitrogen metabolism in microorganisms. Water Res 4, 393-450.

Palmer, M.E., Yan, N.D., Somers, K.M., 2014. Climate change drives coherent trends in physics and oxygen content in North American lakes. Climatic Change 124(1-2), 285-299.

Park, J.H., Duan, L., Kim, B., Mitchell, M.J., Shibata, H., 2010. Potential effects of climate change and variability on watershed biogeochemical processes and water quality in Northeast Asia. Environ Int 36(2), 212-225.

Patoine, A., Graham, M.D., Leavitt, P.R., 2006. Spatial variation of nitrogen fixation in lakes of the northern Great Plains. Limnology and Oceanography 51, 1665–1677.

Powers, S.M., Julian, J.P., Doyle, M.W., Stanley, E.H., 2013. Retention and transport of nutrients in a mature agricultural impoundment. Journal of Geophysical Research: Biogeosciences 118(1), 91-103.

Powers, S.M., Tank, J.L., Robertson, D.M., 2015. Control of nitrogen and phosphorus transport by reservoirs in agricultural landscapes. Biogeochemistry 124(1-3), 417-439.

Renwick, W.H., Smith, S.V., Bartley, J.D., Buddemeier, R.W., 2005. The role of impoundments in the sediment budget of the conterminous United States. Geomorphology 71(1-2), 99-111.

Rosenberg, D.M., McCully, P., Pringle, C.M., 2000. Global-scale environmental effects of hydrological
alterations: introduction. BioScience 50(746-751).

Rydin, E., 2000. Potentially mobile phosphorus in Lake Erken sediment. Water Res 34(7), 2307-2042.

Rysgaard, S., Risgaard-Petersen, N., Sloth, N.P., Jensen, K., Nielsen, L.P., 1994. Oxygen regulation of nitrification and denitrification in sediments. Limnology and Oceanography 39(7), 1643-1652.

Sahoo, G.B., Schladow, S.G., 2008. Impacts of climate change on lakes and reservoirs dynamics and restoration policies. Sustainability Science 3(2), 189-199.

Sahoo, G.B., Schladow, S.G., Reuter, J.E., Coats, R., 2010. Effects of climate change on thermal properties of lakes and reservoirs, and possible implications. Stochastic Environmental Research and Risk Assessment 25(4), 445-456.

Salas, H.J., Martino, P., 1991. A simplified phosphorus trophic state model for warm-water tropical lakes. Water Res 25, 341-350.

Schindler, D.E., Kitchell, J.F., He, X., Carpenter, S.R., Hodgson, J.R., Cottingham, K.L., 1993. Food Web Structure and Phosphorus Cycling in Lakes. Transactions of the American Fisheries Society 122(5), 756-772.

Schindler, D.W., 1974. Eutrophication and recovery in experimental lakes: Implications for lake management. Science 184(4139), 897-899.

Schindler, D.W., 1977. Evolution of phosphorus limitation in lakes. Science 195(4275), 260-262.

Schindler, D.W., Hecky, R.E., Findlay, D.L., Stainton, M.P., Parker, B.R., Paterson, M.J., Beaty, K.G., Lyng, M., Kasian, S.E., 2008. Eutrophication of lakes cannot be controlled by reducing nitrogen input: results of a 37-year whole-ecosystem experiment. Proceedings of the National Academy of Sciences 105(32), 11254-11258.

Schneider, P., Hook, S.J., 2010. Space observations of inland water bodies show rapid surface warming since 1985. Geophysical Research Letters 37(22), n/a-n/a.

Seitzinger, S.P., 1988. Denitrification in freshwater and coastal marine ecosystems: Ecological and geochemical significance. Limnology and Oceanography 33(4, part 2), 702-724.

Seitzinger, S.P., Styles, R.V., Boyer, E.W., Alexander, R.B., Billen, G., Howarth, R.W., Mayer, B., Van Breemen, N., 2002. Nitrogen retention in rivers: model development and application to watersheds in the northeastern U.S.A. Biogeochemistry 57/58, 199-237.

Shaw, J.F.H., Prepas, E.E., 1990. Exchange of phosphorus form shallow sediments at nine Alberta lakes. J. Environ. Qual. 19, 249-256.

Shostell, J., Bukaveckas, P.A., 2004. Seasonal and interannual variation in nutrient fluxes from tributary inputs, consumer recycling and algal growth in a eutrophic river impoundment. Aquatic Ecology 38, 359-373.

Smith, R.A., Schwarz, G.E., Alexander, R.B., 1997. Regional interpretation of water-quality monitoring data. Water Resources Research 33(12), 2781–2798.

Smith, S.V., Renwick, W.H., Bartley, J.D., Buddemeier, R.W., 2002. Distribution and significance of small, artificial water bodies across the United States landscape. Sci Total Environ 299, 21-36.

Smith, V.H., 2003. Eutrophication of freshwater and coastal marine ecosystems a global problem. Environmental Science and Pollution Research 10(2), 126-139.

Smith, V.H., Schindler, D.W., 2009. Eutrophication science: where do we go from here? Trends Ecol Evol 24(4), 201-207.

Søndergaard, M., Jensen, H.S., Jeppesen, E., 2003. Role of sediment and internal loading of phosphorus in shallow lakes. Hydrobiologia 506-509, 135-145.

Søndergaard, M., Jensen, J.P., Jeppesen, E., 1999. Internal phosphorus loading in shallow Danish lakes. Hydrobiologia 408/409, 145-152.

Stumm, W., Morgan, J.J., 1996. Aquatic Chemistry: Chemical Equilibria and Rates in Natural Waters, Wiley Interscience, New York.

Surasinghe, T., Baldwin, R.F., 2014. Ghost of land-use past in the context of current land cover: evidence from salamander communities in streams of Blue Ridge and Piedmont ecoregions. Canadian Journal of Zoology 92(6), 527-536.

Team, R.C., 2014. A Language and Environment for Statistical Computing. R Foundation for Statistical Computing, Vienna, Austria.

Teodoru, C., Wehrli, B., 2005. Retention of Sediments and Nutrients in the Iron Gate I Reservoir on the Danube River. Biogeochemistry 76(3), 539-565.

Tranvik, L.J., Downing, J.A., Cotner, J.B., Loiselle, S.A., Striegl, R.G., Ballatore, T.J., Dillon, P., Finlay, K., Fortino, K., Knoll, L.B., Kortelainen, P., Kutser, T., Larsen, S., Laurion, I., Leech, D.M., McCallister, S.L., McKnight, D.M., Melack, J.M., Overholt, E., Porter, J.H., Prairie, Y.T., Renwick, W.H., Roland, F., Sherman, B., Schindler, D.W., Sobek, S., Tremblay, A., Vanni, M.J., Verschoor, A.M., von Wachenfeldt, E., Weyhenmeyer, G.A.,

2009. Lakes and reservoirs as regulators of carbon cycling and climate. Limnology and Oceanography 54, 2298–2314.

Turner, R.E., Rabalais, N.N., 2003. Linking Landscape and Water Quality in the Mississippi River Basin for 200 Years. BioScience 53(6), 563.

Vanni, M.J., Renwick, W.H., Bowling, A.M., Horgan, M.J., Christian, A.D., 2011. Nutrient stoichiometry of linked catchment-lake systems along a gradient of land use. Freshwater Biology 56(5), 791-811.

Westra, S., Alexander, L.V., Zwiers, F.W., 2013. Global increasing trends in annual maximum daily precipitation. Journal of Climate 26(11), 3904-3918.

Wetzel, R.G., 2001. Limnology: Lake and River Ecosystems, 3rd Edition, Academic Press., San Diego, California.

Whitehead, P.G., Wilby, R.L., Battarbee, R.W., Kernan, M., Wade, A.J., 2009. A review of the potential impacts of climate change on surface water quality. Hydrological Sciences Journal 54(1), 101-123.

Wilkinson, G.N., Rogers, C.E., 1973. Symbolic description of factorial models for analysis of variance. Applied Statistics 22(3), 392-399.

Williamson, C.E., Saros, J.E., Vincent, W.F., Smol, J.P., 2009. Lakes and reservoirs as sentinels, integrators, and regulators of climate change. Limnology and Oceanography 54, 2273-2282.

Wodka, M.C., Effler, S.W., 1985. Phosphorus deposition from the epilimnion of Onondaga Lake. Limnology and Oceanography 30, 833-843.

Wollheim, W.M., Vörösmarty, C.J., Bouwman, A.F., Green, P., Harrison, J., Linder, E., Peterson, B.J., Seitzinger, S.P., Syvitski, J.P.M., 2008. Global N removal by freshwater aquatic systems using a spatially distributed, within-basin approach. Global Biogeochemical Cycles 22(2), 1-14.

Wyman, B., Stevenson, L.H., 1991. Dictionary of Environmental Science, Facts On File, Inc., New York, New York.

Tables

Table 2.1. The net fluxes (mean ± S.D.) of ammonium (NH_4^+), soluble reactive phosphorus (SRP), and nitrate-nitrite ($NO_3^- - NO_2^-$) as a percentage of the nutrient inputs for each treatment. Negative values represent net nutrient retention/loss and positive values represent net nutrient export to the reservoir.

	Treatment			
Nutrient	**A**	**B**	**C**	**D**
NH_4^+	-25 ± 37	43 ± 73	-70 ± 21	-31 ± 64
SRP	-76 ± 8	-68 ± 7	-38 ± 27	-50 ± 27
$NO_3^- - NO_2^-$	-90 ± 6	-70 ± 24	-95 ± 5	-94 ± 2

Table 2.2. Statistical results from a one-way repeated-measures ANOVA testing the effects and interactions of oxygen treatment and time on DO concentrations and NH_4^+, SRP, and $NO_3^- - NO_2^-$ release rates. DF denotes degrees of freedom, and significant effects ($p < 0.05$) are in bold.

Measurement	**Repeated measures ANOVA test**	**DF**	**F-value**	***p*-value**
DO	Oxygen treatment	1,7	220.35	**<0.0001**
	Time	17,119	147.97	**<0.0001**
	Oxygen treatment x Time	17,119	123.8	**<0.0001**
NH_4^+	Oxygen treatment	1,7	10.0094	**0.002**
	Time	6,42	10.1884	**0.002**
	Oxygen treatment x Time	6,42	4.8431	**0.046**
SRP	Oxygen treatment	1,7	1.49	0.23
	Time	6,42	0.77	0.38
	Oxygen treatment x Time	6,42	3.73	0.06
$NO_3^- - NO_2^-$	Oxygen treatment	1,7	9.45	**0.003**
	Time	6,42	18.86	**<0.0001**
	Oxygen treatment x Time	6,42	8.32	**0.006**

Figures

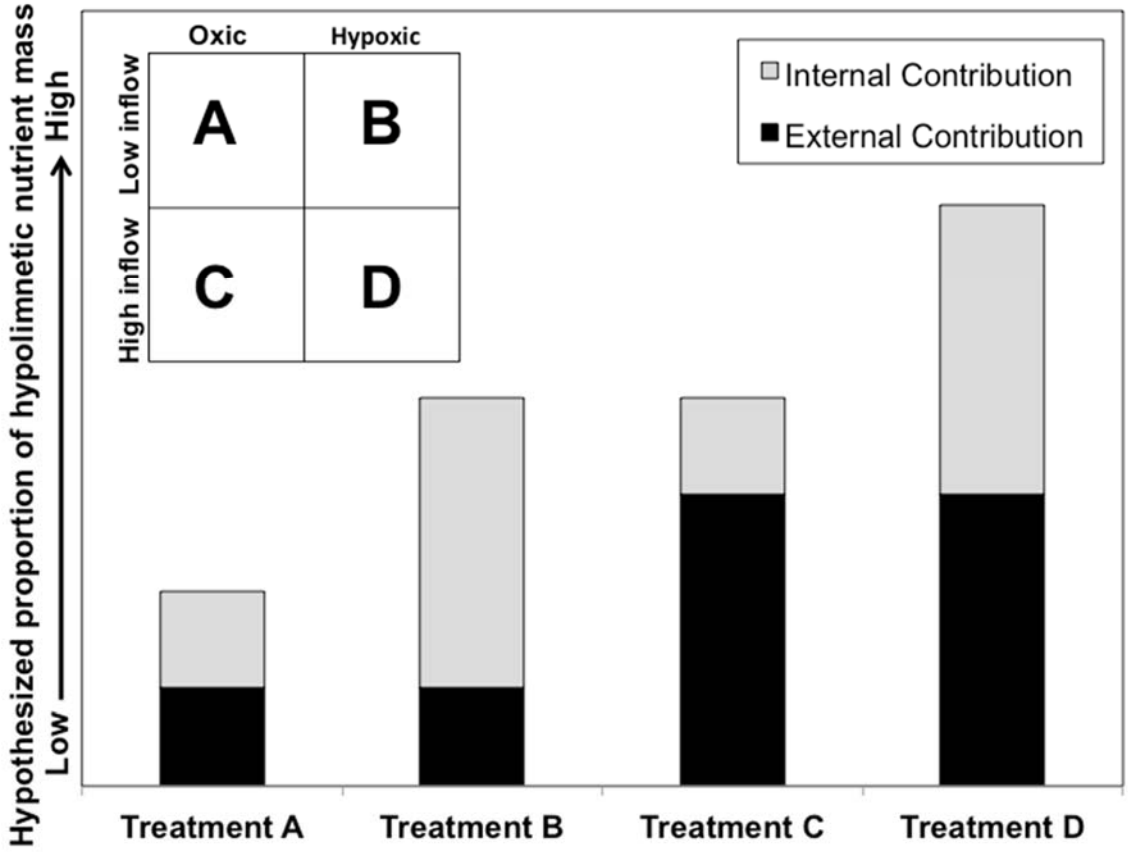

Figure 2.1. We manipulated hypolimnetic oxygen conditions and external nutrient loads to Falling Creek Reservoir. Assuming equivalent internal and external loads, the hypotheses for our four treatments are identified with letters, A – D. Treatment A was the reference treatment, with oxic hypolimnetic conditions and low inflow volumes (low internal and low external loads). Treatment B had hypoxic hypolimnetic conditions and low inflow volumes (high internal and low external loads) and Treatment C was its converse, with oxic hypolimnetic conditions and high inflow volumes (low internal and high external loads). Treatment D had a hypoxic hypolimnion and high inflow volumes (high internal and high external loads).

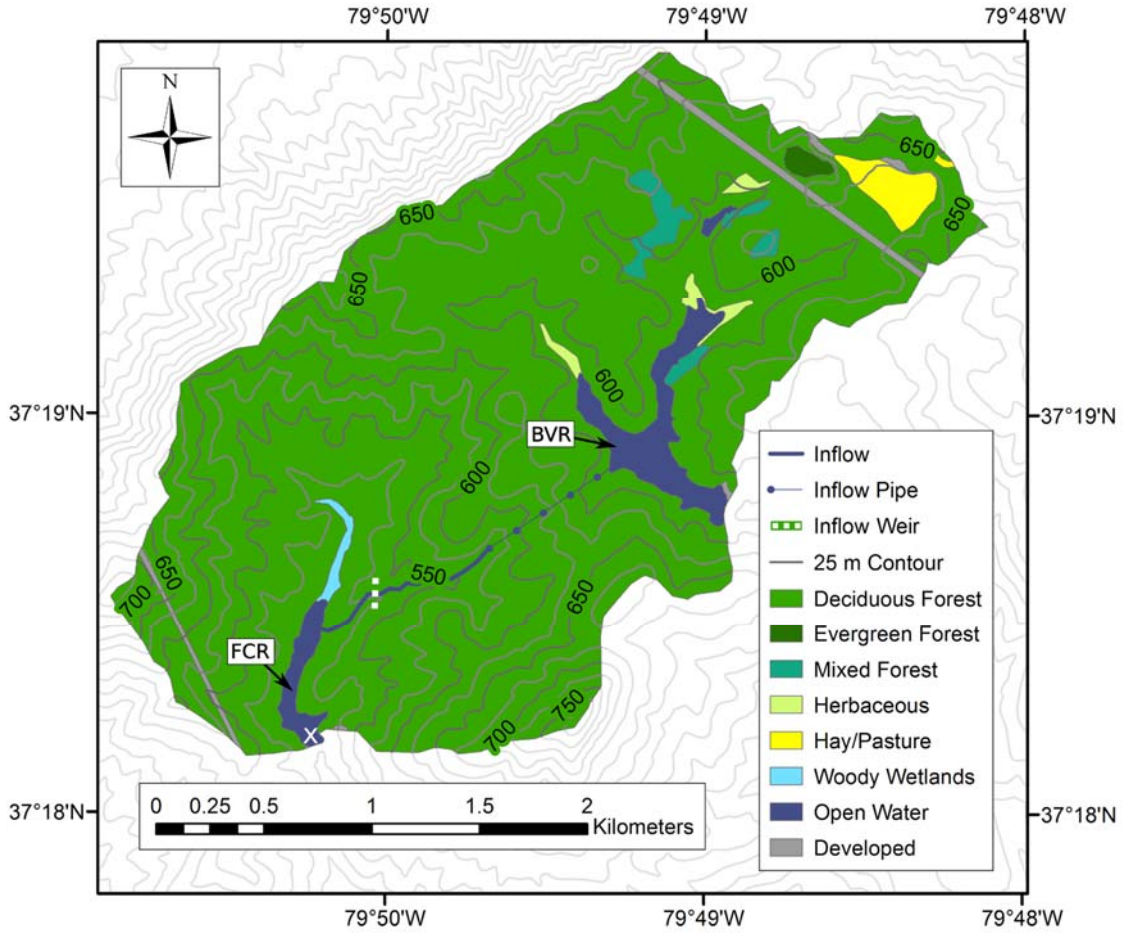

Figure 2.2. Falling Creek Reservoir (FCR) and Beaverdam Reservoir (BVR on figure) catchments located in Vinton, Virginia, USA. FCR receives water primarily from one tributary that flows from the upstream Beaverdam Reservoir. The inflow pipe originates in the epilimnion of Beaverdam Reservoir and is underground for ~750 m until it reaches an open stream that flows ~950 m before it enters FCR. Water samples were collected from the deepest site of FCR (denoted by the "X") and at the gauged weir (denoted by the three white squares). All inflow volumes for this experiment were recorded at the weir.

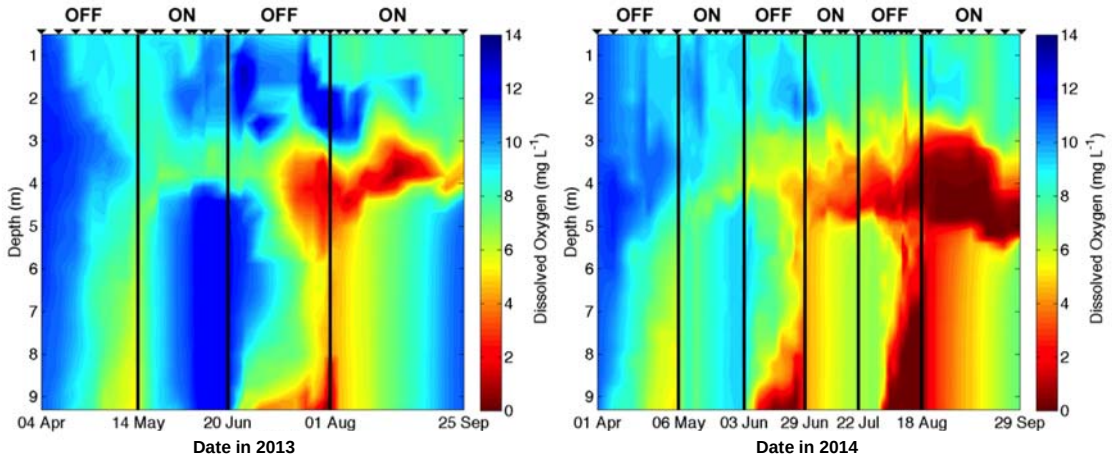

Figure 2.3. Dissolved oxygen concentrations in FCR from 04 April to 25 September 2013 and 01 May to 29 September 2014. The HOx system was deactivated for two periods in 2013 and three periods in 2014 as denoted by the "OFF". Similarly, the HOx system was activated for two periods in 2013 and three periods in 2014 as denoted by the "ON". All sample days are denoted by inverted black triangles; data were interpolated between sample days for the figure.

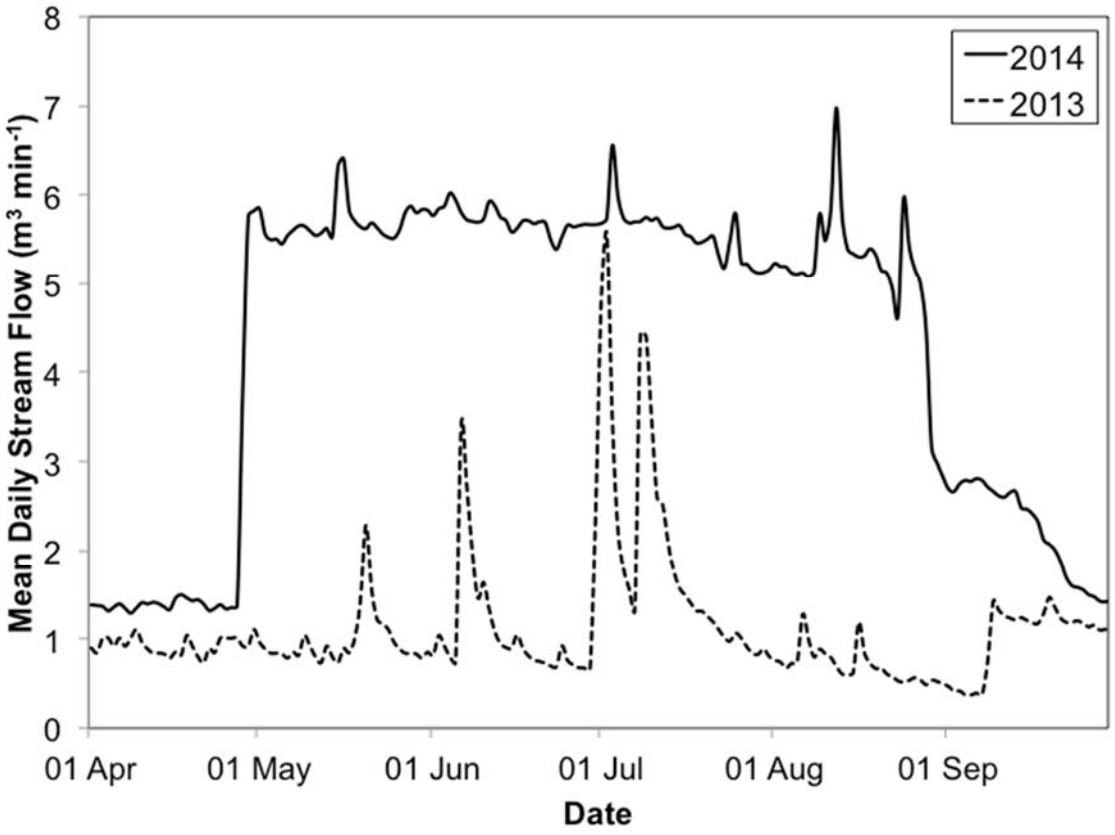

Figure 2.4. Stream flow data calculated from the weir located on FCR's upstream tributary from April to September 2013 and 2014. In 2013, the inflow pipe from Beaverdam Reservoir into the FCR tributary was closed, so the only water entering FCR through the tributary was runoff from the catchment. In 2014, we increased the volume of water entering FCR by opening the inflow pipe at the upper Beaverdam Reservoir.

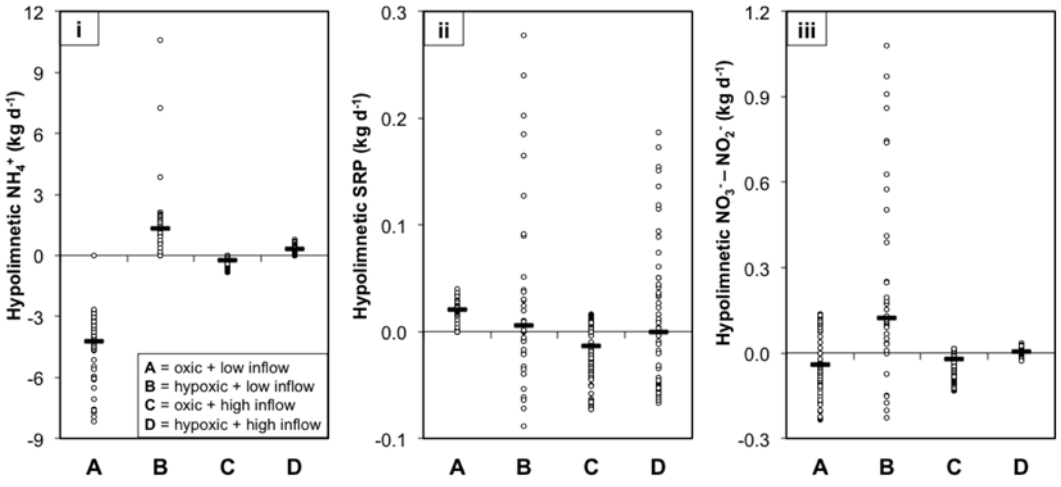

Figure 2.5. The standardized hypolimnetic masses of NH_4^+ (i), SRP (ii), and $NO_3^- - NO_2^-$ (iii), displayed for all days within a treatment. All masses are given in kg d^{-1}. The black dash represents the median of each treatment. Treatments A and B were composed of one period, Treatment C had three periods, and Treatment D had two periods. The data in this figure were aggregated across periods for Treatments C and D.

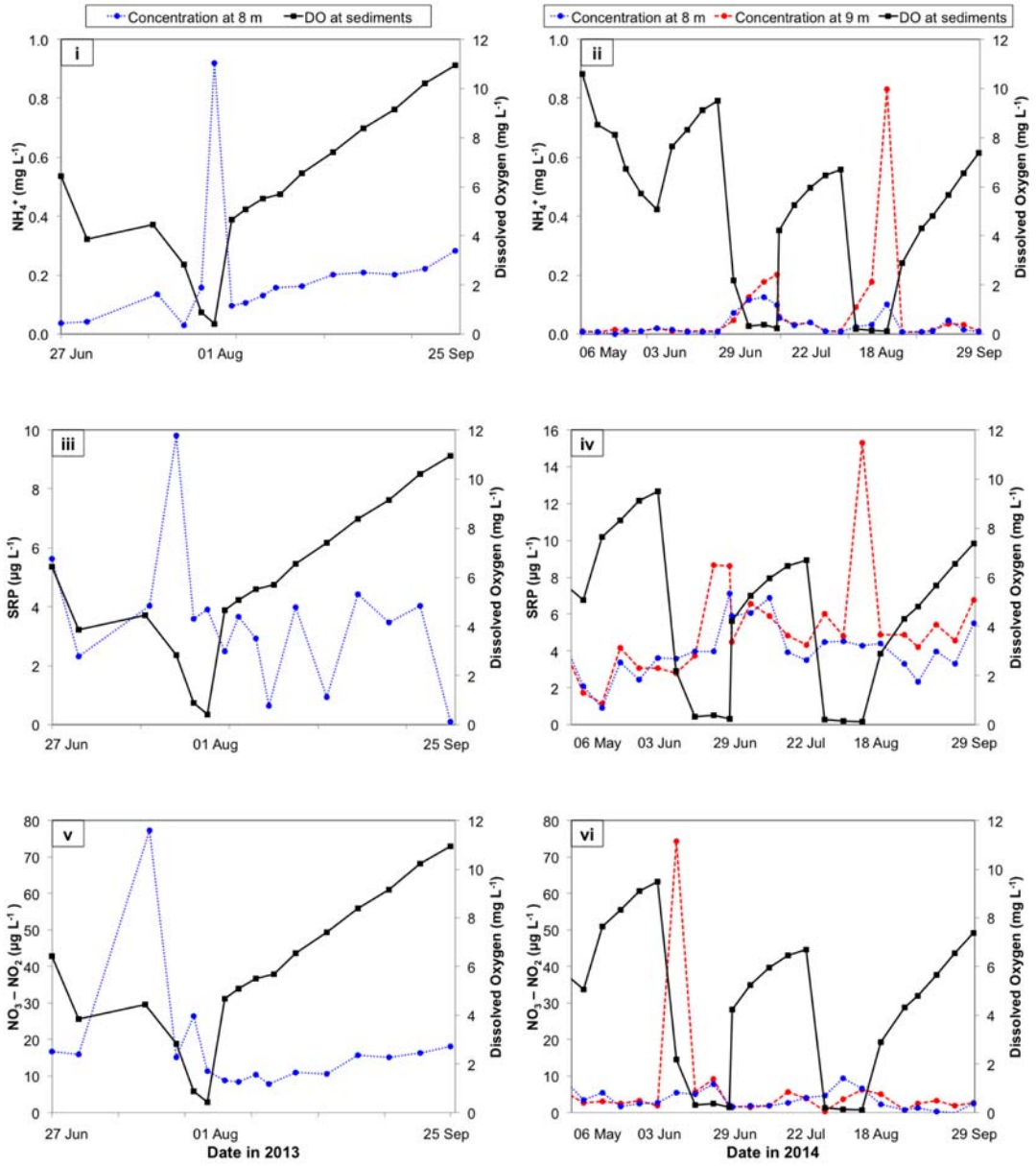

Figure 2.6. NH_4^+ (i, ii), SRP (iii, iv), and $NO_3^- - NO_2^-$ (v, vi) concentrations measured at 8 m depth in 2013, 8 m and 9 m depths in 2014, and dissolved oxygen (DO) concentrations at the sediments. Dissolved oxygen and NH_4^+ concentrations are given in mg L^{-1} and SRP and $NO_3^- - NO_2^-$ concentrations are given in µg L^{-1}. All measurements were collected at the deepest site of FCR from 27 June to 25 September 2013 and 01 May to 29 September 2014.

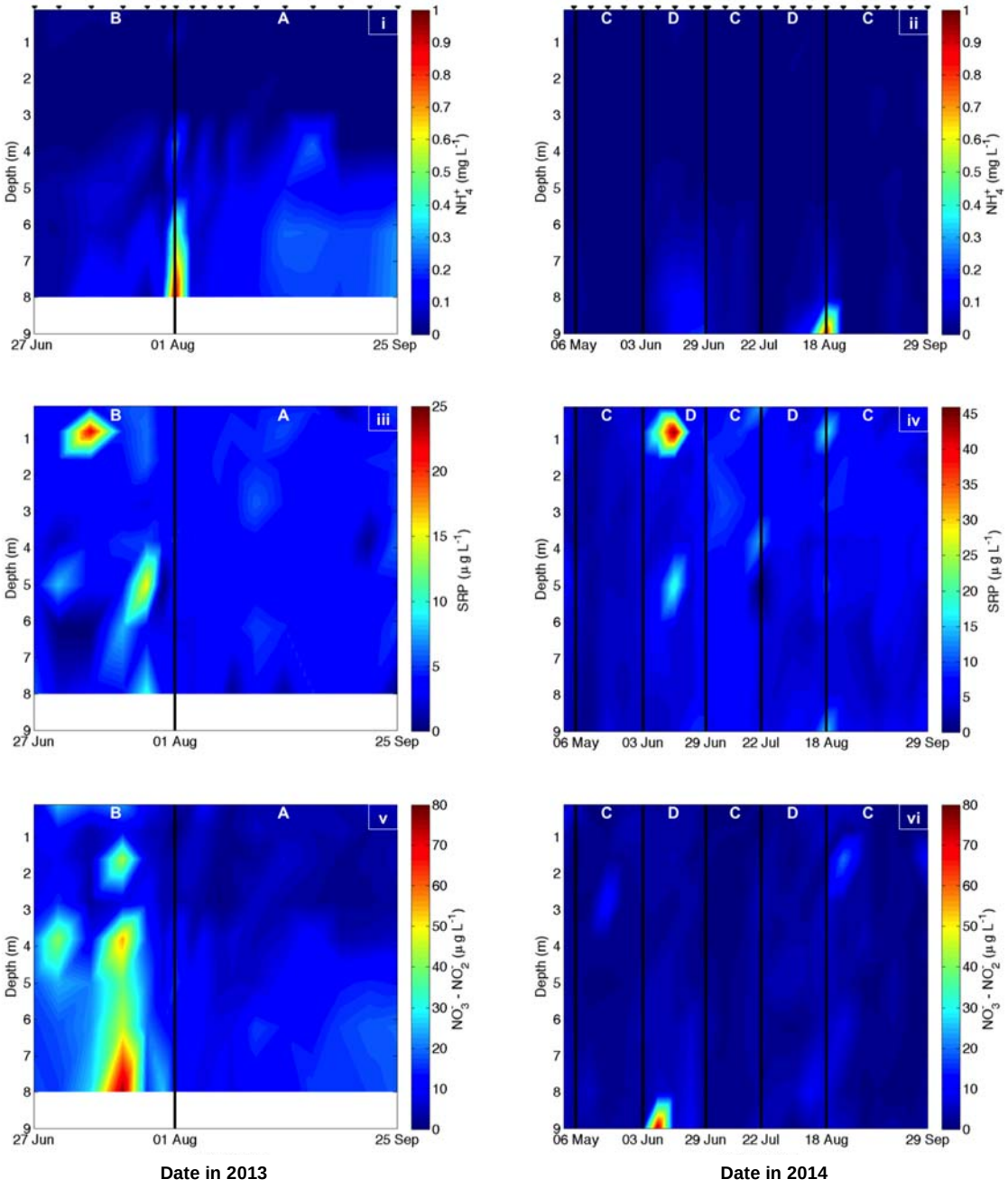

Figure 2.7. Water column NH_4^+ (i, ii), SRP (iii, iv), and NO_3^- – NO_2^- (v, vi) concentrations in FCR in 2013 and 2014, respectively. NH_4^+ concentrations are given in mg L^{-1} and SRP and NO_3^- – NO_2^- concentrations are given in µg L^{-1}; note the difference in color scales among panels. All measurements were collected at the deepest site of FCR from 27 June to 25 September 2013 and

01 May to 29 September 2014. All sample days are denoted by inverted black triangles and data were interpolated between sample days for the figures. The black lines represent transitions between treatments labeled in white font as A, B, C, or D.

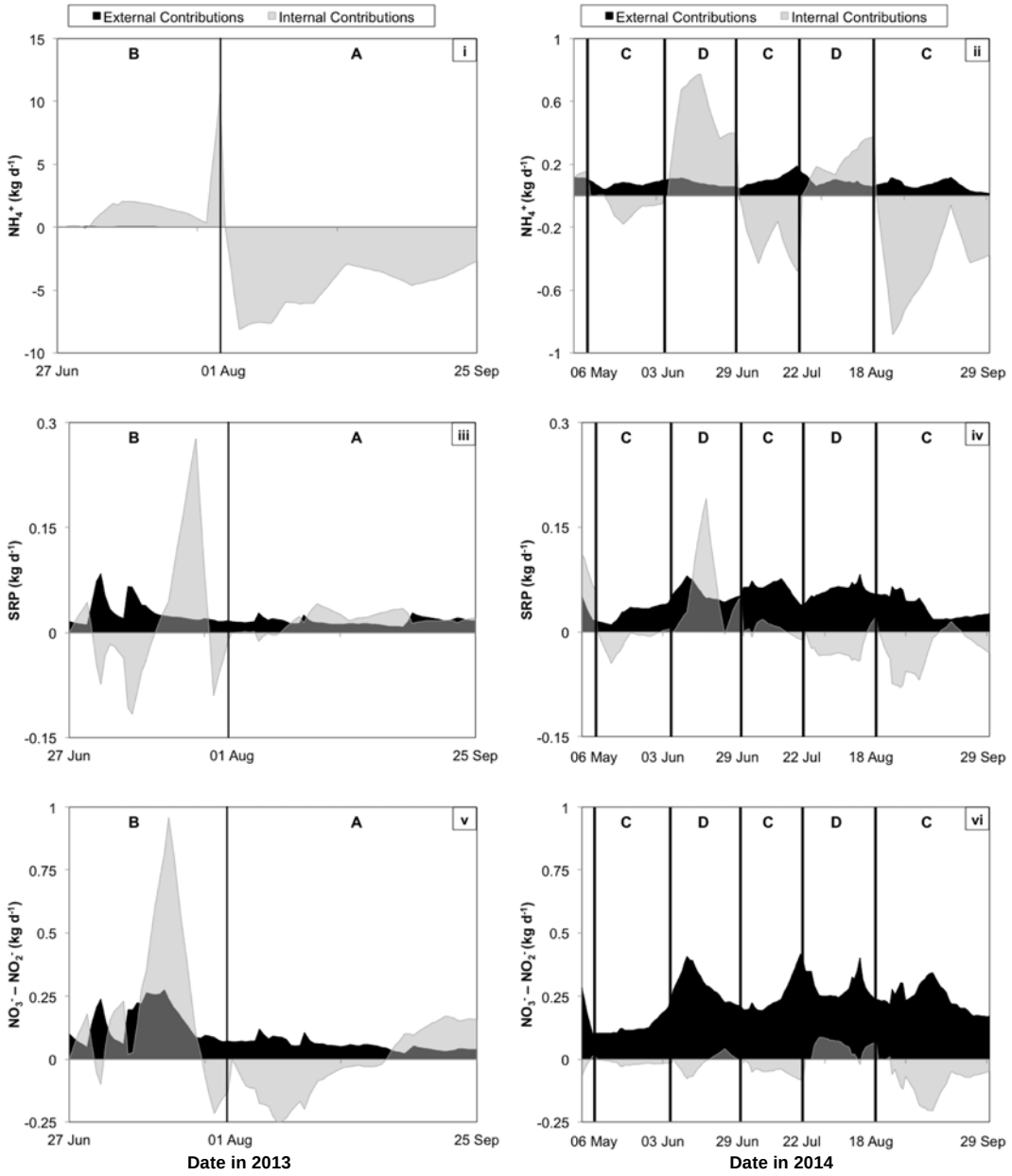

Figure 2.8. The internal (gray area) and external (black area) contributions of hypolimnetic NH_4^+ (i, ii), SRP (iii, iv), and $NO_3^- - NO_2^-$ (v, vi) in 2013 and 2014, respectively. All loads are given in kg d^{-1}. The black lines represent transitions between treatments labeled as A, B, C, or D. Note that the scales on the y-axes for NH_4^+ differ between 2013 and 2014 but are the same for SRP and $NO_3^- - NO_2^-$.

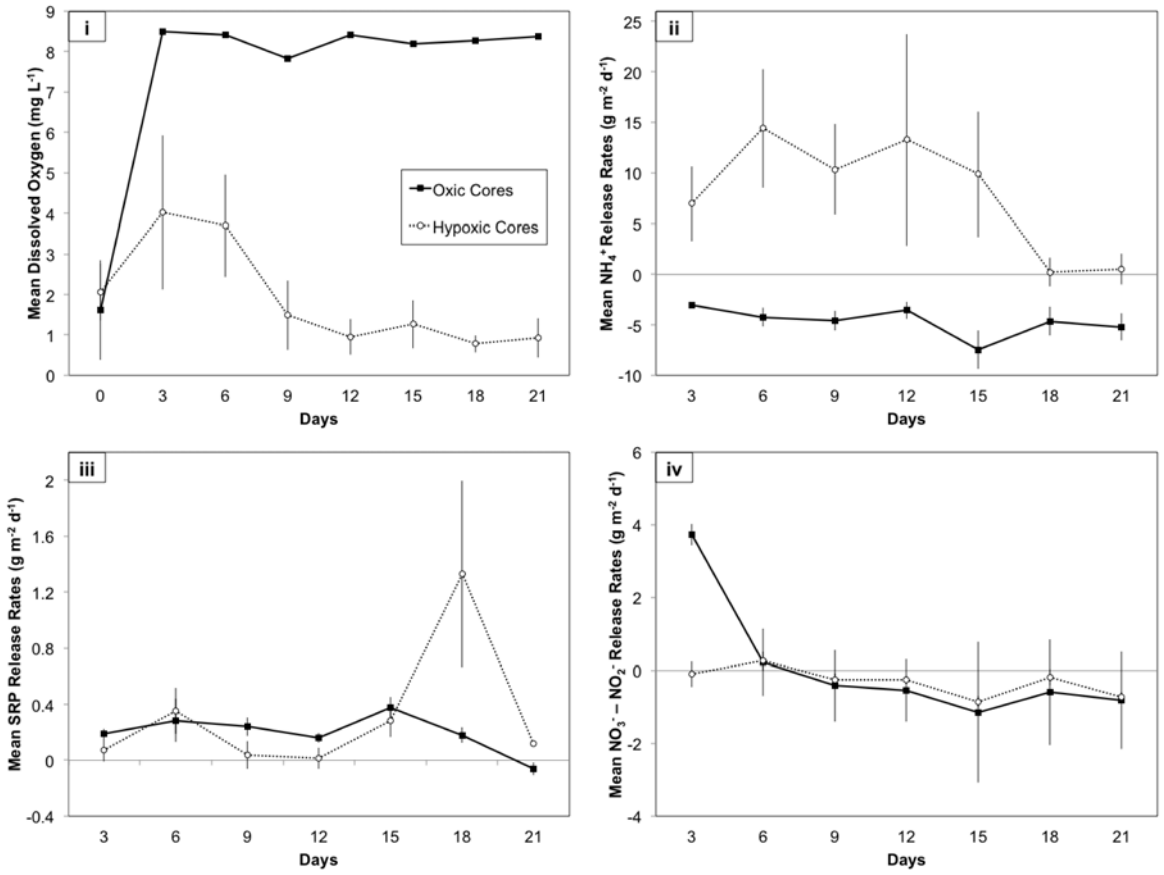

Figure 2.9. Mean dissolved oxygen concentrations (i) and mean release rates of NH_4^+ (ii), SRP (iii), and $NO_3^- - NO_2^-$ (iv) in the incubations of the hypoxic and oxic sediment cores. Dissolved oxygen concentrations are given in mg L^{-1} and all nutrient release rates are given in g m^{-2} d^{-1}. The oxic sediment cores are represented by the solid black lines and the hypoxic sediment cores are the dashed lines.

Conclusions

My data strongly suggest that side stream supersaturation (SSS) is a viable option for improving water quality in Falling Creek Reservoir (FCR), a shallow, eutrophic drinking water reservoir. As detailed in Chapter 1, I found that the SSS system effectively oxygenated the hypolimnion of FCR at a rate of ~1 mg/L/week. Additionally, SSS operation increased hypolimnetic dissolved oxygen (DO) concentrations up to 600 m from the SSS system. The two major concerns that have plagued the use of oxygenation systems in other ecosystems, destratification and warming of the sediments, did not occur in FCR. Rather, Schmidt stability (an index of the strength of thermal stratification) was not affected by the system activation. SSS operation also inhibited the internal release of iron (Fe), manganese (Mn), and phosphorus (P), from the sediments into the water column. In a comprehensive review of all previous hypolimnetic oxygenation system deployments, I found that our activation of SSS in FCR is the only known successful SSS operation in a shallow (<10 m depth) waterbody.

The whole-ecosystem manipulations of hypolimnetic oxygen conditions and inflow volumes to FCR further demonstrated the importance of controlling internal nutrient loads to improve water quality. As described in in Chapter 2, my results provide substantial evidence that internal dissolved nitrogen (N) and P loads strongly influence the hypolimnetic mass of nutrients in FCR, regardless of inflow volumes. My results from the sediment core incubations also demonstrated the dominance of internal loads in FCR and that the reservoir has accumulated a substantial quantity of N and P in its sediments since its construction over 100 years ago. Throughout the manipulations, FCR commonly functioned as net nutrient sink and reduced nutrient export to downstream. In particular, FCR retained a remarkably large amount of NO_3^- – NO_2^- inputs (a mean of 70-95% of all input loads).

It is likely that the legacy of historical agricultural land use in the catchment still has a profound effect on the nutrient dynamics in the reservoir, despite >80 years since catchment reforestation. FCR's history of accumulated nutrients in the sediments likely contributed substantially to its high internal loading rates during hypoxia. My findings indicate that it is critical to take reservoir catchment history and waterbody characteristics into account when predicting the effects of hypolimnetic hypoxia and increased storms on reservoir nutrient budgets.

As the construction of reservoirs increases globally (Chao 1995, Downing et al. 2006a, Rosenberg et al. 2000, Smith et al. 2002), reservoirs will increasingly play an important and dynamic role in biogeochemical processes in the landscape over the next decades to centuries. Longer-term studies are necessary to evaluate the efficacy of SSS operation in FCR. Specifically, multiple years of monitoring of FCR are required to determine if continuous hypolimnetic oxygenation is able to suppress the internal loading of Fe, Mn, N, and P as FCR experiences increased hypolimnetic hypoxia and magnitude of storms, simultaneously. Management efforts at Falling Creek Reservoir need to carefully consider the how multiple aspects of global change, waterbody characteristics, and land use history will interact to alter nutrient and metal budgets in the future.

References

AWWA, 1987. Research needs for the treatment of iron and manganese. American Water Works Association 79, 119-122.

Beutel, M.W., 2006. Inhibition of ammonia release from anoxic profundal sediments in lakes using hypolimnetic oxygenation. Ecological Engineering 28(3), 271-279.

Beutel, M.W., Horne, A.J., 1999. A review of the effects of hypolimnetic oxygenation on lake and reservoir water quality. Lake and Reservoir Management 15(4), 285-297.

Chao, B.F., 1995. Anthropogenic impact on global geodynamics due to reservoir water impoundment. Geophysical Research Letters 22(24), 3529-3532.

Cooke, G.D., Welch, E.B., Peterson, S., Nichols, S.A., 2005. Restoration and Management of Lakes and Reservoirs, Third Edition, CRC Press, Boca Raton, Florida.

Delpla, I., Jung, A.V., Baures, E., Clement, M., Thomas, O., 2009. Impacts of climate change on surface water quality in relation to drinking water production. Environ Int 35(8), 1225-1233.

Downing, J.A., Prairie, Y.T., Cole, J.J., Duarte, C.M., Tranvik, L.J., Striegl, R.G., McDowell, R.W., Kortelainen, P., Caraco, N.F., Melack, J., Middelburg, J.J., 2006. The global abundance and size distribution of lakes, ponds, and impoundments. Limnology and Oceanography 51, 2388-2397.

Jiménez Cisneros, B.E., Oki, T., Arnell, N.W., Benito, G., Cogley, J.G., Döll, P., Jiang, T., Mwakalila, S.S., 2014. Freshwater resources. In: Climate Change 2014: Impacts, Adaptation, and Vulnerability. Part A: Global and Sectoral Aspects. Contribution of Working Group II to the Fifth Assessment Report of the Intergovernmental Panel on Climate Change. ield, C.B., Barros, V.R., Dokken, D.J., Mach, K.J., Mastrandrea, M.D., Bilir, T.E., Chatterjee, M., Ebi, K.L., Estrada, Y.O., Genova, R.C., Girma, B., Kissel, E.S., Levy, A.N., MacCracken, S., Mastrandrea, P.R. and White, L.L. (eds), pp. 229-269, Cambridge, United Kingdom and New York, NY, USA.

Matthews, D.A., Effler, S.W., 2006. Assessment of long-term trends in the oxygen resources of a recovering urban lake, Onondaga Lake, New York. Lake and Reservoir Management 22(1), 19-32.

McGinnis, D.F., Little, J.C., 2002. Predicting diffused-bubble oxygen transfer rate using the discrete-bubble model. Water Res 36, 4627-4635.

Mortimer, C.H., 1941. The exchange of dissolved substances between mud and water in lakes. Journal of Ecology 29, 280-329.

Nowlin, W.H., Evarts, J.L., Vanni, M.J., 2005. Release rates and potential fates of nitrogen and phosphorus from sediments in a eutrophic reservoir. Freshwater Biology 50(2), 301-322.

Paerl, H.W., Huisman, J., 2009. Climate change: a catalyst for global expansion of harmful cyanobacterial blooms. Environ Microbiol Rep 1(1), 27-37.

Powers, S.M., Tank, J.L., Robertson, D.M., 2015. Control of nitrogen and phosphorus transport by reservoirs in agricultural landscapes. Biogeochemistry 124(1-3), 417-439.

Rosenberg, D.M., McCully, P., Pringle, C.M., 2000. Global-scale environmental effects of hydrological alterations: introduction. BioScience 50(746-751).

Sahoo, G.B., Schladow, S.G., 2008. Impacts of climate change on lakes and reservoirs dynamics and restoration policies. Sustainability Science 3(2), 189-199.

Sahoo, G.B., Schladow, S.G., Reuter, J.E., Coats, R., 2010. Effects of climate change on thermal properties of lakes and reservoirs, and possible implications. Stochastic Environmental Research and Risk Assessment 25(4), 445-456.

Schindler, D.W., 1974. Eutrophication and recovery in experimental lakes: Implications for lake management. Science 184(4139), 897-899.

Schindler, D.W., 1977. Evolution of phosphorus limitation in lakes. Science 195(4275), 260-262.

Schindler, D.W., Hecky, R.E., Findlay, D.L., Stainton, M.P., Parker, B.R., Paterson, M.J., Beaty, K.G., Lyng, M., Kasian, S.E., 2008. Eutrophication of lakes cannot be controlled by reducing nitrogen input: results of a 37-year whole-ecosystem experiment. Proceedings of the National Academy of Sciences 105(32), 11254-11258.

Singleton, V.L., Little, J.C., 2006. Designing hypolimnetic aeration and oxygenation systems - A Review. Environmental Science and Technology 40(24), 7512-7520.

Smith, S.V., Renwick, W.H., Bartley, J.D., Buddemeier, R.W., 2002. Distribution and significance of small, artificial water bodies across the United States landscape. Sci Total Environ 299, 21-36.

Smith, V.H., 1982. The nitrogen and phosphorous dependence of algal biomass in lakes - and empirical and theoretical analysis. Limnology and Oceanography 27(6), 1101-1112.

Smith, V.H., Schindler, D.W., 2009. Eutrophication science: where do we go from here? Trends Ecol Evol 24(4), 201-207.

Teodoru, C., Wehrli, B., 2005. Retention of Sediments and Nutrients in the Iron Gate I Reservoir on the Danube River. Biogeochemistry 76(3), 539-565.

Tranvik, L.J., Downing, J.A., Cotner, J.B., Loiselle, S.A., Striegl, R.G., Ballatore, T.J., Dillon, P., Finlay, K., Fortino, K., Knoll, L.B., Kortelainen, P., Kutser, T., Larsen, S., Laurion, I., Leech, D.M., McCallister, S.L., McKnight, D.M., Melack, J.M., Overholt, E., Porter, J.H., Prairie, Y.T., Renwick, W.H., Roland, F., Sherman, B., Schindler, D.W., Sobek, S., Tremblay, A., Vanni, M.J., Verschoor, A.M., von Wachenfeldt, E., Weyhenmeyer, G.A.,

2009. Lakes and reservoirs as regulators of carbon cycling and climate. Limnology and Oceanography 54, 2298–2314.

Williamson, C.E., Saros, J.E., Vincent, W.F., Smol, J.P., 2009. Lakes and reservoirs as sentinels, integrators, and regulators of climate change. Limnology and Oceanography 54, 2273-2282.

Wyman, B., Stevenson, L.H., 1991. Dictionary of Environmental Science, Facts On File, Inc., New York, New York

Zaw, M., Chiswell, B., 1999. Iron and manganese dynamics in lake water. Water Res 33(8), 1900-1910.

Appendix A: Stream Flow Data

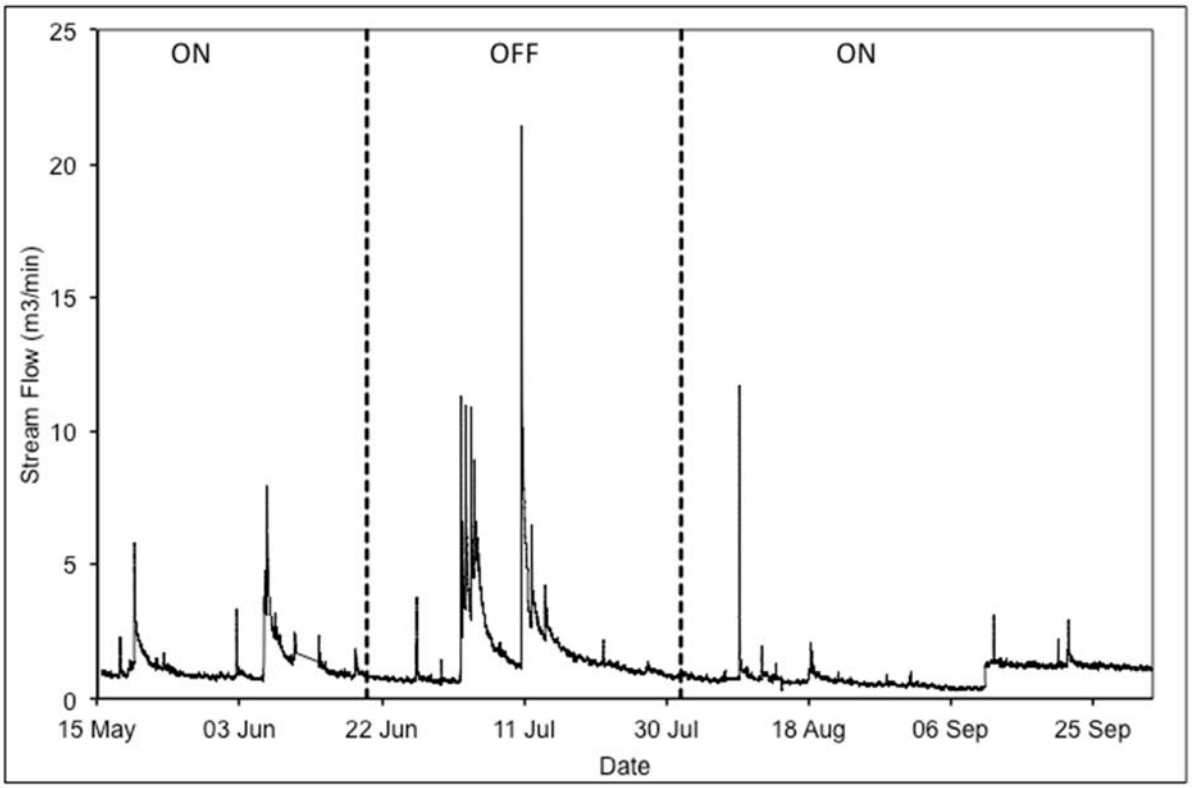

Figure A.1: Stream flow data calculated from the weir located on Falling Creek Reservoir's only upstream tributary from 15 May to 25 September 2013. The SSS system was activated until 20 June (denoted by the "ON"), deactivated again until 1 August (denoted by the "OFF"), and finally reactivated for the remainder of the sampling period (denoted by the "ON").